NASA Contractor Report 177638

# Hypersonic Shock/Boundary-Layer Interaction Database: New and Corrected Data

Gary S. Settles and Lori J. Dodson

Department of Mechanical Engineering
Penn State University
University Park, PA 16802

Prepared for
Ames Research Center
CONTRACT NAG2-781
April 1994

National Aeronautics and
Space Administration

**Ames Research Center**
Moffett Field, California 94035-1000

# Hypersonic Shock/Boundary-Layer Interaction Database: New and Corrected Data

## Table of Contents

# Introduction

As described fully in Ref. 1, an effort was begun in 1989 at the Penn State University Gas Dynamics Laboratory to perform a critical review of the available hypersonic data and to assemble a selected database for purposes of CFD code validation and turbulence modeling. The effort was sponsored by the NASP Program through NASA-Ames Research Center, and was a part of an overall task to develop compressible turbulence models. Ref. 1, a database report on hypersonic shock wave/turbulent boundary-layer interactions, was the product of phase 1 of that effort. Phase 2 produced a similar database, reported in Ref. 2, covering the topics of attached hypersonic boundary layers in pressure gradients and compressible turbulent mixing layers. The present report represents the result of the third and final phase, namely, recent additions and corrections to the hypersonic shock wave/ turbulent boundary-layer interaction database originally given in Ref. 1.

The new datasets included here are those which have come to our attention since the completion of Phase 1 of the database effort at the end of 1990, and which were able to pass the acceptance criteria originally applied in Phase 1. Those criteria are listed by name below, but the reader is directed to Ref. 1 for details of their application:

(NECESSARY CRITERIA)

1) BASELINE APPLICABILITY
2) SIMPLICITY
3) SPECIFIC APPLICABILITY
4) WELL-DEFINED EXPERIMENTAL BOUNDARY CONDITIONS
5) WELL-DEFINED EXPERIMENTAL ERROR BOUNDS
6) CONSISTENCY CRITERION
7) ADEQUATE DOCUMENTATION OF DATA
8) ADEQUATE SPATIAL RESOLUTION OF DATA

(DESIRABLE CRITERIA)

1) TURBULENCE DATA
2) REALISTIC TEST CONDITIONS
3) NON-INTRUSIVE INSTRUMENTATION
4) REDUNDANT MEASUREMENTS
5) FLOW STRUCTURE AND PHYSICS

# Discussion of New Data

Ref.: 3-6
Author: Kussoy and Horstman
Geometry: 3-D Fin
Mach number: 8.2
Data: $p_{wall}$ ,$q_{wall}$ ,$c_f$ , flowfield pitot surveys

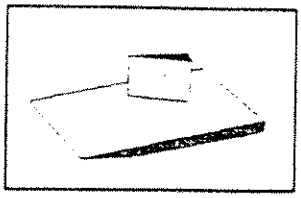

Ref.: 7-9
Author: Rodi and Dolling
Geometry: 3-D Fin
Mach number: 4.9
Data: $p_{wall}$, $q_{wall}$, surface-flow traces

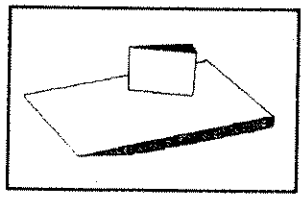

Ref.: 10-11
Author: Lee and Settles
Geometry: 3-D Fin
Mach number: 3, 4
Data: $c_h$

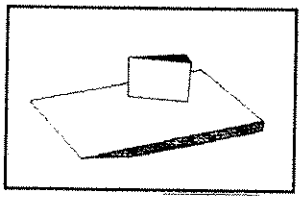

Ref.: 12-13
Author: Hsu and Settles
Geometry: 3-D Fin
Mach number: 3, 4
Data: flowfield density maps

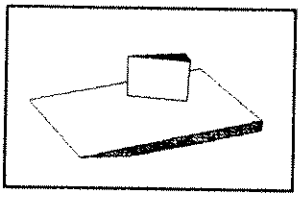

Ref.: 14
Author: Kussoy and Horstman
Geometry: Crossing Oblique Shock Waves
Mach number: 8.3
Data: $p_{wall}$, $q_{wall}$, flowfield pitot surveys

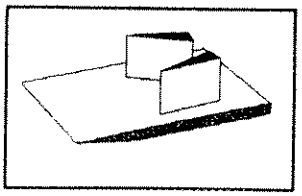

Ref.: 15-17
Author: Garrison and Settles
Geometry: Crossing Oblique Shock Waves
Mach number: 4
Data: $p_{wall}$, $c_f$, flowfield pitot surveys

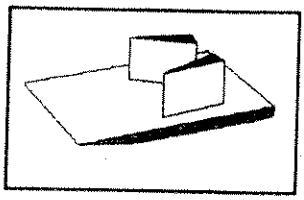

Ref.: 18-20
Author: Kuntz *et al.*
Geometry: 2-D Compression Corner
Mach number: 3
Data: $p_{wall}$, mean & fluctuating flowfield surveys (2-channel LDV)

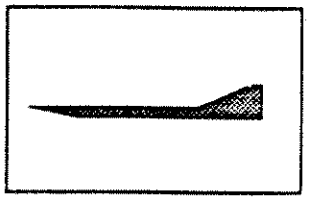

The new data since 1991 can be characterized in 3 groups as follows: 1) Mach 8 single- and double-fin (crossing-shock) interactions, 2) more advanced measurements of supersonic single- and double-fin interactions, and 3) more advanced measurements of a supersonic 2-D compression corner.

The new Mach 8 data are the result of a concerted experimental program by Kussoy and Horstman in the NASA-Ames Research Center 3.5-foot hypersonic wind tunnel (Refs. 3-6 and 14). These carefully-documented datasets fulfill several of the needs pointed out in Ref. 1 and its companion technical paper (Ref. 21), including Mach number firmly within the hypersonic regime, more-complex interaction types, and more emphasis on 3-D interactions.

The new supersonic single-fin-interaction datasets are the results of research programs at Penn State (Refs. 10-13) and the University of Texas-Austin (Refs. 7-9) aimed at providing advanced data for code validation and turbulence modeling. They feature heat transfer data to supplement the skin friction data already including in Ref. 1, and flowfield density maps obtained non-intrusively by conical holographic interferometry.

The new supersonic double-fin or crossing-shock interaction data (Refs. 15, 16) feature surface pressures, skin friction coefficients, and one plane of flowfield pitot-pressure data for this important inlet-type interaction. Readers interested in this interaction should also see Refs. 14 and 22-23.

Finally, the new 2-D compression corner data listed here (Refs. 18-20) were actually available previously, and were included in the literature search of Ref. 1, but, due to an oversight, were not subjected to an evaluation. That was unfortunate, since this dataset provides valuable LDV data to supplement the mean-flow and hot-wire data previously available for supersonic compression corners.

However, the availability of Mach 3 LDV compression corner data in Refs. 18-20 creates the following dilemma: The LDV magnitudes of Reynolds stresses in these interactions are 2 to 4 times larger than the levels found using hot-wire anemometry by Smits et al., Refs. 1 and 24) in a similar experiment. The LDV authors speculate (see discussion just prior to Conclusions of Ref. 18) that this discrepancy is due to inherent errors

in slanted-hot-wire calibrations. However, it is not reasonable to discount the hot-wire data on the basis of this speculation alone. Moreover, discussions with D. W. Kuntz concerning the LDV dataset appear to confirm that the higher LDV values of Reynolds stress are not simply due to shock unsteadiness, since pdf plots of the data do not reveal bimodal distributions. Though the hot-wire and LDV experiments were conducted in different test facilities varying in size by a factor of two, the test conditions were similar enough that the discrepancy cannot be thus explained. Given such an unresolved discrepancy, we have decided to retain both sets of data in the present database with the following warning:

**Note: One or both of the Smits (Ref. 24) and Kuntz (Ref. 18) 2-D compression corner datasets is incorrect insofar as the levels of turbulent Reynolds stresses are concerned. It is not presently possible to determine where the error lies. Thus both experiments are included in the database in order to show possible limits on Reynolds stresses in such interactions, or possible error levels in the experiments. Beyond that, there is only the time-honored disclaimer, *caveat emptor*.**

# Discussion of Corrected Data

---

Ref.: 25, private communication
Author: Zheltovodov, A. A., *et al*
Geometry: 2-D Compression Corner
Mach number: 3
Data: $p_{wall}$, $c_h$, mean and fluctuating flowfield surveys (pitot and hot-wire anemometry)

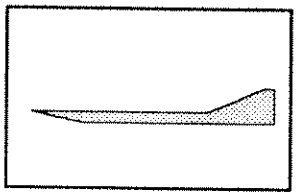

---

Two small but significant errors were found in this dataset as it is presented in Ref. 1. First, although the step height h = 15 mm, is correctly given for the mean-flow test geometry shown on page 108 of Ref. 1, no value is given for h in the case of the heat transfer model shown on the next page. In fact, h = 6 mm is the correct value for the heat transfer model.

Second, in the tabulated data on page 119 of Ref. 1 and in the data file ZHELT.DAT, a typographical error appears. In the heading:

**********Heat Transfer Data on Model FFS25**********
M1 = 3.01, $\alpha$1 = 280 W/m**2 K

The correct value of the incoming flat-plate heat transfer rate $\alpha$1 should be 180 W/m$^2$K. This correction has been verified by e-mail correspondence with A. A. Zheltovodov. The diskette accompanying the present report contains a corrected data file designated ZHELT2.DAT.

Ref.: 26
Author: Kim, K-S, *et al*
Geometry: 3-D Fin
Mach number: 3, 4
Data: $p_{wall}$, $c_f$, surface-flow angles

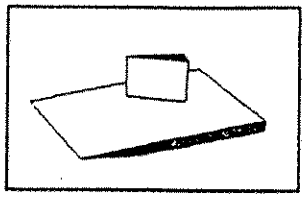

Based on a suggestion by D. J. Monson, the laser-skin-friction data reduction scheme of Kim (Ref. 26) was re-examined by Garrison (Ref. 17). It was found that, in the case of high peak skin friction levels in swept interactions where few laser interference fringes were available, Kim's approach led to a significant overestimate of the skin friction coefficient (Ref. 27). Garrison then repeated experiments at the peak points of Kim's strongest single-fin interaction (Mach 4, $\alpha$ =20 degrees) and found lower skin friction values than those originally found by Kim. Kim's original skin friction distribution for this case, as tabulated in Ref. 1, is:

MACH 4, ALPHA = 20 DEGREES

| BETA | CF | ERROR BAR |
|---|---|---|
| 56.00 | 9.868E-4 | 2.774E-5 |
| 51.00 | 9.835E-4 | 4.131E-5 |
| 48.80 | 1.114E-3 | 4.380E-5 |
| 44.00 | 1.199E-3 | 4.645E-5 |
| 40.50 | 1.820E-3 | 8.979E-5 |
| 39.50 | 1.655E-3 | 3.913E-5 |
| 31.00 | 2.649E-3 | 9.820E-5 |
| 26.30 | 9.494E-3 | 6.718E-4 |
| 23.30 | 7.733E-3 | 5.920E-4 |
| 21.00 | 5.749E-3 | 4.377E-4 |

With Garrison's correction of the 8th and 9th data points in this table, the corrected skin friction distribution is:

MACH 4, ALPHA = 20 DEGREES

| BETA | CF | ERROR BAR |
|---|---|---|
| 56.00 | 9.868E-4 | 2.774E-5 |
| 51.00 | 9.835E-4 | 4.131E-5 |
| 48.80 | 1.114E-3 | 4.380E-5 |
| 44.00 | 1.199E-3 | 4.645E-5 |
| 40.50 | 1.820E-3 | 8.979E-5 |
| 39.50 | 1.655E-3 | 3.913E-5 |
| 31.00 | 2.649E-3 | 9.820E-5 |
| 26.50 | 5.070E-3 | 5.000E-4 |
| 22.00 | 5.510E-3 | 5.000E-4 |

21.00 5.749E-3 4.377E-4

A corrected data file with the name KIM2.DAT has been included on the diskette accompanying the present report.

This error is an unfortunate one, since it changes the conclusions of Ref. 26. In fact, the computational solutions described there are in much better agreement with the corrected data than they were with the original, erroneous data. However, an examination of this dataset indicates that such peak-skin-friction errors occurred only in the strongest interaction (Mach 4, $\alpha$ =20 degrees), so that the results given in Refs. 1 and 26 and the conclusions drawn in ref. 26 for the weaker interactions are still believed to be valid.

---

Ref.: 28, 29
Author: Smits, A. J., *et al*
Geometry: 2-D Compression Corner
Mach number: 3
Data: $p_{wall}$, $c_f$, mean & fluctuating flowfield surveys (pitot and hot-wire anemometry)

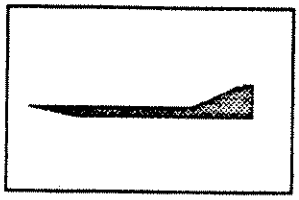

---

Since the publication of Ref. 1, several computational groups have made use of the mean-flow component of this dataset, which was tabulated and appeared in the ASCII file named SETTLES.DAT which was on the diskette included with Ref. 1. The dataset has thus had a rather thorough "workout," and several errors and problems were found as follows.

To put the mean-flow dataset in perspective, note that it consists of 1970's-vintage 2-D compression corner data taken by Settles *et al.* This work was originally reported in Refs. 30-33, which contain some discrepancies attributable to the original experimenters as described below. It was also submitted as a test case for the 1980-81 AFOSR-HTTM-Stanford Conference on Complex Turbulent Flows, whence Ref. 28 was prepared. Ref. 28 is still a complete and almost-up-to-date discussion and tabulation of the dataset, but this reference is, by its nature, not widely available. Unfortunately, the later tabulation of the same dataset for Ref. 29 involved re-reduction of the raw data by persons other than the original experimenters, whereupon additional discrepancies occurred. An attempt is made here to resolve these issues.

1) Tabulation of Freestream and Incoming-Flow Conditions

Ref. 1 contains no proper tabulation of freestream and incoming-flow conditions for the four compression-corner cases included in the dataset. This information, from Ref. 28, is now included in the present data file SETTLES2.DAT and in the printed tabulation reproduced in this report, along with a list of definitions of terms. It should be noted that minor revisions of some of the incoming conditions, especially PINF values, have been made on account of a re-examination of the dataset after Ref. 28 was prepared.

2) Correction of Wall-Pressure Distributions

The manner in which the wall pressures were presented in Ref. 1 was inconsistent, confusing, and erroneous in places. The revised distributions are presented in terms of Pwall/PINF, with PINF tabulated nearby, and have been gone over carefully for errors.

3) Correction of Confusion Surrounding Skin-Friction Distributions

By far the worst problem with this dataset as presented in Ref. 1 concerns the skin friction distributions. The problem arose because the original experimenters chose to present the skin friction coefficient in two different forms: wall shear stress normalized by $\rho_\infty u_\infty^2$ ("CFINF" in Ref. 1) and normalized by $\rho_{edge} u_{edge}^2$ ("CF" in Ref. 1). In retrospect, the former form is the proper skin friction coefficient, while the latter is confusing and essentially worthless. This unfortunate situation has been cleared up in the present tabulation and SETTLES2.DAT file by deleting the "CF" column and renaming the "CFINF" column "CF," which is now unequivocally defined as the wall shear stress normalized by $\rho_\infty u_\infty^2$.

To make matters worse, early publications such as Ref. 33, due to a misunderstanding between experimental and computational authors, compared properly-defined computed skin friction distributions with the above improperly-defined experimental values. Thus Figs. 3 and 9 of Ref. 33 show data points which are significantly smaller than they should be. This mistake was later discovered and corrected, but the confusion factor still exists in the early literature. Hopefully the present report will clear up this confusion.

4) Mean Profile Corrections

A recheck of the mean flowfield profiles of this dataset uncovered some minor errors and needed clarifications. These have been corrected and implemented in the present SETTLES2.DAT file.

# Closure

The publication of this report brings to an end the effort by the Penn State Gas Dynamics Lab, under NASA-Ames support, to establish a database for hypersonic boundary layers, interacting flows, and compressible mixing. There remains only the necessity to comment on the limitations of the present database for users of advanced turbulence models.

In general, none of the experiments included in this database contains enough information to properly specify the boundary conditions of any *turbulent-flow* computation. Assumptions must always be made. As an example of a reasonable assumption, Horstman (Ref. 34) carries out a finite-difference boundary-layer calculation for the test surface ahead of a shock/boundary-layer interaction. At the point where the computed boundary-layer displacement thickness matches that of the experiment, Horstman uses the computed boundary-layer turbulence quantities as input conditions. A similar approach is adopted by Morrison *et al.* (Ref. 35), who attempt to find a location where all three computed boundary-layer thicknesses and the skin friction coefficient are within 15% of the experimentally-determined values.

Both these approaches are reasonable, and similar schemes may work as well, if it is established that the incoming turbulent boundary-layer is in equilibrium in the experiment. However, in shock interaction cases where the incoming boundary-layer is not in equilibrium (of which there are none in the present database), much more documentation and detail of the incoming boundary layer would be required in the experiment in order to provide proper information for a computational simulation.

# References


1) Settles, G. S., and Dodson, L. J., "Hypersonic Shock/Boundary-Layer Interaction Database," NASA CR 177577, April 1991.
2) Settles, G. S., and Dodson, L. J., "Hypersonic Turbulent Boundary-Layer and Free Shear Layer Database," NASA CR in press.
3) Kussoy, M. I., and Horstman, K. C., "Documentation of Two- and Three-Dimensional Shock-Wave/Turbulent Boundary-Layer Interaction Flows at Mach 8.2," NASA TM 103838, May 1991.
4) Kussoy, M. I., and Horstman, K. C., "Three-Dimensional Shock-Wave/Turbulent Boundary-Layer Interactions," *AIAA Journal*, Vol. 31, Jan. 1993, pp. 8-9.
5) Kussoy, M. I., Kim, K-S., and Horstman, K. C., "An Experimental Study of a Three-Dimensional Shock-Wave/Turbulent Boundary-Layer Interaction at Hypersonic Mach Number," AIAA Paper 91-1761, June 1991.
6) Knight, D.D., Horstman, C. C., and Monson, D. J., "The Hypersonic Shock-Wave/Turbulent Boundary-Layer Interaction Generated by a Sharp Fin at Mach 8.2," AIAA Paper 92-0747, Jan. 1992.
7) Rodi, P.E., Dolling, D.S. and Knight, D.D., "An Experimental/Computational Study of Heat Transfer in Sharp Fin Induced Turbulent Interactions at Mach 5," AIAA Paper 91-1764, June 1991.
8) Rodi, P.E. and Dolling, D.S., "An Experimental/Computational Study of Sharp Fin Induced Shock Wave/Turbulent Boundary Layer Interactions at Mach 5: Experimental Results," AIAA Paper 92-0749, January 1992.
9) Rodi, P.E., "An Experimental/Computational Study of Heat Transfer in Sharp Fin Induced Shock Wave/Turbulent Boundary Layer Interactions at Low Hypersonic Mach Numbers," Ph.D. Dissertation, Department of Aerospace Engineering and Engineering Mechanics, The University of Texas at Austin, December 1991.
10) Lee, Y., Settles, G. S., and Horstman, C. C., "Heat Transfer Measurements and CFD Comparison of Swept Shock Wave/Boundary-Layer Interactions," AIAA Paper 92-3665, July 1992, (to be published in *AIAA Journal)*.
11) Lee, Y., "Heat Transfer Measurements in Swept Shock Wave/Turbulent Boundary-Layer Interactions," Ph.D. Dissertation, Department of Mechanical Engineering, Penn State University, June 1992.
12) Hsu, J. C., and Settles, G. S., "Holographic Flowfield Density Measurements in Swept Shock-Wave/Turbulent Boundary-Layer Interactions," AIAA Paper 92-0746, Jan. 1992.

13) Hsu, J. C., "Holographic Flowfield Density Measurements in Swept Shock-Wave/Turbulent Boundary-Layer Interactions," Ph.D. Dissertation, Department of Mechanical Engineering, Penn State University, pending.
14) Kussoy, M. I., and Horstman, K. C., "Intersecting Shock-Wave/Turbulent Boundary-Layer Interactions at mach 8.3,"NASA TM 103909, February 1992.
15) Garrison, T. J., Settles, G. S., Narayanswami, N., and Knight, D. D., "Structure of Crossing Shock-Wave/Turbulent Boundary-Layer Interactions," AIAA Paper 92-3670, July 1992, (to be published in *AIAA Journal).*
16) Garrison, T. J., Ph.D. Dissertation, Department of Mechanical Engineering, Penn State University, pending.
17) Garrison, T. J., and Settles, G. S., "Laser Interferometer Measurements of Crossing-Shock Wave/Turbulent Boundary-Layer Interactions," AIAA Paper 93-3072, July 1993.
18) Kuntz, D.W., Amatucci, V.A. and Addy, A.L., "Turbulent Boundary-Layer Properties Downstream of the Shock-Wave/Boundary-Layer Interaction," *AIAA Journal*, Vol. 25, 1987, pp. 668-675.
19) Kuntz, D.W., Amatucci, V.A. and Addy, A.L., "An Experimental Study of the Shock-Wave-Turbulent Boundary-Layer Interaction," *Proc. Intl. Symposium on Laser Anemometry*, ASME FED Vol. 33, ed. A. Dybbs and P. A. Pfund, 1985, pp. 173-178.
20) Kuntz, D.W., "An Experimental Investigation of the Shock-Wave-Turbulent Boundary-Layer Interaction," Ph.D. Thesis, Dept. of Mechanical and Industrial Engineering, Univ. of Illinois at Urbana-Champagne, 1985.
21) Settles, G. S., and Dodson, L. J., "Hypersonic Shock/Boundary-Layer Interaction Database," AIAA Paper 91-1763, June 1991, (to published in *AIAA Journal* ).
22) Garrison, T. J., and Settles, G. S., "Interaction Strength and Model Geometry Effects on the Structure of Crossing Shock-Wave/Turbulent Boundary-Layer Interactions," AIAA Paper 93-0780, Jan. 1993.
23) Garrison, T. J., and Settles, G. S., "Flowfield Visualization of Crossing Shock-Wave/Boundary Layer Interactions," AIAA Paper 92-0750, Jan. 1992.
24) Smits, A.J. and Muck, K.C., "Experimental Study of Three Shock Wave/Turbulent Boundary Layer Interactions," *Journal of Fluid Mechanics*, Vol. 182, Sept. 1987, pp. 291-314.
25) Zheltovodov, A.A., Zaylichny, E.G., Trofimov, V.M. and Yakovlev, V.N., "Investigation of Heat Transfer and Turbulence in Supersonic Separation," Russian *ITPM Preprint 22-87*, 1987.
26) Kim, K-S, Lee, Y., Alvi, F. S., and Settles, G. S., "Skin-Friction Measurements and Computational Comparison of Swept Shock/Boundary-Layer Interactions," *AIAA Journal*, Vol. 29, October 1991, pp. 1643-1650.
27) Garrison, T. J., private communication, 1992.
28) Settles, G.S., Gilbert, R.B. and Bogdonoff, S.M., "Data Compilation For Shock Wave/Turbulent Boundary Layer Interaction Experiments On Two-Dimensional Compression Corners," *Princeton University Report 1489-MAE*, Princeton Univ., 1980.

29) Fernholz, H.H., Finley, P.J., Dussauge, J.P. and Smits, A.J., "A Survey of Measurements and Measuring Techniques in Rapidly Distorted Compressible Turbulent Boundary Layers," *AGARDograph 315*, 1989.

30) Settles, G. S., Fitzpatrick, T. J. and Bogdonoff, S. M., "Detailed Study of Attached and Separated Compression Corner Flowfields in High Reynolds Number Supersonic Flow," *AIAA Journal*, Vol. 17, No. 6, June 1979, pp. 579.

31) Settles, G. S., Vas, I. E. and Bogdonoff, S. M., "Details of a Shock-Separated Turbulent Boundary Layer at a Compression Corner," *AIAA Journal*, Vol. 14, No. 12, December 1976, pp. 1709-1715.

32) Settles, G. S., "An Experimental Study of Compressible Turbulent Boundary Layer Separation at High Reynolds Numbers," Ph.D. Dissertation, Aerospace and Mechanical Sciences Dept., Princeton University, Sept. 1975.

33) Horstman, C. C., Settles, G. S., Vas, I. E., Bogdonoff S. M., Hung, C. M., "Reynolds Number Effects on Shock-Wave Turbulent Boundary-Layer Interactions,"*AIAA Journal*, Vol. 15, August 1977, pp. 1152-1158.

34) Horstman, C. C., private communication, April 26, 1993.

35) Morrison, J. H., Gatski, T. B., Sommer, T, P., Zhang, H. S., and So, R. M. C., "Evaluation of Near-Wall Turbulent Closure Model in Predicting Compressible Ramp Flows," Paper presented at the International Conference on Near-Wall Turbulent Flows, Tempe, AZ, March 15-17, 1993.

# Appendix: Data Tabulation

There follows a tabulation of pertinent data from the new and corrected datasets which make up the hypersonic shock/boundary-layer interaction database. For each dataset, a brief discussion of the data is given for the benefit of users. However, users are strongly encouraged to consult the original references for more detail on what was measured and how it was accomplished. Similarly, no attempt has been made to tabulate all available data from each of these studies, but rather only those data most pertinent to the issues of turbulence modeling and code validation. In several cases, additional data may be had from the original publications. Moreover, of the data selected for inclusion, only initial profiles and samples are printed in this report, since brevity is required and paper tabulations are no longer of much use when machine-readable data are readily available. A 3.5" double-sided high-density diskette is also provided in original copies of this report. This disk contains the complete data-tables of this Appendix in machine-readable ASCII files, formatted for MS-DOS computers. Individual ASCII files are given for each of the datasets, with filenames keyed to first authors as follows:

New Datasets:
GARRISON.DAT
HSU.DAT
KUNTZ.DAT
KUSSOY3.DAT (single-fin)
KUSSOY4.DAT (crossing-shocks)
LEE.DAT
RODI.DAT

Corrected Datasets:
SETTLES2.DAT

Ref.: 15-17
Author: Garrison and Settles
Geometry: Crossing Oblique Shock Waves
Mach number: 3 and 4
Data: $p_{wall}$, $c_f$ , flowfield pitot surveys

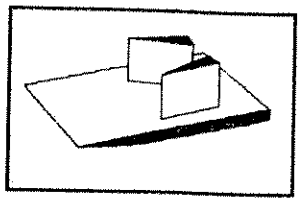

The experiments were carried out using a double-fin test geometry mounted on a flat plate in the supersonic wind tunnel facility of the Penn State Gas Dynamics Laboratory. The flat-plate boundary-layers at Mach 3 and 4 are the same as those previously documented in Ref. 1(KIM.DAT). These are equilibrium turbulent boundary-layers developing naturally on a flat-plate at high Reynolds number, and are essentially adiabatic.

Opposing fins produced oblique shocks of opposite families, which intersected along the centerline of the flat plate. All test geometries were symmetric about this centerline. Fin angles-of-attack of 7x7, 9x9, 11x11, and 13x13 degrees were tested at Mach 3 and 4. A 15x15 degree case was also tested at Mach 4.

All data are described by a right-handed Cartesian x,y,z coordinate system. The origin of coordinates is on the centerline of the flat plate at the location of the fin leading-edges, ie 21.3 cm downstream of the flat-plate leading-edge. The x and z coordinates lie in the plane of the flat plate when $y = 0$, and in planes parallel to but above it for $y > 0$. The z coordinate is positive in the downstream direction, while the x coordinate is positive to the right of the plate centerline when viewed from the downstream direction. The z and x-locations of points within a given interaction are normalized by a reference "incoming" boundary-layer thickness, which is taken as $\delta_0 = 3.5$ mm for all test conditions.

The data file GARRISON.DAT contains tabulations of measured wall static pressures, skin friction distributions, and a single pitot-survey plane in these interactions. The wall static pressures were measured only on the centerlines of the symmetric interactions studied. Skin friction data, obtained by way of a laser-based technique (Ref. 17) were measured both on the centerline and on certain spanwise "cuts" at specific streamwise locations denoted by $z/\delta_0$ values cited in the data file. The flowfield pitot survey data were obtained in a single x-y plane located at $z/\delta_0 = 32.33$ in the Mach 4, 15x15 deg interaction. While the flowfield features in this plane are discussed in Refs. 15, 22, and 23, the procedure of these flowfield surveys has not yet been described elsewhere in print. Interested readers should consult Ref. 16 when it becomes available.

GARRISON.DAT

SURFACE PRESSURE, SKIN FRICTION AND PITOT SURVEY DATA
SYMMETRIC CROSSING-SHOCK/TRUBULENT BOUNDARY-LAYER
INTERACTIONS AT MACH 3 AND 4

NOMENCLATURE & DEFINITIONS

CF = SKIN FRICTION COEFFICIENT
d0 = INITIAL REFERENCE BOUNDARY LAYER THICKNESS AT L.E. LOCATION
(DEFINED AS 3.5mm FOR ALL CASES)
H = FIN HEIGHT (= 8.25 cm)
P0 = FREESTREAM STAGNATION PRESSURE
Pw = WALL STATIC PRESSURE
Pinf = FREESTREAM STATIC PRESSURE
pt2 = PITOT PRESSURE
Re = REYNOLDS NUMBER
T0 = FREESTREAM STAGNATION TEMPERATURE
Tw = WALL TEMPERATURE
Taw = ADIABATIC WALL TEMPERATURE
W = WIDTH BETWEEN FIN LEADING EDGES (= 9.4 cm)
X = SPANWISE COORDINATE ORIGINATING ON TUNNEL CENTERLINE
Y = VERTICAL COORDINATE ORIGINATING ON FLAT PLATE
Z = STREAMWISE COORDINATE ORIGINATING AT FIN LEADING
EDGE POSITION (21.3 cm DOWNSTREAM OF PLATE L.E.)

INCOMING AND FREESTREAM FLOW CONDITIONS

MACH 3
p0 = 750 kPa
Pinf = 20.4 kPa
T0 = 295 K
Re/m = 6.2E+07
Tw/Taw = 1.06 (roughly adiabatic)

MACH 4
p0 = 1500 kPa
Pinf = 99 kPa
T0 = 295 K
Re/m = 6.8E+07
Tw/Taw = 1.06 (roughly adiabatic)

INCOMING BOUNDARY LAYER PARAMETERS AT X=178 mm FROM FLAT-PLATE LEADING EDGE

Mach 3 (actual freestream Mach number was 2.91 for this survey)
Delta = 3.02 mm
Delta* = 0.895 mm
Theta = 0.184 mm
Re(theta) = 9751

Mach 4 (actual freestream Mach number was 3.88 for this survey)
Delta = 2.87 mm
Delta* = 0.950 mm
Theta = 0.128 mm
Re(theta) = 9082

CENTERLINE WALL PRESSURE DISTRIBUTIONS AT MACH 3

| z/d0 | 13x13deg pw/pinf | 11x11deg pw/pinf | 9x9 deg pw/pinf | 7x7 deg pw/pinf |
|---|---|---|---|---|
| 8.9989 | 0.98581 | 1.0117 | 0.98868 | 1.0094 |
| 13.353 | 1.0402 | 1.0466 | 1.0279 | 1.0421 |
| 14.079 | 1.1602 | 1.0538 | 1.0259 | 1.0492 |
| 15.349 | 1.8911 | 1.1163 | 1.0329 | 1.0494 |
| 16.619 | 2.3104 | 1.4548 | 1.1263 | 1.1021 |
| 17.889 | 2.5082 | 1.8144 | 1.2572 | 1.1076 |
| 19.703 | 2.7039 | 2.1856 | 1.5965 | 1.238 |
| 20.429 | 2.7521 | 2.2983 | 1.7418 | 1.3429 |
| 21.699 | 2.8214 | 2.4087 | 1.8828 | 1.4387 |
| 22.969 | 3.0462 | 2.5744 | 2.0228 | 1.5298 |
| 24.239 | 3.1559 | 2.6327 | 2.1465 | 1.6709 |
| 26.779 | 3.5511 | 2.8183 | 2.3665 | 1.8083 |
| 28.049 | 4.1086 | 2.9662 | 2.4964 | 1.8918 |
| 29.319 | 4.6118 | 3.0773 | 2.5828 | 1.9614 |
| 30.589 | 4.7936 | 3.1915 | 2.6621 | 2.0121 |
| 32.403 | 5.1768 | 3.3939 | 2.7606 | 2.1142 |
| 33.129 | 5.2627 | 3.5051 | 2.7924 | 2.1403 |
| 34.399 | 5.5767 | 3.6958 | 2.8237 | 2.176 |
| 35.669 | 5.8293 | 3.8576 | 2.8857 | 2.2187 |
| 36.395 | 5.8524 | 3.905 | 2.9237 | 2.2262 |
| 39.479 | 5.2015 | 4.5838 | 3.0998 | 2.3517 |
| 41.475 | 4.0826 | 5.0753 | 3.1133 | 2.3967 |
| 43.289 | 2.8807 | 4.7789 | 3.0065 | 2.4035 |
| 44.559 | 2.5063 | 4.2625 | 3.0881 | 2.4294 |
| 45.829 | 2.2481 | 4.0106 | 3.5857 | 2.5234 |
| 47.099 | 1.856 | 3.2963 | 3.367 | 2.5321 |
| 48.369 | 1.7024 | 3.0198 | 3.4325 | 2.5874 |
| 49.639 | 1.4198 | 2.554 | 3.0653 | 2.6657 |
| 50.909 | 1.2915 | 2.2812 | 2.8738 | 2.7229 |
| 52.179 | 1.1545 | 2.0177 | 2.5945 | 2.8016 |
| 53.449 | 0.86939 | 1.4938 | 1.9485 | 2.7956 |
| 54.719 | 0.91548 | 1.5216 | 2.0365 | 2.8324 |
| 55.989 | 1.0919 | 1.5773 | 1.9042 | 2.8415 |
| 57.259 | 0.67488 | 1.0862 | 1.463 | 2.5718 |
| 58.529 | 0.64068 | 1.0748 | 1.3134 | 2.4989 |

CENTERLINE WALL PRESSURE DISTRIBUTIONS AT MACH 4

| z/d0 | 15x15dg pw/pinf | 13x13dg pw/pinf | 11x11dg pw/pinf | 9x9 deg pw/pinf | 7x7 deg pw/pinf |
|---|---|---|---|---|---|
| 8.9989 | 1.0222 | 1.0521 | 1.0414 | 1.017 | 1.0348 |
| 10.269 | 0.9665 | 1.0342 | 1.0223 | 0.9968 | 1.0149 |
| 11.539 | 0.9395 | 1.032 | 1.0234 | 0.9901 | 1.0244 |
| 13.353 | 1.0421 | 1.0425 | 1.0286 | 1.0061 | 1.0147 |
| 14.079 | 1.294 | 1.0385 | 1.0213 | 0.9964 | 1.0076 |
| 15.349 | 2.1077 | 1.1262 | 1.0234 | 0.9862 | 1.0341 |
| 16.619 | 2.4778 | 1.6252 | 1.1204 | 1.0193 | 0.98821 |
| 17.889 | 2.6778 | 2.0441 | 1.3119 | 0.9908 | 1.0496 |
| 19.703 | 2.8588 | 2.4136 | 1.7294 | 1.1418 | 1.0794 |
| 20.429 | 2.9773 | 2.5618 | 1.9245 | 1.2605 | 1.0901 |
| 21.699 | 3.1775 | 2.6111 | 2.0294 | 1.3798 | 1.1642 |
| 22.969 | 3.7023 | 2.8273 | 2.2436 | 1.5371 | 1.2685 |
| 24.239 | 3.6624 | 2.8554 | 2.3429 | 1.6749 | 1.4579 |
| 26.779 | 4.9227 | 3.2875 | 2.5475 | 1.8806 | 1.5641 |
| 28.049 | 5.7257 | 3.7931 | 2.7016 | 2.0213 | 1.66 |
| 29.319 | 6.6439 | 4.2784 | 2.8324 | 2.1385 | 1.7643 |
| 30.589 | 7.1743 | 4.7166 | 3.0702 | 2.2943 | 1.9303 |
| 32.403 | 8.3968 | 5.5558 | 3.5395 | 2.4402 | 1.9557 |
| 33.129 | 8.6098 | 5.7968 | 3.7123 | 2.4759 | 2.0409 |
| 34.399 | 9.0073 | 6.2965 | 4.0336 | 2.5166 | 2.028 |
| 35.669 | 9.2383 | 6.7298 | 4.3787 | 2.607 | 2.0385 |
| 36.395 | 10.721 | 6.8432 | 4.5646 | 2.6698 | 2.2459 |
| 39.479 | 13.412 | 7.3227 | 5.2796 | 3.023 | 2.3496 |
| 40.749 | 8.6375 | 7.7677 | 5.6155 | 3.1161 | 2.4002 |
| 41.475 | 9.2485 | 13.345 | 5.2701 | 3.2661 | 2.4571 |
| 43.289 | 5.3859 | 11.602 | 5.4409 | 3.4952 | 2.6021 |
| 44.559 | 4.1633 | 9.4111 | 5.817 | 3.6986 | 2.6408 |
| 45.829 | 3.6298 | 6.8483 | 5.6632 | 3.9345 | 2.6414 |
| 47.099 | 2.7678 | 5.742 | 6.2548 | 3.9294 | 2.7945 |
| 48.369 | 2.5314 | 4.4132 | 5.519 | 4.064 | 2.8262 |

| | | | | | |
|---|---|---|---|---|---|
| 49.639 | 2.0387 | 3.815 | 4.8841 | 4.1929 | 2.9251 |
| 50.909 | 1.8894 | 3.1747 | 4.1704 | 4.2237 | 2.8757 |
| 52.179 | 1.6542 | 2.2633 | 3.0053 | 4.4283 | 2.9868 |
| 53.449 | 1.2176 | 2.3245 | 3.1682 | 3.8959 | 3.3574 |
| 54.719 | 1.3379 | 2.5095 | 3.0227 | 4.5734 | 2.9917 |
| 55.989 | 1.9329 | 1.645 | 2.2605 | 4.6809 | 3.1566 |
| 57.259 | 1.0041 | 1.4239 | 1.9605 | 4.5097 | |
| 58.529 | 1.0719 | | | 4.2253 | |

**********

SKIN FRICTION DISTRIBTIONS AT MACH 3

**********

CENTERLINE SKIN FRICTION DISTRIBUTIONS

**********

7X7 DEGREE INTERACTION

| z/δ0 | CF EE+03 | ERROR+03 |
|---|---|---|
| 11.611 | 1.41 | 0.141 |
| 15.24 | 1.436 | 0.1436 |
| 18.869 | 1.303 | 0.1303 |
| 22.497 | 1.196 | 0.1196 |
| 26.126 | 1.043 | 0.1043 |
| 29.754 | 0.937 | 0.0937 |
| 33.383 | 0.858 | 0.0858 |
| 37.011 | 0.762 | 0.0762 |
| 40.64 | 0.734 | 0.0734 |
| 44.269 | 0.713 | 0.0713 |

11x11 DEGREE INTERACTION

| z/δ0 | CF EE+03 | ERROR+03 |
|---|---|---|
| 7.9829 | 1.462 | 0.1462 |
| 11.611 | 1.407 | 0.1407 |
| 15.24 | 1.173 | 0.1173 |
| 18.869 | 0.594 | 0.0594 |
| 22.272 | 0.336 | 0.03452 |
| 26.126 | 0.135 | 0.135 |
| 29.754 | 0.13 | 0.13 |
| 33.383 | 0.631 | 0.0631 |
| 37.011 | 1.831 | 0.1831 |
| 40.64 | 1.883 | 0.1883 |

SPANWISE SKIN FRICTION DISTRIBUTIONS

**********

7X7 DEGREE INTERACTION @ Z/δ0=40.6

| X/δ0 | CF EE+03 | ERROR+03 |
|---|---|---|
| 0 | 0.734 | 0.0734 |
| 1.8143 | 1.227 | 0.1227 |
| 2.7214 | 1.733 | 0.1733 |
| 3.6286 | 2.35 | 0.235 |
| 5.4429 | 2.63 | 0.263 |
| 6.35 | 3.005 | 0.3005 |
| 7.2571 | 3.04 | 0.4 |
| 7.9393 | 2.34 | 0.234 |

11X11 DEGREE INTERACTION

| Z/δ0 = 29.8 | | | Z/δ0 = 37.0 | | |
|---|---|---|---|---|---|
| X/δ0 | CF EE+03 | ERROR+03 | X/δ0 | CF EE+03 | ERROR+03 |
| 0 | 0.13 | 0.03078 | 0 | 1.831 | 0.1831 |
| 0.9071 | 1.364 | 0.1364 | 1.8143 | 4.096 | 0.4096 |
| 2.7214 | 2.966 | 0.2966 | 3.6286 | 4.573 | 0.53478 |
| 4.5357 | 3.828 | 0.3828 | 5.4429 | 3.897 | 0.3897 |
| 5.4429 | 3.79 | 0.379 | | | |
| 6.4661 | 3.744 | 0.3744 | | | |

**********

SKIN FRICTION DISTRIBTIONS FOR MACH 4, 15x15 DEGREE INTERACTION

**********

CENTERLINE SKIN FRICTION DISTRIBUTION

**********

| z/δ0 | CF EE+03 | ERROR+03 |
|---|---|---|
| 12.417 | 1.099 | 0.1099 |
| 16.495 | 0.564 | 0.0564 |
| 18.564 | 0.304 | 0.05 |
| 23.753 | 0 | 0.1 |
| 25.567 | 1.022 | 0.183 |
| 27.381 | 1.918 | 0.1918 |
| 31.01 | 1.845 | 0.1845 |
| 34.638 | 1.877 | 0.1877 |
| 38.267 | 3.116 | 0.3116 |

SPANWISE SKIN FRICTION DISTRIBUTION

**********

Z/δ0 = 25.3

| X/δ0 | CF EE+03 | ERROR+03 |
|---|---|---|
| 0 | 1.022 | 0.1022 |
| 0.90714 | 0.582 | 0.06028 |
| 2.0973 | 2.368 | 0.2368 |
| 2.6053 | 1.053 | 0.1053 |
| 3.9697 | 2.905 | 0.2905 |
| 5.1598 | 4.049 | 0.4049 |
| 6.125 | 5.344 | 0.5344 |
| 6.5314 | 4.552 | 0.4552 |
| 7.2571 | 3.931 | 0.3931 |

**********

FLOWFIELD PITOT SURVEY DATA
MACH 4, 15x15 DEGREE INTERACTION
SPANWISE PLANE "L" LOCATED AT Z/δ0 = 32.33

**********

| X mm | Y mm | pt2/p0 |
|---|---|---|
| 15.270480 | 2.374900 | 2.388831E-01 |
| 15.262860 | 3.276600 | 2.325127E-01 |
| 15.260320 | 4.295140 | 2.599282E-01 |
| 15.252700 | 5.300980 | 2.548075E-01 |
| 15.252700 | 6.286500 | 2.372937E-01 |
| 15.245080 | 7.297420 | 2.744129E-01 |
| 15.247620 | 8.336280 | 2.922414E-01 |
| 15.240000 | 9.362440 | 2.909256E-01 |
| 15.247620 | 10.370820 | 2.919231E-01 |
| 15.252700 | 11.361420 | 2.777345E-01 |
| 15.245080 | 12.400280 | 2.742993E-01 |
| 15.245080 | 13.413740 | 2.915159E-01 |
| 15.245080 | 14.417040 | 2.960328E-01 |
| 15.242540 | 15.394960 | 2.921575E-01 |
| 15.245080 | 16.375380 | 2.882945E-01 |
| 15.247620 | 17.330420 | 2.891678E-01 |
| 15.245080 | 18.321020 | 2.746836E-01 |
| 15.250160 | 19.372580 | 2.869852E-01 |
| 15.247620 | 20.474940 | 3.033747E-01 |
| 15.255240 | 21.531580 | 2.963852E-01 |
| 15.247620 | 22.532340 | 3.063171E-01 |
| 15.252700 | 23.515320 | 3.039299E-01 |
| 15.247620 | 24.490680 | 3.075611E-01 |
| 15.247620 | 25.486360 | 2.924217E-01 |

NOTE: THE EXCERPT SHOWN HERE IS FOR SAMPLE PURPOSES ONLY. SPACE LIMITATIONS PRECLUDE A COMPLETE LISTING.

Ref.: 12-13
Author: Hsu and Settles
Geometry: 3-D Fin
Mach number: 3, 4
Data: flowfield density maps

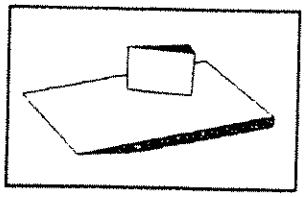

The experiments were carried out using a single sharp unswept fin mounted at angle-of-attack on a flat plate in the supersonic wind tunnel facility of the Penn State Gas Dynamics Laboratory. The flat-plate boundary-layers at Mach 3 and 4 are the same as those previously documented in Ref. 1 (KIM.DAT). These are equilibrium turbulent boundary-layers developing naturally on a flat plate at high Reynolds number, and are essentially adiabatic.

The swept, single-fin shock/boundary-layer interaction was studied by way of conical holographic interferometry, wherein the holographic test beam was focused at or near the virtual origin of the quasiconical swept interaction. The light rays then coincided with the rays of the interaction, rendering the interaction two-dimensional insofar as the quasiconical approximation is valid. Users of these data who are unfamiliar with this approach should first consult the cited references and Alvi and Settles, *AIAA Journal*, Vol. 30, Sept. 1992, pp. 2252-2258.

Holographic interferograms obtained as described above and in the cited references were reduced to provide flowfield density data, assuming that each interaction was a two-dimensional flow in the angular coordinates $\beta$ and $\phi$ defined in the diagram below. $\beta$ is the azimuthal coordinate measured from the freestream direction, and is positive in the direction illustrated. $\phi$ is the elevation coordinate measured from the plane of the flat plate, and is also positive in the direction illustrated. Both $\beta$ and $\phi$ have vertices at the virtual conical origin (VCO) of the interaction, which is located on the flat plate ahead of the fin leading edge, along a line extrapolated from the inviscid shock angle, $\beta_0$. The distance from the fin leading edge to the VCO for the three interactions studied here were: $48\pm6$ mm for the Mach 3, $\alpha = 10°$ case, $33\pm3$ mm for the Mach 3, $\alpha = 16°$ case, and $21\pm3$ mm for the Mach 4, $\alpha = 20°$ case.

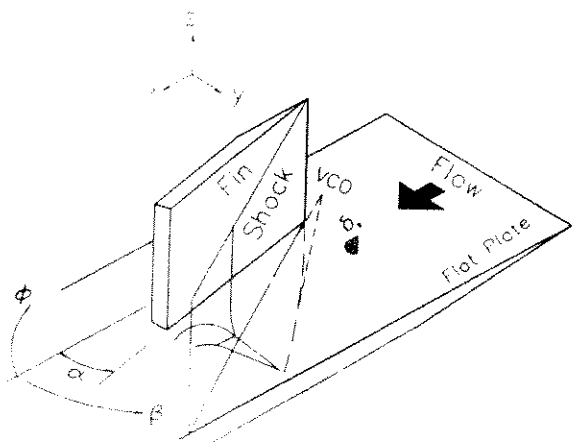


The data file HSU.DAT contains preliminary information and density data files for each of these 3 interactions. The extensive flowfield density data are given in columnar form, the number of $\beta$ columns ranging from 18 to 36 and the number of $\phi$ rows ranging from 58 to 100, depending on the overall angular extent of the interaction in question. At each flowfield location defined by a $\beta,\phi$ pair, the measured static density is given along with its normalization by the freestream static density.

Density data from conical holographic interferogram
of swept shock wave/turbulent B. L. interaction

Mach 3.0 Fin Angle 10.1 degrees

Penn State Gas Dynamics Laboratory, March 1991

**********

INCOMING BOUNDARY LAYER PARAMETERS AT X=178 mm FROM FLAT-PLATE LEADING EDGE

Mach 3 (actual freestream Mach number was 2.91 for this survey)
Delta = 3.02 mm
Delta* = 0.895 mm
Theta = 0.184 mm
Cf = 0.001520
Re(theta) = 9751

**********

Case: m3a10/m3a10a
Beta Column Count= 18
Phi Row Count= 58
Freestream Mach Number= 2.95
Angle of Attack= 10.1
Fin L.E. from flat plate L.E., X= 10.414 cm
Fin L.E. from side wall, Y= 3.333750 cm
Freestream stagnation Temperature.= 296.3000 K
Freestream stagnation Pressure= 0.6892000 MPa
Freestream Density Rhoinf = 0.6189000 Kg/m^3
Reynolds number 6.19E+07/m
Tw/Taw = 1.06 (roughly adiabatic)

**********

| Col.# | Beta | Phi | Rho | Rho/Rhoinf |
|---|---|---|---|---|
| 1 | 34.473 | 9.235 | 0.621 | 1.00 |
| 1 | 34.473 | 9.198 | 0.621 | 1.00 |
| 1 | 34.473 | 9.161 | 0.621 | 1.00 |
| 1 | 34.473 | 9.124 | 0.621 | 1.00 |
| 1 | 34.473 | 9.087 | 0.621 | 1.00 |
| 1 | 34.473 | 9.051 | 0.621 | 1.00 |
| 1 | 34.473 | 9.014 | 0.621 | 1.00 |
| 1 | 34.473 | 8.977 | 0.621 | 1.00 |
| 1 | 34.473 | 8.940 | 0.621 | 1.00 |
| 1 | 34.473 | 8.903 | 0.621 | 1.00 |
| 1 | 34.473 | 8.866 | 0.621 | 1.00 |
| 1 | 34.473 | 8.830 | 0.621 | 1.00 |
| 1 | 34.473 | 8.793 | 0.621 | 1.00 |
| 1 | 34.473 | 8.756 | 0.621 | 1.00 |
| 1 | 34.473 | 8.719 | 0.621 | 1.00 |
| 1 | 34.473 | 8.682 | 0.621 | 1.00 |
| 1 | 34.473 | 8.646 | 0.621 | 1.00 |
| 1 | 34.473 | 8.609 | 0.621 | 1.00 |
| 1 | 34.473 | 8.572 | 0.621 | 1.00 |
| 1 | 34.473 | 8.535 | 0.621 | 1.00 |
| 1 | 34.473 | 8.498 | 0.621 | 1.00 |
| 1 | 34.473 | 8.462 | 0.621 | 1.00 |
| 1 | 34.472 | 8.277 | 0.623 | 1.01 |
| 1 | 34.475 | 8.080 | 0.623 | 1.01 |

EXCERPT ONLY
SEE HSU.DAT



Density data from conical holographic interferogram
of swept shock wave/turbulent B. L. interaction

Mach 3.0 Angle 16.0 degrees

Penn State Gas Dynamics Laboratory, March 1991

**********

INCOMING BOUNDARY LAYER PARAMETERS AT X=178 mm FROM FLAT-PLATE LEADING EDGE

Mach 3 (actual freestream Mach number was 2.91 for this survey)
Delta = 3.02 mm
Delta* = 0.895 mm
Theta = 0.184 mm
Cf = 0.001520
Re(theta) = 9751

**********

Case: m3a16/m3a16
Beta Column Count= 24
Phi Row Count= 92
Freestream Mach Number= 2.950000
Angle of Attack= 16.00000
Fin L.E. from flat plate L.E., X= 11.68400 cm
Fin L.E. from side wall, Y= 2.698750 cm
Freestream stagnation Temperature.= 289.0000 K
Freestream stagnation Pressure= 0.7565000 MPa
Freestream Density Rhoinf = 0.6238000 Kg/m^3
Reynolds number 6.19E+07/m
Tw/Taw = 1.06 (roughly adiabatic)

**********

| Col.# | Beta | Phi | Rho | Rho/Rhoinf |
|---|---|---|---|---|
| 1 | 46.111 | 14.523 | 0.623 | 1.00 |
| 1 | 46.111 | 14.520 | 0.623 | 1.00 |
| 1 | 46.111 | 14.517 | 0.623 | 1.00 |
| 1 | 46.111 | 14.514 | 0.623 | 1.00 |
| 1 | 46.111 | 14.511 | 0.623 | 1.00 |
| 1 | 46.111 | 14.508 | 0.623 | 1.00 |
| 1 | 46.111 | 14.505 | 0.623 | 1.00 |
| 1 | 46.111 | 14.502 | 0.623 | 1.00 |
| 1 | 46.111 | 14.499 | 0.623 | 1.00 |
| 1 | 46.111 | 14.496 | 0.623 | 1.00 |
| 1 | 46.111 | 14.493 | 0.623 | 1.00 |
| 1 | 46.111 | 14.490 | 0.623 | 1.00 |
| 1 | 46.111 | 14.487 | 0.623 | 1.00 |
| 1 | 46.111 | 14.484 | 0.623 | 1.00 |
| 1 | 46.111 | 14.480 | 0.623 | 1.00 |
| 1 | 46.111 | 14.477 | 0.623 | 1.00 |
| 1 | 46.111 | 14.474 | 0.623 | 1.00 |
| 1 | 46.111 | 14.471 | 0.623 | 1.00 |
| 1 | 46.111 | 14.468 | 0.623 | 1.00 |
| 1 | 46.111 | 14.465 | 0.623 | 1.00 |
| 1 | 46.111 | 14.462 | 0.623 | 1.00 |
| 1 | 46.111 | 14.459 | 0.623 | 1.00 |
| 1 | 46.111 | 14.456 | 0.623 | 1.00 |
| 1 | 46.111 | 14.453 | 0.623 | 1.00 |
| 1 | 46.111 | 14.450 | 0.623 | 1.00 |

EXCERPT ONLY
SEE HSU.DAT

Density data from conical holographic interferogram
of swept shock wave/turbulent B. L. interaction

Mach 4 Angle 20 degrees

Penn State Gas Dynamics Laboratory, March 1991

**********

INCOMING BOUNDARY LAYER PARAMETERS AT X=178 mm FROM FLAT-PLATE LEADING EDGE

Mach 4 (actual freestream Mach number was 3.88 for this survey)
Delta = 2.87 mm
Delta* = 0.950 mm
Theta = 0.128 mm
Cf = 0.001325
Re(theta) = 9082

**********

Case: m4a20/m4a20
Beta Column Count= 36
Phi Row Count= 100
Freestream Mach Number= 3.930000
Angle of Attack= 20.00000
Fin L.E. from flat plate L.E., X= 10.00125 cm
Fin L.E. from side wall, Y= 2.460625 cm
VCO from fin leading edge= 17 mm (along the inviscid shock)
Freestream stagnation Temperature.= 294.8000 K
Freestream stagnation Pressure= 1.385840 MPa
Freestream Density Rhoinf = 0.4841200 Kg/M^3
Reynolds number 6.79E+07/m
Tw/Taw = 1.06 (roughly adiabatic)

**********

| Col.# | Beta | Phi | Rho | Rho/Rhoinf |
|---|---|---|---|---|
| 1 | 49.284 | 13.244 | 0.485 | 1.00 |
| 1 | 49.284 | 13.238 | 0.485 | 1.00 |
| 1 | 49.284 | 13.233 | 0.485 | 1.00 |
| 1 | 49.284 | 13.227 | 0.485 | 1.00 |
| 1 | 49.284 | 13.222 | 0.485 | 1.00 |
| 1 | 49.284 | 13.216 | 0.485 | 1.00 |
| 1 | 49.284 | 13.211 | 0.485 | 1.00 |
| 1 | 49.284 | 13.205 | 0.485 | 1.00 |
| 1 | 49.284 | 13.200 | 0.485 | 1.00 |
| 1 | 49.284 | 13.195 | 0.485 | 1.00 |
| 1 | 49.284 | 13.189 | 0.485 | 1.00 |
| 1 | 49.284 | 13.184 | 0.485 | 1.00 |
| 1 | 49.284 | 13.178 | 0.485 | 1.00 |
| 1 | 49.284 | 13.173 | 0.485 | 1.00 |
| 1 | 49.284 | 13.167 | 0.485 | 1.00 |
| 1 | 49.284 | 13.162 | 0.485 | 1.00 |
| 1 | 49.284 | 13.156 | 0.485 | 1.00 |
| 1 | 49.284 | 13.151 | 0.485 | 1.00 |
| 1 | 49.284 | 13.145 | 0.485 | 1.00 |
| 1 | 49.284 | 13.140 | 0.485 | 1.00 |
| 1 | 49.284 | 13.134 | 0.485 | 1.00 |
| 1 | 49.284 | 13.129 | 0.485 | 1.00 |
| 1 | 49.284 | 13.124 | 0.485 | 1.00 |

EXCERPT ONLY
SEE HSU.DAT

Author: Kuntz, D. W., *et al*
Geometry: 2-D Compression Corner
Mach Number: 3
Data: $p_{wall}$, mean & fluctuating flowfield surveys (two channel Laser Doppler Velocimetry)

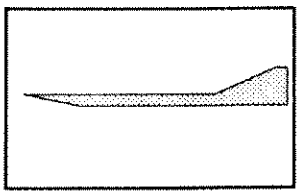

Kuntz, D. W., Amatucci, V. A., and Addy, A. L., "An Experimental Study of the Shock Wave-Turbulent Boundary Layer Interaction," Presented at the Winter Annual Meeting of the American Society of Mechanical Engineers, Miami Beach, Florida, November 17-22, 1985, and published in the International Symposium on Laser Anemometry, FED-Vol. 33, ed. A. Dybbs and P. A. Pfund, pp. 173-178.

Kuntz, D. W., Amatucci, V. A., and Addy, A. L., "Turbulent Boundary-Layer Properties Downstream of the Shock-Wave/Boundary-Layer Interaction," *AIAA Journal*, Vol. 25, No. 5, pp. 668-675, May, 1987.

Kuntz, D. W., "An Experimental Investigation of the Shock Wave-Turbulent Boundary Layer Interaction," Ph.D. Thesis, Dept. of Mechanical and Industrial Engineering, Univ. of Illinois at Urbana-Champaign, Urbana, Illinois, 1985.

Experiments were conducted in a supersonic wind tunnel with a 10.2 x 10.2 cm test section. The models were two-dimensional compression corners which spanned the test section. Experiments were conducted with corner angles of 8, 12, 16, 20, and $24^{o}$.

The freestream Mach number, determined from surface pressure measurements, was approximately 2.94, and the stagnation pressure was maintained at approximately 483 kPa (70 psia) for all data points.

The primary measurement tool used in this investigation was a two-color laser Doppler velocimeter system. This system was used to obtain two-component mean velocity and turbulent property measurements in both the upstream and redeveloping downstream boundary layers within the flowfields. In addition to the LDV measurements, surface static pressure measurements, surface streak pattern measurements, and high-speed Schlieren photographs were also taken.

Measurements made in the wind tunnel in the absence of the compression corner models indicated that the undisturbed turbulent boundary layer had a thickness of 8.27 mm ($u_e = 0.99\ u_\infty$), a displacement thickness of 3.11 mm and a momentum thickness of 0.57 mm.

The tabular data includes the surface static pressure distribution, the LDV data from a single traverse made upstream of the interaction, and the LDV data from the traverses made downstream of the interaction. Each traverse made downstream of the interaction includes data taken at a single point above the shock wave. The coordinate systems used are presented in the accompanying figure, and the definitions of the quantities listed are included in the accompanying table. The reader is referred to the AIAA Journal article cited above for a detailed discussion of the corrections applied to the LDV data, the errors associated with the LDV data, and estimates of the measurement accuracies.

Definitions of the Tabular LDV Data

| Variable Name | Description | Units | Definition | Note |
|---|---|---|---|---|
| x | Longitudinal Position | mm | See Figure | |
| y | Vertical Position | mm | See Figure | |
| Vt | Total Velocity | m/s | $\sqrt{(V0)^2 + (V1)^2}$ | 1 |
| theta | Flow Angle | deg | See Figure | |
| V0 | Average Velocity, Ch 0 | m/s | See Figure | |
| V1 | Average Velocity, Ch 1 | m/s | See Figure | |
| var0 | Variance, Ch 0 | $m^2/s^2$ | $\frac{\sum_n (v0 - V0)^2}{n-1}$ | 2 |
| var1 | Variance, Ch 1 | $m^2/s^2$ | $\frac{\sum_n (v1 - V1)^2}{n-1}$ | |
| s01 | Reynolds Stress Term | $m^2/s^2$ | $\overline{(v0 - V0)\,(v1 - V1)}$ | 3 |
| s001 | Triple Product | $m^3/s^3$ | $\overline{(v0 - V0)^2 (v1 - V1)}$ | |
| s110 | Triple Product | $m^3/s^3$ | $\overline{(v0 - V0)\,(v1 - V1)^2}$ | |
| s000 | Triple Product | $m^3/s^3$ | $\overline{(v0 - V0)^3}$ | |
| s111 | Triple Product | $m^3/s^3$ | $\overline{(v1 - V1)^3}$ | |
| sk0 | Skewness, Ch 0 | - | $(s000) / (\sqrt{var0})^3$ | |

| Variable Name | Description | Units | Definition | Note |
|---|---|---|---|---|
| sk1 | Skewness, Ch 1 | - | $(s111)/(\sqrt{var1})^3$ | |
| ku0 | Flatness, Ch 0 | - | $\left[(s0000)/(\sqrt{var0})^4\right]-3.0$ | 4 |
| ku1 | Flatness, Ch 1 | - | $\left[(s1111)/(\sqrt{var1})^4\right]-3.0$ | |

Notes:

1 V denotes average velocity, v denotes instantaneous velocity. Upstream of the compression corner, Channel 0 is parallel to the tunnel floor and Channel 1 is perpendicular to the tunnel floor. Downstream of the compression corner, Channel 0 is parallel to the ramp surface, and Channel 1 is perpendicular to the ramp surface.

2 The variance is the square of the standard deviation. The turbulence intensity would be found by taking the square root of the variance and dividing by the appropriate reference quantity (such as a reference velocity or a local velocity).

3 The overbar denotes a simple average of the instantaneous measurements.

4 The quantity s0000 was calculated in a similar manner as s000.

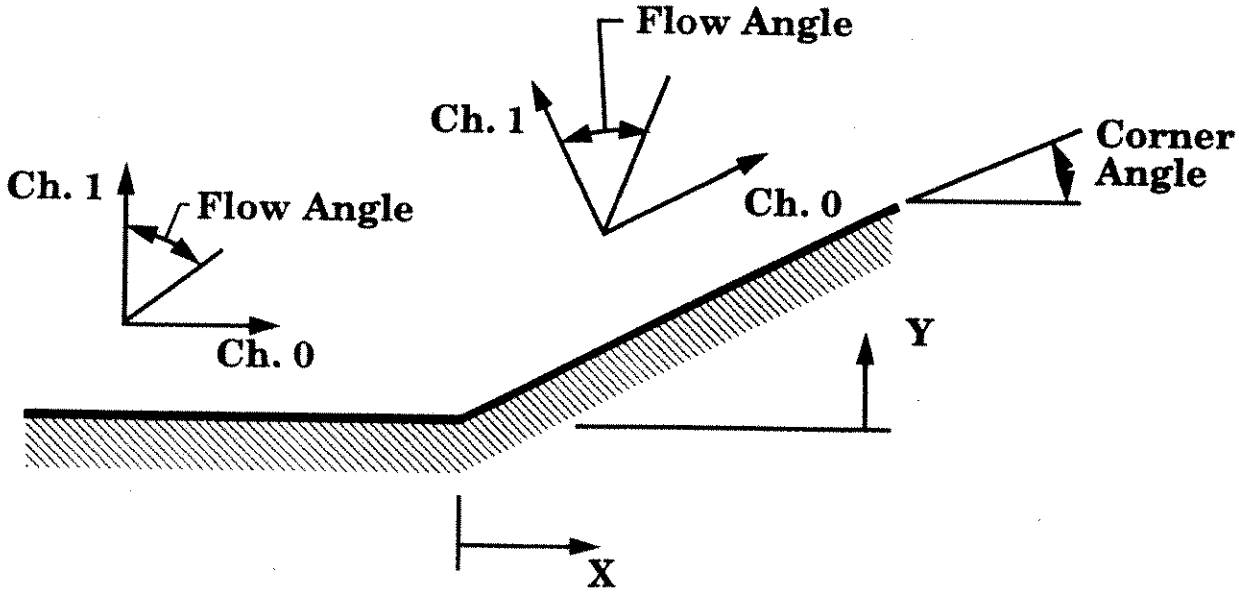


Coordinate System

**********

Kuntz et al 2-D Compression Corner Data

**********

20. Degree Compression Corner

**********

M-inf = 2.94
p0 = 483 kPa
t0 = 30 deg C
delta-0 = 8.27 mm

Separation Location = -1.63*delta-0
Reattachment Location = 0.52*delta-0 (measured parallel to the ramp surface)

Mean Surface Static Pressure Distribution

| x (mm) | p/p-inf |
|---|---|
| -71.12 | 1.000 |
| -66.04 | 0.992 |
| -60.96 | 0.986 |
| -55.88 | 0.996 |
| -50.80 | 0.996 |
| -48.26 | 0.998 |
| -45.72 | 0.995 |
| -43.18 | 0.992 |
| -40.64 | 0.999 |
| -38.10 | 1.008 |
| -35.56 | 0.999 |
| -33.02 | 1.009 |
| -30.48 | 0.994 |
| -27.94 | 1.007 |
| -25.40 | 0.991 |
| -22.86 | 0.992 |
| -20.32 | 1.000 |
| -17.78 | 1.042 |
| -15.24 | 1.168 |
| -12.70 | 1.529 |
| -10.16 | 1.677 |
| -7.62 | 1.817 |
| -5.08 | 1.899 |
| -2.54 | 1.970 |
| 0.36 | 2.060 |
| 2.39 | 2.192 |
| 4.77 | 2.356 |
| 7.16 | 2.562 |
| 9.55 | 2.692 |
| 11.93 | 2.792 |
| 14.32 | 2.951 |
| 16.71 | 2.995 |
| 19.09 | 3.096 |
| 21.48 | 3.185 |
| 23.87 | 3.225 |
| 26.26 | 3.277 |
| 28.64 | 3.352 |
| 31.03 | 3.392 |
| 33.42 | 3.437 |
| 35.80 | 3.468 |
| 38.19 | 3.496 |
| 40.58 | 3.487 |
| 42.96 | 3.480 |

NOTE: DUE TO SPACE LIMITATIONS, ONLY THE 20° DATA ARE TABULATED HERE. SEE DISKETTE FILE KUNTZ.DAT FOR COMPLETE TABULATIONS FOR ALL FIVE COMPRESSION CORNERS.

Laser Doppler Velocimeter Data

Basic data, x = -20.0 mm.

| y | Vt | theta | V0 | V1 | var0 | var1 | s01 |
|---|---|---|---|---|---|---|---|
| 15.00 | 629.83 | 90.02 | 629.83 | -0.24 | 123.974 | 67.884 | -22.16 |
| 14.00 | 631.15 | 89.97 | 631.15 | 0.31 | 82.210 | 74.888 | 1.03 |
| 13.00 | 631.04 | 90.01 | 631.04 | -0.06 | 83.261 | 66.507 | -10.52 |
| 12.00 | 631.18 | 89.97 | 631.18 | 0.28 | 82.380 | 63.546 | -6.84 |
| 11.00 | 630.37 | 89.98 | 630.37 | 0.25 | 91.020 | 64.016 | -3.13 |
| 10.00 | 628.97 | 89.97 | 628.97 | 0.38 | 144.848 | 64.641 | -14.42 |
| 9.50 | 628.92 | 90.02 | 628.92 | -0.18 | 139.109 | 93.333 | 11.20 |
| 9.00 | 625.96 | 90.05 | 625.96 | -0.54 | 179.863 | 89.770 | 10.54 |
| 8.50 | 624.47 | 90.02 | 624.47 | -0.23 | 224.517 | 94.184 | -0.82 |
| 8.00 | 623.16 | 90.05 | 623.16 | -0.55 | 268.612 | 109.647 | -12.23 |
| 7.50 | 621.40 | 89.94 | 621.40 | 0.65 | 279.304 | 128.847 | -31.07 |
| 7.00 | 616.24 | 89.99 | 616.24 | 0.14 | 330.528 | 130.878 | -18.25 |
| 6.50 | 609.41 | 89.90 | 609.40 | 1.02 | 501.894 | 148.948 | -102.43 |
| 6.00 | 601.19 | 90.03 | 601.19 | -0.27 | 592.226 | 181.281 | -67.81 |
| 5.50 | 588.01 | 89.96 | 588.01 | 0.39 | 798.860 | 191.253 | -120.55 |
| 5.00 | 580.70 | 90.00 | 580.70 | 0.04 | 931.395 | 195.745 | -163.73 |
| 4.50 | 569.92 | 90.08 | 569.92 | -0.80 | 945.322 | 235.213 | -159.33 |
| 4.00 | 555.81 | 90.12 | 555.81 | -1.20 | 1274.509 | 236.399 | -211.54 |
| 3.50 | 544.79 | 90.25 | 544.78 | -2.38 | 1255.189 | 245.164 | -219.28 |
| 3.00 | 528.84 | 90.21 | 528.84 | -1.94 | 1530.370 | 278.494 | -270.16 |
| 2.50 | 510.50 | 90.21 | 510.50 | -1.86 | 1616.059 | 239.195 | -228.87 |
| 2.25 | 502.73 | 90.28 | 502.73 | -2.46 | 1738.444 | 252.180 | -283.66 |
| 2.00 | 490.31 | 90.28 | 490.30 | -2.41 | 1962.803 | 235.178 | -324.92 |
| 1.75 | 482.27 | 90.39 | 482.26 | -3.29 | 1865.482 | 237.170 | -291.96 |
| 1.50 | 468.59 | 90.35 | 468.59 | -2.83 | 1853.864 | 225.861 | -283.13 |

Higher order moment data, x = -20.0 mm.

| y | s001 | s110 | s000 | s111 | sk0 | sk1 | ku0 | ku1 |
|---|---|---|---|---|---|---|---|---|
| 15.00 | 2.0235E+02 | -9.3537E+01 | -2.2967E+03 | 6.8859E+01 | -1.6639E+00 | 1.2311E-01 | 5.4483E+00 | 4.2745E-01 |
| 14.00 | -5.0543E+02 | -3.6605E+02 | -1.0831E+03 | -2.9269E+02 | -1.4531E+00 | -4.5163E-01 | 8.0608E+00 | 2.1114E+00 |
| 13.00 | 1.5715E+02 | -4.0176E+01 | -1.1367E+03 | 7.3030E+01 | -1.4961E+00 | 1.3465E-01 | 8.9324E+00 | 2.7036E-01 |
| 12.00 | 2.3253E+01 | 3.8892E+01 | -7.4730E+02 | 4.5761E+01 | -9.9945E-01 | 9.0336E-02 | 5.9122E+00 | 3.4205E-01 |
| 11.00 | -2.3082E+02 | -2.2224E+01 | -1.6080E+03 | -3.4294E+01 | -1.8517E+00 | -6.6954E-02 | 9.2173E+00 | 4.2448E-01 |
| 10.00 | 1.7118E+02 | -2.1015E+01 | -3.3750E+03 | -1.6216E+01 | -1.9360E+00 | -3.1202E-02 | 7.7342E+00 | 1.9883E-01 |
| 9.50 | -1.2724E+03 | -1.6979E+03 | -3.2023E+03 | -1.4625E+03 | -1.9518E+00 | -1.6220E+00 | 7.4695E+00 | 1.2167E+01 |
| 9.00 | -9.8147E+02 | -9.4948E+02 | -4.4037E+03 | -8.4440E+02 | -1.8256E+00 | -9.9278E-01 | 5.6903E+00 | 6.4585E+00 |
| 8.50 | -8.2099E+02 | -1.1794E+03 | -6.3828E+03 | -6.7499E+02 | -1.8973E+00 | -7.3847E-01 | 5.6451E+00 | 5.6307E+00 |
| 8.00 | -6.2678E+02 | -1.7881E+03 | -5.4699E+03 | -6.2733E+02 | -1.2425E+00 | -5.4639E-01 | 2.0279E+00 | 7.0365E+00 |
| 7.50 | -6.0594E+02 | -2.3652E+03 | -6.9227E+03 | -1.5742E+03 | -1.4831E+00 | -1.0764E+00 | 3.3418E+00 | 7.2633E+00 |
| 7.00 | -1.5415E+03 | -2.5645E+03 | -7.9463E+03 | -1.1649E+03 | -1.3224E+00 | -7.7804E-01 | 2.9939E+00 | 5.5822E+00 |
| 6.50 | 1.6567E+03 | -2.2157E+03 | -1.2144E+04 | -4.1840E+02 | -1.0800E+00 | -2.3016E-01 | 1.3151E+00 | 3.9066E+00 |

| | | | | | | | | |
|---|---|---|---|---|---|---|---|---|
| 6.00 | -7.5540E+01 | -3.6699E+03 | -1.1941E+04 | -2.6558E+03 | -8.2853E-01 | -1.0881E+00 | 5.5174E-01 | 7.2079E+00 |
| 5.50 | 1.5719E+03 | -3.3634E+03 | -1.6858E+04 | -7.7005E+02 | -7.4663E-01 | -2.9114E-01 | 5.9426E-01 | 2.8110E+00 |
| 5.00 | 1.7549E+03 | -2.5210E+03 | -1.5825E+04 | -1.6705E+02 | -5.5672E-01 | -6.0995E-02 | 9.4438E-03 | 2.1575E+00 |
| 4.50 | 6.9012E+02 | -3.8577E+03 | -1.5033E+04 | -9.2446E+02 | -5.1723E-01 | -2.5627E-01 | 3.4463E-01 | 2.5078E+00 |
| 4.00 | -6.0964E+02 | -2.1747E+03 | -1.8942E+04 | 4.4923E+02 | -4.1631E-01 | 1.2359E-01 | 1.1514E-01 | 1.3522E+00 |
| 3.50 | 1.0611E+03 | -2.0295E+03 | -1.6478E+04 | 3.8577E+02 | -3.7056E-01 | 1.0049E-01 | 6.4845E-02 | 1.0624E+00 |
| 3.00 | 1.1746E+03 | -2.0313E+03 | -1.3114E+04 | -6.7744E+00 | -2.1905E-01 | -1.4576E-03 | -2.6129E-01 | 2.1297E+00 |
| 2.50 | 8.3028E+02 | -5.5184E+01 | -7.5547E+03 | 9.3189E+00 | -1.1629E-01 | 2.5191E-03 | -1.5630E-01 | 1.0117E+00 |
| 2.25 | 1.6478E+03 | -5.1679E+02 | -1.3447E+04 | -6.5488E+02 | -1.8552E-01 | -1.6353E-01 | -2.4052E-01 | 1.3350E+00 |
| 2.00 | 2.3778E+03 | -5.0284E+02 | -1.1720E+04 | 1.4881E+02 | -1.3477E-01 | 4.1262E-02 | -2.9848E-01 | 3.8375E-01 |
| 1.75 | 1.6490E+03 | -1.0535E+03 | 1.9196E+03 | -2.3046E+02 | 2.3825E-02 | -6.3098E-02 | -2.1967E-01 | 1.1392E+00 |
| 1.50 | 2.3348E+03 | -1.3341E+03 | -9.4191E+03 | 1.1719E+03 | -1.1800E-01 | 3.4524E-01 | -1.9256E-01 | 3.1097E+00 |

Basic data, x = 15.0 mm.

| y | Vt | theta | V0 | V1 | var0 | var1 | s01 |
|---|---|---|---|---|---|---|---|
| 25.00 | 626.64 | 110.04 | 588.69 | -214.76 | 89.488 | 83.653 | -40.67 |
| 15.00 | 590.13 | 103.08 | 574.82 | -133.58 | 138.698 | 1179.915 | -41.62 |
| 14.50 | 584.99 | 101.68 | 572.88 | -118.42 | 143.080 | 1220.481 | -85.82 |
| 14.00 | 579.89 | 100.38 | 570.40 | -104.46 | 346.483 | 1524.398 | -351.28 |
| 13.50 | 573.35 | 99.45 | 565.56 | -94.17 | 702.691 | 1821.974 | -637.51 |
| 13.00 | 562.01 | 98.48 | 555.86 | -82.87 | 1556.716 | 2070.953 | -1091.02 |
| 12.50 | 534.57 | 97.12 | 530.45 | -66.26 | 4221.431 | 2317.852 | -2184.88 |
| 12.00 | 523.41 | 97.25 | 519.22 | -66.07 | 5794.362 | 2657.328 | -2846.59 |
| 11.50 | 457.37 | 94.88 | 455.72 | -38.88 | 9134.602 | 2521.922 | -3574.67 |
| 11.00 | 419.16 | 93.62 | 418.32 | -26.43 | 10370.281 | 2475.441 | -3922.39 |
| 10.50 | 389.49 | 93.14 | 388.91 | -21.33 | 11522.217 | 2797.428 | -4310.29 |
| 10.00 | 364.97 | 93.54 | 364.28 | -22.54 | 12994.065 | 2594.220 | -4163.35 |
| 9.50 | 354.50 | 94.25 | 353.52 | -26.30 | 11880.019 | 2700.931 | -4253.63 |
| 9.00 | 331.57 | 94.79 | 330.41 | -27.71 | 12764.326 | 2801.589 | -4324.87 |
| 8.50 | 291.62 | 93.95 | 290.93 | -20.10 | 14428.071 | 3244.977 | -4959.70 |
| 8.00 | 231.80 | 93.48 | 231.37 | -14.05 | 11345.315 | 2985.999 | -4142.82 |
| 7.75 | 217.11 | 93.14 | 216.79 | -11.87 | 10872.860 | 3098.062 | -4195.36 |
| 7.50 | 207.76 | 92.54 | 207.55 | -9.22 | 10031.171 | 2955.841 | -3868.81 |
| 7.25 | 201.24 | 92.78 | 201.01 | -9.76 | 9021.621 | 2923.591 | -3668.41 |
| 7.00 | 179.28 | 91.23 | 179.24 | -3.86 | 7698.342 | 2660.897 | -3053.32 |

Higher order moment data, x = 15.0 mm.

| y | s001 | s110 | s000 | s111 | sk0 | sk1 | ku0 | ku1 |
|---|---|---|---|---|---|---|---|---|
| 25.00 | 3.8656E+02 | -2.3489E+02 | -7.6392E+02 | 1.4088E+02 | -9.0240E-01 | 1.8413E-01 | 2.9275E+00 | 1.1219E-01 |
| 15.00 | -2.6332E+02 | -5.4143E+03 | -2.3439E+03 | -1.3941E+04 | -1.4349E+00 | -3.4398E-01 | 7.8909E+00 | 1.5692E-01 |
| 14.50 | -5.3550E+02 | -3.5512E+03 | -1.9059E+03 | -1.7902E+04 | -1.1136E+00 | -4.1986E-01 | 4.1317E+00 | 2.5554E-01 |
| 14.00 | 2.9727E+04 | -2.7298E+04 | -3.3843E+04 | -5.9964E+03 | -5.2474E+00 | -1.0075E-01 | 4.7258E+01 | 1.7821E+00 |
| 13.50 | 7.0572E+04 | -5.4221E+04 | -9.3617E+04 | 1.1285E+04 | -5.0258E+00 | 1.4510E-01 | 3.5415E+01 | 1.8272E+00 |
| 13.00 | 1.1299E+05 | -6.2639E+04 | -2.0633E+05 | 6.5404E+02 | -3.3593E+00 | 6.9399E-03 | 1.4209E+01 | 9.2126E-01 |
| 12.50 | 2.3912E+05 | -9.7709E+04 | -6.1925E+05 | 5.4779E+03 | -2.2577E+00 | 4.9089E-02 | 5.4012E+00 | 7.8636E-01 |
| 12.00 | 3.6922E+05 | -1.3696E+05 | -9.8090E+05 | 8.2362E+03 | -2.2239E+00 | 6.0125E-02 | 5.4016E+00 | 8.2041E-01 |
| 11.50 | 2.2738E+05 | -7.2436E+04 | -8.1353E+05 | 6.2758E+03 | -9.3183E-01 | 4.9553E-02 | 3.0818E-01 | 9.2357E-01 |
| 11.00 | 2.1316E+05 | -9.3639E+04 | -8.0677E+05 | 5.4406E+04 | -7.6395E-01 | 4.4174E-01 | 2.4558E-01 | 5.4881E-01 |
| 10.50 | 2.0007E+05 | -9.9943E+04 | -7.9622E+05 | 7.0847E+04 | -6.4377E-01 | 4.7883E-01 | -3.8348E-02 | 5.2800E-01 |
| 10.00 | 1.5987E+05 | -7.4827E+04 | -1.0101E+06 | 6.2538E+04 | -6.8196E-01 | 4.7330E-01 | 1.8900E-01 | 4.3730E-01 |
| 9.50 | 1.6260E+05 | -8.1249E+04 | -6.2072E+05 | 5.7436E+04 | -4.7937E-01 | 4.0918E-01 | -3.0599E-01 | 3.7710E-01 |
| 9.00 | 1.5333E+05 | -8.8085E+04 | -6.9643E+05 | 7.3656E+04 | -4.8292E-01 | 4.9671E-01 | -3.0711E-01 | 4.5722E-01 |
| 8.50 | 3.7100E+04 | -4.4120E+04 | -3.7368E+05 | 5.6335E+04 | -2.1562E-01 | 3.0476E-01 | -6.8503E-01 | 2.5830E-02 |
| 8.00 | -1.2782E+05 | 2.4610E+04 | 3.8752E+05 | 1.4066E+04 | 3.2068E-01 | 8.6208E-02 | -4.7752E-01 | -1.7768E-01 |
| 7.75 | -1.8393E+05 | 5.8723E+04 | 4.6173E+05 | -4.9383E+03 | 4.0726E-01 | -2.8638E-02 | -3.3945E-01 | -1.9150E-01 |
| 7.50 | -1.9670E+05 | 6.7295E+04 | 4.4413E+05 | -8.5046E+03 | 4.4206E-01 | -5.2922E-02 | -2.1879E-01 | -2.7334E-01 |
| 7.25 | -1.9442E+05 | 7.3813E+04 | 4.9625E+05 | -1.7954E+04 | 5.7912E-01 | -1.1357E-01 | -5.5344E-02 | -2.9367E-01 |
| 7.00 | -1.6831E+05 | 7.2865E+04 | 3.8035E+05 | -2.4550E+04 | 5.6311E-01 | -1.7886E-01 | 1.2360E-01 | -2.1235E-01 |

Basic data, x = 20.0 mm.

| y | Vt | theta | V0 | V1 | var0 | var1 | s01 |
|---|---|---|---|---|---|---|---|
| 30.00 | 625.05 | 110.03 | 587.25 | -214.08 | 136.945 | 126.725 | -77.50 |
| 17.50 | 582.26 | 100.97 | 571.61 | -110.81 | 119.179 | 1047.679 | -84.41 |
| 17.00 | 579.03 | 99.93 | 570.36 | -99.82 | 118.294 | 1259.272 | -135.87 |
| 16.50 | 576.45 | 99.82 | 568.01 | -98.29 | 189.085 | 1855.030 | -130.32 |
| 16.00 | 571.51 | 97.78 | 566.25 | -77.36 | 159.283 | 1544.215 | -190.19 |
| 15.50 | 566.68 | 97.12 | 562.32 | -70.22 | 558.570 | 1451.326 | -432.08 |
| 15.00 | 560.39 | 97.06 | 556.14 | -68.84 | 979.371 | 1923.282 | -775.45 |
| 14.50 | 546.04 | 96.17 | 542.88 | -58.68 | 2660.936 | 2009.862 | -1433.50 |
| 14.00 | 526.37 | 95.67 | 523.79 | -52.03 | 5104.213 | 2545.022 | -2422.73 |
| 13.50 | 516.33 | 95.35 | 514.08 | -48.15 | 4362.667 | 1901.045 | -1910.74 |
| 12.50 | 440.56 | 93.86 | 439.56 | -29.67 | 9047.953 | 1922.597 | -2681.29 |
| 12.00 | 410.01 | 94.06 | 408.99 | -29.00 | 10749.297 | 2177.956 | -3260.18 |
| 11.50 | 393.82 | 94.34 | 392.69 | -29.80 | 9239.213 | 2076.666 | -2929.18 |
| 11.00 | 378.32 | 94.12 | 377.34 | -27.20 | 8944.463 | 2288.416 | -3042.51 |
| 10.50 | 335.24 | 93.23 | 334.71 | -18.90 | 11318.126 | 2961.173 | -4106.47 |
| 10.00 | 308.70 | 92.79 | 308.34 | -15.04 | 11402.291 | 3121.934 | -4045.75 |
| 9.75 | 263.09 | 92.83 | 262.77 | -13.00 | 10810.626 | 3038.149 | -3913.95 |
| 9.50 | 244.09 | 91.86 | 243.96 | -7.92 | 10332.898 | 2927.825 | -3753.18 |
| 9.25 | 238.82 | 91.89 | 238.69 | -7.87 | 9913.989 | 3076.881 | -3762.51 |
| 9.00 | 222.19 | 91.21 | 222.14 | -4.71 | 8949.622 | 2750.721 | -3424.42 |
| 8.75 | 209.10 | 90.03 | 209.10 | -0.12 | 7419.993 | 2305.558 | -2680.20 |

Higher order moment data, x = 20.0 mm.

| y | s001 | s110 | s000 | s111 | sk0 | sk1 | ku0 | ku1 |
|---|---|---|---|---|---|---|---|---|
| 30.00 | 1.9534E+03 | -1.8259E+03 | -2.5761E+03 | 1.7093E+03 | -1.6074E+00 | 1.1982E+00 | 6.0317E+00 | 5.5374E+00 |
| 17.50 | -9.8253E+02 | -7.9655E+02 | -1.5069E+03 | -3.1088E+04 | -1.1582E+00 | -9.1674E-01 | 4.8702E+00 | 9.2906E-01 |
| 17.00 | -7.4653E+02 | 4.9095E+02 | 3.5741E+01 | -4.4977E+04 | 2.7779E-02 | -1.0065E+00 | 2.8440E+00 | 1.2101E+00 |
| 16.50 | -4.3219E+02 | -2.2999E+03 | -2.6020E+03 | -7.1754E+04 | -1.0007E+00 | -8.9809E-01 | 5.3332E+00 | 4.5549E-01 |
| 16.00 | 2.1981E+03 | -2.5348E+03 | -2.0406E+03 | -6.7117E+04 | -1.0151E+00 | -1.1060E+00 | 2.8211E+00 | 2.2282E+00 |
| 15.50 | 3.8359E+04 | -2.8690E+04 | -5.7306E+04 | -2.7934E+04 | -4.3409E+00 | -5.0522E-01 | 2.9728E+01 | 3.0239E+00 |
| 15.00 | 8.0443E+04 | -4.6852E+04 | -1.2359E+05 | -4.1117E+04 | -4.0325E+00 | -4.8748E-01 | 2.1020E+01 | 2.2281E+00 |
| 14.50 | 1.7635E+05 | -7.4881E+04 | -3.9775E+05 | -2.6500E+04 | -2.8978E+00 | -2.9410E-01 | 9.0649E+00 | 1.8928E+00 |
| 14.00 | 3.4152E+05 | -1.5396E+05 | -8.9468E+05 | 7.3953E+03 | -2.4534E+00 | 5.7599E-02 | 6.3587E+00 | 1.9725E+00 |
| 13.50 | 1.6840E+05 | -5.7302E+04 | -4.8785E+05 | -1.2573E+04 | -1.6930E+00 | -1.5169E-01 | 2.7021E+00 | 1.7742E+00 |
| 12.50 | 2.0158E+05 | -8.0167E+04 | -8.5224E+05 | 3.2897E+04 | -9.9023E-01 | 3.9023E-01 | 7.8096E-01 | 1.8299E+00 |
| 12.00 | 1.7734E+05 | -6.8434E+04 | -7.0653E+05 | 3.4743E+04 | -6.3396E-01 | 3.4181E-01 | -2.8864E-01 | 8.0596E-01 |
| 11.50 | 1.3043E+05 | -6.9456E+04 | -6.0370E+05 | 4.6776E+04 | -6.7978E-01 | 4.9427E-01 | 1.9807E-01 | 5.4240E-01 |
| 11.00 | 1.5922E+05 | -8.6112E+04 | -6.0859E+05 | 6.2820E+04 | -7.1943E-01 | 5.7385E-01 | 6.6930E-01 | 7.9868E-01 |
| 10.50 | 1.5846E+05 | -9.8766E+04 | -5.3539E+05 | 8.5750E+04 | -4.4464E-01 | 5.3215E-01 | -3.2403E-01 | 3.4728E-01 |
| 10.00 | 6.5949E+04 | -6.7144E+04 | -2.9542E+05 | 9.2451E+04 | -2.4263E-01 | 5.3000E-01 | -6.2171E-01 | 4.7395E-01 |
| 9.75 | -5.5026E+04 | -1.2227E+04 | 2.3742E+05 | 3.3472E+04 | 2.1122E-01 | 1.9988E-01 | -5.5706E-01 | -1.5128E-01 |
| 9.50 | -1.1349E+05 | 3.4203E+04 | 2.9972E+05 | -1.4262E+02 | 2.8535E-01 | -9.0025E-04 | -4.3791E-01 | -2.3955E-01 |
| 9.25 | -1.4336E+05 | 4.9116E+04 | 4.0197E+05 | 2.7771E+03 | 4.0721E-01 | 1.6271E-02 | -4.0499E-01 | -2.6189E-02 |
| 9.00 | -1.5916E+05 | 6.7628E+04 | 4.0545E+05 | -1.7404E+04 | 4.7888E-01 | -1.2064E-01 | -2.4824E-01 | -9.9814E-02 |
| 8.75 | -1.4929E+05 | 8.1233E+04 | 3.5037E+05 | -3.9535E+04 | 5.4818E-01 | -3.5712E-01 | -9.5127E-02 | 1.4733E-01 |

Basic data, x = 25.0 mm.

| y | Vt | theta | V0 | V1 | var0 | var1 | s01 |
|---|---|---|---|---|---|---|---|
| 30.00 | 626.37 | 110.03 | 588.48 | -214.53 | 116.729 | 112.293 | -61.55 |
| 21.00 | 582.87 | 102.00 | 570.12 | -121.23 | 155.986 | 1425.719 | -150.71 |
| 20.00 | 570.86 | 98.36 | 564.79 | -83.02 | 122.455 | 1089.978 | -183.06 |
| 19.50 | 569.84 | 97.80 | 564.57 | -77.36 | 123.037 | 1127.853 | -184.15 |
| 19.00 | 568.04 | 97.67 | 562.95 | -75.83 | 116.420 | 1092.864 | -122.31 |
| 18.50 | 568.34 | 97.34 | 563.68 | -72.64 | 127.254 | 1297.951 | -194.44 |
| 18.00 | 563.44 | 96.28 | 560.06 | -61.64 | 313.597 | 1293.862 | -246.48 |
| 17.50 | 559.09 | 95.54 | 556.48 | -53.96 | 636.543 | 1329.822 | -479.81 |
| 17.00 | 553.18 | 95.34 | 550.78 | -51.44 | 1232.820 | 1755.841 | -843.11 |
| 16.50 | 542.42 | 94.90 | 540.44 | -46.34 | 2954.674 | 2145.133 | -1632.37 |
| 16.00 | 533.09 | 94.43 | 531.49 | -41.20 | 3425.741 | 1713.136 | -1468.81 |
| 15.50 | 494.33 | 92.88 | 493.71 | -24.85 | 6781.567 | 1857.436 | -2372.84 |
| 15.00 | 466.01 | 92.80 | 465.46 | -22.73 | 8955.245 | 1897.946 | -2654.63 |
| 14.50 | 425.61 | 91.99 | 425.36 | -14.75 | 11422.480 | 2308.966 | -3540.95 |
| 14.00 | 395.42 | 91.44 | 395.30 | -9.93 | 10095.002 | 2461.667 | -3628.77 |
| 13.50 | 370.51 | 90.98 | 370.45 | -6.35 | 10252.772 | 2483.062 | -3573.02 |
| 13.00 | 349.15 | 90.94 | 349.10 | -5.73 | 10481.388 | 2760.578 | -3859.39 |
| 12.50 | 327.70 | 90.66 | 327.68 | -3.79 | 9921.190 | 2886.565 | -3720.75 |
| 12.00 | 287.47 | 91.72 | 287.34 | -8.64 | 9915.507 | 2609.335 | -3329.53 |
| 11.50 | 262.50 | 90.60 | 262.49 | -2.74 | 8279.528 | 2605.469 | -3027.36 |
| 11.25 | 256.57 | 90.98 | 256.53 | -4.41 | 8133.522 | 2522.247 | -2978.68 |
| 11.00 | 243.29 | 90.19 | 243.28 | -0.81 | 7449.190 | 2347.077 | -2612.77 |
| 10.75 | 242.05 | 90.94 | 242.02 | -3.97 | 6912.335 | 2183.193 | -2368.04 |
| 10.50 | 242.77 | 90.98 | 242.74 | -4.16 | 6219.900 | 2228.734 | -2177.42 |

Higher order moment data, x = 25.0 mm.

| y | s001 | s110 | s000 | s111 | sk0 | sk1 | ku0 | ku1 |
|---|---|---|---|---|---|---|---|---|
| 30.00 | 1.0848E+03 | -9.0001E+02 | -1.4515E+03 | 8.7687E+02 | -1.1509E+00 | 7.3690E-01 | 3.8514E+00 | 2.6182E+00 |
| 21.00 | -1.0916E+03 | -5.6806E+01 | -2.8102E+03 | -3.2378E+04 | -1.4425E+00 | -6.0145E-01 | 8.9597E+00 | -5.9189E-02 |
| 20.00 | -1.0516E+03 | 4.7604E+03 | 1.9878E+02 | -3.9193E+04 | 1.4669E-01 | -1.0891E+00 | 3.2863E-01 | 9.2733E-01 |
| 19.50 | -2.5350E+02 | 4.1905E+03 | -1.1169E+03 | -5.2028E+04 | -8.1840E-01 | -1.3736E+00 | 5.0109E+00 | 2.6084E+00 |
| 19.00 | -4.9211E+02 | 7.3092E+01 | -1.0166E+03 | -5.2026E+04 | -8.0927E-01 | -1.4400E+00 | 4.6724E+00 | 3.2664E+00 |
| 18.50 | -8.4431E+02 | 7.1117E+03 | -1.7772E+02 | -6.7371E+04 | -1.2380E-01 | -1.4407E+00 | 1.9550E+00 | 2.9015E+00 |
| 18.00 | 1.1772E+04 | -5.3387E+03 | -2.2419E+04 | -5.9449E+04 | -4.0370E+00 | -1.2774E+00 | 3.3174E+01 | 4.1372E+00 |
| 17.50 | 4.9437E+04 | -3.1479E+04 | -7.3126E+04 | -3.6655E+04 | -4.5534E+00 | -7.5587E-01 | 2.9177E+01 | 4.8896E+00 |
| 17.00 | 8.3165E+04 | -4.2205E+04 | -1.5214E+05 | -3.6103E+04 | -3.5147E+00 | -4.9070E-01 | 1.4415E+01 | 2.9889E+00 |
| 16.50 | 2.3224E+05 | -1.0222E+05 | -5.2941E+05 | -2.0284E+04 | -3.2963E+00 | -2.0416E-01 | 1.2181E+01 | 2.8638E+00 |
| 16.00 | 1.8708E+05 | -6.9380E+04 | -5.3534E+05 | -2.0070E+04 | -2.6699E+00 | -2.8305E-01 | 7.9896E+00 | 2.9946E+00 |
| 15.50 | 2.4055E+05 | -1.0197E+05 | -8.9539E+05 | 4.4802E+04 | -1.6033E+00 | 5.5966E-01 | 2.4774E+00 | 1.9726E+00 |
| 15.00 | 2.5415E+05 | -1.0253E+05 | -1.0237E+06 | 3.7822E+04 | -1.2080E+00 | 4.5743E-01 | 1.1223E+00 | 1.4435E+00 |
| 14.50 | 1.9004E+05 | -7.2911E+04 | -8.3207E+05 | 3.4392E+04 | -6.8158E-01 | 3.0998E-01 | -4.1959E-01 | 1.0799E+00 |
| 14.00 | 1.1536E+05 | -7.5146E+04 | -3.6914E+05 | 5.0609E+04 | -3.6394E-01 | 4.1437E-01 | -5.8653E-01 | 5.1758E-01 |
| 13.50 | 6.8860E+04 | -6.6587E+04 | -2.5143E+05 | 6.0382E+04 | -2.4219E-01 | 4.8800E-01 | -6.8628E-01 | 3.1534E-01 |
| 13.00 | 4.1469E+04 | -4.3360E+04 | -1.6556E+05 | 4.9190E+04 | -1.5429E-01 | 3.3914E-01 | -7.3506E-01 | 3.3524E-01 |
| 12.50 | -3.8953E+04 | -1.4391E+04 | 8.8186E+03 | 4.3798E+04 | 8.9239E-03 | 2.8241E-01 | -6.4540E-01 | 5.4739E-03 |
| 12.00 | -1.0579E+05 | 1.3224E+04 | 3.3166E+05 | 1.6363E+04 | 3.3590E-01 | 1.2277E-01 | -5.6003E-01 | 6.3626E-02 |
| 11.50 | -1.4079E+05 | 5.1260E+04 | 3.9152E+05 | -1.3699E+04 | 5.1970E-01 | -1.0300E-01 | -2.3951E-01 | 6.0997E-02 |
| 11.25 | -1.3313E+05 | 5.0441E+04 | 4.0582E+05 | -1.6867E+04 | 5.5325E-01 | -1.3315E-01 | -1.3291E-01 | -1.8215E-01 |
| 11.00 | -1.2533E+05 | 5.1658E+04 | 3.6842E+05 | -1.7805E+04 | 5.7303E-01 | -1.5658E-01 | 5.1980E-03 | -6.7729E-02 |
| 10.75 | -1.3458E+05 | 6.7742E+04 | 3.6316E+05 | -2.9108E+04 | 6.3191E-01 | -2.8535E-01 | 1.7596E-01 | 2.5672E-01 |
| 10.50 | -1.3023E+05 | 7.0130E+04 | 3.2338E+05 | -3.7301E+04 | 6.5923E-01 | -3.5451E-01 | 4.3812E-01 | 2.7816E-01 |

Basic data, x = 30.0 mm.

| y | Vt | theta | V0 | V1 | var0 | var1 | s01 |
|---|---|---|---|---|---|---|---|
| 35.00 | 624.48 | 109.98 | 586.90 | -213.34 | 129.288 | 125.705 | -69.78 |
| 24.00 | 579.99 | 101.54 | 568.27 | -116.02 | 143.351 | 1552.255 | -172.52 |
| 23.00 | 571.95 | 99.36 | 564.34 | -92.99 | 130.643 | 1521.529 | -189.30 |
| 22.00 | 567.87 | 98.11 | 562.18 | -80.16 | 129.090 | 1504.931 | -166.66 |
| 21.00 | 562.10 | 96.01 | 559.01 | -58.85 | 125.275 | 928.417 | -164.27 |
| 20.50 | 559.95 | 95.53 | 557.35 | -53.92 | 160.173 | 985.826 | -144.43 |
| 20.00 | 558.72 | 95.60 | 556.06 | -54.49 | 244.115 | 1306.696 | -233.82 |
| 19.50 | 557.56 | 96.46 | 554.02 | -62.69 | 784.258 | 2502.344 | -689.92 |
| 19.00 | 551.23 | 96.49 | 547.70 | -62.30 | 1904.883 | 3403.986 | -1418.14 |
| 18.50 | 542.59 | 94.88 | 540.63 | -46.14 | 1999.413 | 2489.680 | -1275.58 |
| 18.00 | 496.65 | 92.19 | 496.28 | -18.95 | 7133.023 | 2451.691 | -2877.18 |
| 17.50 | 478.02 | 92.21 | 477.67 | -18.41 | 8306.979 | 2661.572 | -3114.20 |
| 17.00 | 454.17 | 91.57 | 454.00 | -12.43 | 10484.967 | 2334.930 | -3267.19 |
| 16.50 | 422.31 | 91.09 | 422.23 | -8.01 | 10159.162 | 2457.900 | -3625.82 |
| 16.00 | 375.68 | 88.85 | 375.61 | 7.53 | 9991.463 | 2650.711 | -3580.15 |
| 15.50 | 365.44 | 89.56 | 365.43 | 2.78 | 10246.301 | 2732.756 | -3765.09 |
| 15.00 | 358.30 | 90.07 | 358.30 | -0.43 | 9307.491 | 2465.418 | -3368.33 |
| 14.50 | 335.83 | 89.96 | 335.83 | 0.25 | 9540.713 | 2579.665 | -3416.04 |
| 14.00 | 319.01 | 89.96 | 319.01 | 0.22 | 8714.416 | 2658.002 | -3243.98 |
| 13.50 | 302.71 | 89.60 | 302.70 | 2.10 | 7788.780 | 2472.115 | -2764.58 |
| 13.25 | 280.01 | 90.97 | 279.97 | -4.76 | 7707.948 | 2328.527 | -2477.17 |
| 13.00 | 264.63 | 90.31 | 264.62 | -1.44 | 6833.139 | 2307.003 | -2270.97 |
| 12.75 | 255.88 | 89.94 | 255.88 | 0.26 | 6430.853 | 2051.967 | -2044.61 |
| 12.50 | 254.14 | 90.49 | 254.14 | -2.19 | 6046.320 | 1999.390 | -1909.44 |

Higher order moment data, x = 30.0 mm.

| y | s001 | s110 | s000 | s111 | sk0 | sk1 | ku0 | ku1 |
|---|---|---|---|---|---|---|---|---|
| 35.00 | 9.7269E+02 | -7.1704E+02 | -1.3465E+03 | 6.7097E+02 | -9.1592E-01 | 4.7607E-01 | 2.3876E+00 | 7.1204E-01 |
| 24.00 | -8.7636E+02 | 4.9649E+02 | -1.7122E+03 | -4.5565E+04 | -9.9758E-01 | -7.4505E-01 | 5.4955E+00 | 5.4545E-02 |
| 23.00 | -1.6812E+03 | 6.2221E+03 | -5.8093E+02 | -7.3279E+04 | -3.8904E-01 | -1.2367E+00 | 3.6625E+00 | 1.0673E+00 |
| 22.00 | -1.8449E+03 | 9.0039E+03 | -9.7353E+02 | -9.8014E+04 | -6.6376E-01 | -1.6789E+00 | 4.2567E+00 | 2.6820E+00 |
| 21.00 | -5.9858E+02 | 8.0793E+03 | -4.1297E+01 | -5.6681E+04 | -2.9452E-02 | -2.0037E+00 | 2.2962E+00 | 5.8606E+00 |
| 20.50 | -5.9273E+02 | 5.1969E+03 | -2.3921E+03 | -5.7164E+04 | -1.1801E+00 | -1.8468E+00 | 7.3663E+00 | 6.1293E+00 |
| 20.00 | 1.5680E+03 | 6.9594E+03 | -6.5136E+03 | -7.7780E+04 | -1.7078E+00 | -1.6467E+00 | 8.5012E+00 | 4.3415E+00 |
| 19.50 | 6.2473E+04 | -3.2793E+04 | -8.8890E+04 | -1.1277E+05 | -4.0473E+00 | -9.0092E-01 | 2.2662E+01 | 1.3627E+00 |
| 19.00 | 1.8856E+05 | -9.2939E+04 | -3.3020E+05 | -8.0955E+04 | -3.9717E+00 | -4.0763E-01 | 1.9233E+01 | 7.7420E-01 |
| 18.50 | 1.1253E+05 | -4.4955E+04 | -2.4063E+05 | -9.2263E+04 | -2.6915E+00 | -7.4270E-01 | 7.9906E+00 | 2.2924E+00 |
| 18.00 | 3.3004E+05 | -1.1783E+05 | -9.8986E+05 | 5.7806E+03 | -1.6431E+00 | 4.7618E-02 | 2.5115E+00 | 1.9143E+00 |
| 17.50 | 2.5615E+05 | -7.0844E+04 | -9.3344E+05 | -3.5639E+04 | -1.2329E+00 | -2.5955E-01 | 9.3274E-01 | 1.5553E+00 |
| 17.00 | 2.3120E+05 | -7.7147E+04 | -9.9893E+05 | 1.2785E+04 | -9.3044E-01 | 1.1332E-01 | -7.1357E-02 | 1.3159E+00 |
| 16.50 | 1.1995E+05 | -4.0623E+04 | -4.7857E+05 | 1.0497E+04 | -4.6736E-01 | 8.6147E-02 | -7.1542E-01 | 7.0695E-01 |
| 16.00 | 3.0521E+04 | -5.2054E+04 | -1.6952E+05 | 5.0908E+04 | -1.6974E-01 | 3.7303E-01 | -7.4556E-01 | 1.3337E-01 |
| 15.50 | 2.2123E+04 | -4.6001E+04 | -9.2314E+04 | 4.7953E+04 | -8.9005E-02 | 3.3567E-01 | -7.9542E-01 | 6.0550E-02 |
| 15.00 | -5.1464E+03 | -1.7339E+04 | -4.2407E+04 | 2.9160E+04 | -4.7227E-02 | 2.3821E-01 | -7.9392E-01 | 7.3480E-02 |
| 14.50 | -6.8719E+04 | 1.0784E+04 | 1.0102E+05 | 1.6315E+04 | 1.0840E-01 | 1.2452E-01 | -8.0221E-01 | -2.2148E-01 |
| 14.00 | -7.8654E+04 | 1.6350E+04 | 1.5907E+05 | 1.4025E+04 | 1.9554E-01 | 1.0234E-01 | -6.8529E-01 | -2.0309E-01 |
| 13.50 | -9.0231E+04 | 3.2244E+04 | 1.9470E+05 | -3.9661E+03 | 2.8325E-01 | -3.2267E-02 | -4.9703E-01 | -1.5090E-01 |
| 13.25 | -1.3454E+05 | 4.9733E+04 | 3.6098E+05 | -1.4454E+04 | 5.3343E-01 | -1.2864E-01 | -2.3624E-01 | -1.3302E-02 |
| 13.00 | -1.4196E+05 | 6.0094E+04 | 3.9046E+05 | -1.9564E+04 | 6.9127E-01 | -1.7656E-01 | 1.3297E-01 | 1.3265E-01 |

| | | | | | | | | |
|---|---|---|---|---|---|---|---|---|
| 12.75 | -1.2296E+05 | 6.3514E+04 | 3.2242E+05 | -3.0446E+04 | 6.2519E-01 | -3.2755E-01 | 2.2083E-01 | 1.1914E-01 |
| 12.50 | -9.8929E+04 | 5.7439E+04 | 2.9082E+05 | -3.3490E+04 | 6.1858E-01 | -3.7460E-01 | 1.4764E-01 | 1.8168E-01 |

Basic data, x = 35.0 mm.

| y | Vt | theta | V0 | V1 | var0 | var1 | s01 |
|---|---|---|---|---|---|---|---|
| 35.00 | 624.59 | 110.05 | 586.74 | -214.13 | 104.275 | 122.313 | -46.92 |
| 27.00 | 570.76 | 99.95 | 562.18 | -98.63 | 130.849 | 1713.864 | -230.35 |
| 26.00 | 566.15 | 98.46 | 560.00 | -83.25 | 142.465 | 1475.569 | -195.48 |
| 25.00 | 564.98 | 97.84 | 559.70 | -77.05 | 152.145 | 1774.390 | -207.48 |
| 24.00 | 559.96 | 96.39 | 556.48 | -62.34 | 126.394 | 1716.906 | -188.26 |
| 23.00 | 557.41 | 95.49 | 554.85 | -53.36 | 152.616 | 1281.892 | -179.61 |
| 22.50 | 554.63 | 94.79 | 552.70 | -46.29 | 235.107 | 1315.710 | -211.62 |
| 22.00 | 550.83 | 94.96 | 548.76 | -47.66 | 969.095 | 2147.524 | -686.17 |
| 21.50 | 549.09 | 94.52 | 547.39 | -43.25 | 1160.417 | 2213.936 | -800.86 |
| 21.00 | 543.60 | 94.13 | 542.19 | -39.11 | 1849.980 | 2328.756 | -1151.68 |
| 20.50 | 533.19 | 94.00 | 531.89 | -37.18 | 3342.092 | 3115.914 | -2057.17 |
| 20.00 | 514.75 | 92.37 | 514.31 | -21.25 | 4210.062 | 1899.129 | -1825.16 |
| 19.50 | 498.74 | 92.06 | 498.41 | -17.96 | 5584.182 | 1828.731 | -1997.69 |
| 19.00 | 467.22 | 91.61 | 467.03 | -13.16 | 7993.199 | 2348.696 | -2800.77 |
| 18.50 | 442.71 | 90.48 | 442.69 | -3.73 | 9992.555 | 2261.464 | -3178.73 |
| 18.00 | 413.25 | 90.64 | 413.23 | -4.61 | 8873.327 | 2409.175 | -3257.43 |
| 17.50 | 387.03 | 89.66 | 387.02 | 2.30 | 9124.133 | 2426.867 | -3296.79 |
| 17.00 | 372.22 | 89.43 | 372.20 | 3.73 | 8740.143 | 2489.362 | -3251.64 |
| 16.50 | 362.23 | 89.98 | 362.23 | 0.14 | 8462.497 | 2501.807 | -3142.15 |
| 16.00 | 337.21 | 89.13 | 337.17 | 5.12 | 7849.018 | 2513.630 | -2861.06 |
| 15.50 | 325.46 | 89.15 | 325.42 | 4.85 | 6912.124 | 2459.199 | -2657.15 |
| 15.25 | 318.00 | 89.08 | 317.96 | 5.12 | 6655.475 | 2286.293 | -2330.65 |
| 15.00 | 310.95 | 88.99 | 310.91 | 5.49 | 6396.124 | 2134.903 | -2232.57 |
| 14.75 | 305.06 | 89.11 | 305.02 | 4.72 | 5943.905 | 2119.469 | -2087.01 |
| 14.50 | 297.82 | 88.72 | 297.75 | 6.65 | 5708.782 | 2081.372 | -1905.93 |
| 14.25 | 294.82 | 88.78 | 294.75 | 6.30 | 5694.945 | 1858.643 | -1690.62 |

Higher order moment data, x = 35.0 mm.

| y | s001 | s110 | s000 | s111 | sk0 | sk1 | ku0 | ku1 |
|---|---|---|---|---|---|---|---|---|
| 35.00 | 5.5544E+02 | -4.7868E+02 | -8.4888E+02 | 3.8190E+02 | -7.9722E-01 | 2.8232E-01 | 1.7099E+00 | 2.6051E-01 |
| 27.00 | -1.6641E+03 | 5.9972E+03 | 1.4294E+02 | -6.6537E+04 | 9.5496E-02 | -9.3777E-01 | 2.2270E+00 | 3.9760E-01 |
| 26.00 | -2.6085E+03 | 8.0258E+03 | -5.3078E+02 | -7.6056E+04 | -3.1214E-01 | -1.3418E+00 | 5.0774E+00 | 1.3055E+00 |
| 25.00 | -2.3016E+03 | 7.9948E+03 | 9.8321E+02 | -1.0809E+05 | 5.2392E-01 | -1.4461E+00 | 5.0227E+00 | 1.2430E+00 |
| 24.00 | -1.6154E+03 | 1.0259E+04 | 2.3172E+02 | -1.2188E+05 | 1.6307E-01 | -1.7133E+00 | 2.9607E+00 | 2.5792E+00 |
| 23.00 | -8.4129E+02 | 7.7841E+03 | -1.2443E+03 | -7.7126E+04 | -6.5998E-01 | -1.6804E+00 | 4.6262E+00 | 3.7140E+00 |
| 22.50 | 7.7657E+03 | -2.2230E+03 | -8.2381E+03 | -8.5458E+04 | -2.2852E+00 | -1.7907E+00 | 2.0185E+01 | 6.4185E+00 |
| 22.00 | 7.1235E+04 | -2.4640E+04 | -1.4792E+05 | -9.7724E+04 | -4.9033E+00 | -9.8197E-01 | 3.2799E+01 | 2.5390E+00 |
| 21.50 | 8.8429E+04 | -3.5974E+04 | -1.6941E+05 | -1.0515E+05 | -4.2856E+00 | -1.0094E+00 | 2.4575E+01 | 2.9380E+00 |
| 21.00 | 1.3737E+05 | -4.6353E+04 | -2.8598E+05 | -9.6787E+04 | -3.5940E+00 | -8.6125E-01 | 1.6091E+01 | 2.4603E+00 |
| 20.50 | 2.6478E+05 | -1.1029E+05 | -5.3800E+05 | -7.1411E+04 | -2.7845E+00 | -4.1057E-01 | 8.0967E+00 | 1.5048E+00 |
| 20.00 | 1.9883E+05 | -7.8660E+04 | -5.7311E+05 | -2.9476E+03 | -2.0980E+00 | -3.5616E-02 | 4.8795E+00 | 3.0404E+00 |
| 19.50 | 1.9652E+05 | -7.5946E+04 | -6.6516E+05 | 5.9358E+03 | -1.5940E+00 | 7.5902E-02 | 2.2496E+00 | 2.5017E+00 |
| 19.00 | 1.8106E+05 | -4.0635E+04 | -6.8592E+05 | -3.6030E+04 | -9.5983E-01 | -3.1654E-01 | 1.8418E-01 | 1.7440E+00 |
| 18.50 | 1.2622E+05 | -3.1055E+04 | -6.3440E+05 | -3.6224E+02 | -6.3511E-01 | -3.3683E-03 | -6.5227E-01 | 1.1997E+00 |
| 18.00 | 5.0434E+04 | -2.8590E+04 | -2.4590E+05 | 7.8855E+03 | -2.9419E-01 | 6.6685E-02 | -7.9999E-01 | 7.5791E-01 |
| 17.50 | 4.3623E+04 | -4.9842E+04 | -1.3176E+05 | 4.2969E+04 | -1.5118E-01 | 3.5941E-01 | -8.2296E-01 | 1.2963E-02 |
| 17.00 | -7.8561E+03 | -2.4856E+04 | -2.4932E+04 | 4.3433E+04 | -3.0512E-02 | 3.4970E-01 | -8.2246E-01 | 1.2451E-01 |
| 16.50 | -1.4774E+04 | -1.4780E+04 | -2.5431E+04 | 2.8099E+04 | -3.2667E-02 | 2.2455E-01 | -6.4084E-01 | 5.2729E-02 |
| 16.00 | -1.0476E+05 | 3.5176E+04 | 1.9640E+05 | -3.0202E+03 | 2.8243E-01 | -2.3965E-02 | -6.3772E-01 | 4.8769E-02 |
| 15.50 | -9.9212E+04 | 3.5533E+04 | 2.0905E+05 | -3.8544E+02 | 3.6377E-01 | -3.1606E-03 | -4.0936E-01 | -1.6722E-01 |
| 15.25 | -1.1035E+05 | 4.6696E+04 | 1.9052E+05 | -4.2296E+03 | 3.5089E-01 | -3.8690E-02 | -3.8998E-01 | -1.5572E-02 |
| 15.00 | -1.1864E+05 | 6.3450E+04 | 2.0898E+05 | -1.7303E+04 | 4.0854E-01 | -1.7541E-01 | -2.6187E-01 | 1.8947E-01 |
| 14.75 | -1.0816E+05 | 6.0815E+04 | 1.9599E+05 | -1.9205E+04 | 4.2770E-01 | -1.9682E-01 | -1.3925E-01 | 3.1196E-01 |
| 14.50 | -1.0545E+05 | 5.5177E+04 | 1.8243E+05 | -2.0418E+04 | 4.2294E-01 | -2.1503E-01 | 6.4236E-02 | 4.3302E-01 |
| 14.25 | -8.7247E+04 | 5.5625E+04 | 1.5297E+05 | -2.6684E+04 | 3.5594E-01 | -3.3301E-01 | -1.1583E-01 | 4.2253E-01 |

Basic data, x = 40.0 mm.

| y | Vt | theta | V0 | V1 | var0 | var1 | s01 |
|---|---|---|---|---|---|---|---|
| 40.00 | 619.79 | 109.82 | 583.10 | -210.10 | 160.320 | 182.309 | -104.23 |
| 29.00 | 560.67 | 97.67 | 555.65 | -74.82 | 139.489 | 1806.798 | -284.33 |
| 28.00 | 561.47 | 98.31 | 555.58 | -81.14 | 254.355 | 2700.398 | -398.69 |
| 27.00 | 554.82 | 95.19 | 552.55 | -50.23 | 118.039 | 929.978 | -138.67 |
| 26.00 | 556.79 | 95.56 | 554.17 | -53.90 | 162.366 | 1626.057 | -278.28 |
| 25.00 | 553.98 | 94.66 | 552.15 | -45.03 | 181.133 | 1539.031 | -239.81 |
| 24.50 | 551.96 | 94.29 | 550.42 | -41.29 | 229.265 | 1288.827 | -237.17 |
| 24.00 | 549.03 | 94.80 | 547.10 | -45.99 | 878.172 | 2446.083 | -818.25 |
| 23.50 | 544.12 | 94.65 | 542.33 | -44.14 | 1880.232 | 2976.443 | -1356.45 |
| 23.00 | 533.08 | 93.62 | 532.02 | -33.67 | 3495.716 | 2723.742 | -1743.19 |
| 22.50 | 526.06 | 93.80 | 524.91 | -34.82 | 4116.333 | 3465.048 | -2464.43 |
| 22.00 | 512.90 | 91.84 | 512.64 | -16.50 | 4196.119 | 1606.409 | -1712.48 |
| 21.50 | 505.23 | 91.70 | 505.01 | -15.01 | 4246.289 | 1381.263 | -1491.23 |
| 21.00 | 478.59 | 91.32 | 478.46 | -11.04 | 6529.839 | 1759.626 | -2159.98 |
| 20.50 | 464.82 | 91.54 | 464.65 | -12.45 | 6774.542 | 1711.446 | -2028.38 |
| 20.00 | 412.31 | 89.80 | 412.31 | 1.46 | 9337.557 | 2167.280 | -3086.90 |
| 19.50 | 376.83 | 88.52 | 376.70 | 9.74 | 9282.037 | 2341.569 | -2976.25 |
| 19.00 | 357.26 | 87.79 | 356.99 | 13.80 | 8143.571 | 2412.743 | -2889.91 |
| 18.50 | 342.47 | 87.76 | 342.21 | 13.41 | 7156.485 | 2280.957 | -2542.66 |
| 18.00 | 328.48 | 87.44 | 328.15 | 14.68 | 6552.400 | 2296.314 | -2392.16 |
| 17.50 | 315.11 | 87.68 | 314.85 | 12.73 | 5720.797 | 2012.192 | -1964.18 |
| 17.00 | 308.10 | 87.95 | 307.90 | 11.00 | 5438.109 | 1939.306 | -1792.37 |
| 16.75 | 302.80 | 87.99 | 302.61 | 10.61 | 5031.649 | 1894.254 | -1620.49 |
| 16.50 | 299.45 | 87.82 | 299.23 | 11.38 | 4677.565 | 1724.155 | -1419.77 |
| 16.25 | 298.18 | 88.30 | 298.05 | 8.84 | 4569.933 | 1603.462 | -1262.32 |
| 16.00 | 296.28 | 88.96 | 296.23 | 5.36 | 4656.351 | 1560.909 | -1308.31 |

Higher order moment data, x = 40.0 mm.

| y | s001 | s110 | s000 | s111 | sk0 | sk1 | ku0 | ku1 |
|---|---|---|---|---|---|---|---|---|
| 40.00 | 2.7865E+03 | -2.6980E+03 | -3.0090E+03 | 2.7714E+03 | -1.4823E+00 | 1.1259E+00 | 5.4265E+00 | 4.2176E+00 |
| 29.00 | -3.0522E+03 | 1.3991E+04 | 5.0491E+02 | -1.0102E+05 | 3.0648E-01 | -1.3153E+00 | 1.7816E-01 | 1.0299E+00 |
| 28.00 | -6.6475E+03 | 1.5742E+04 | 5.6858E+02 | -1.2707E+05 | 1.4016E-01 | -9.0554E-01 | 4.3650E+00 | -4.3938E-01 |
| 27.00 | -2.2949E+03 | 1.0293E+04 | 4.2514E+02 | -6.2722E+04 | 3.3151E-01 | -2.2116E+00 | 8.8029E-01 | 6.0398E+00 |
| 26.00 | -2.7956E+03 | 1.7665E+04 | 3.4196E+02 | -1.2058E+05 | 1.6528E-01 | -1.8389E+00 | 2.3652E+00 | 3.0068E+00 |
| 25.00 | 1.5204E+03 | 1.0191E+04 | -2.7967E+03 | -9.4839E+04 | -1.1472E+00 | -1.5708E+00 | 9.7585E+00 | 4.1478E+00 |
| 24.50 | 2.9443E+03 | 7.4575E+03 | -5.8891E+03 | -8.1598E+04 | -1.6965E+00 | -1.7635E+00 | 9.5235E+00 | 5.2612E+00 |
| 24.00 | 7.8211E+04 | -3.9038E+04 | -1.1114E+05 | -9.8057E+04 | -4.2707E+00 | -8.1053E-01 | 2.7039E+01 | 2.0043E+00 |
| 23.50 | 1.5293E+05 | -6.8416E+04 | -2.7849E+05 | -9.6991E+04 | -3.4158E+00 | -5.9729E-01 | 1.3894E+01 | 1.5195E+00 |
| 23.00 | 2.3682E+05 | -7.7289E+04 | -6.4013E+05 | -8.8036E+04 | -3.0972E+00 | -6.1932E-01 | 1.0321E+01 | 2.0140E+00 |
| 22.50 | 2.9622E+05 | -1.0824E+05 | -6.4967E+05 | -7.8669E+04 | -2.4600E+00 | -3.8569E-01 | 6.3796E+00 | 1.1810E+00 |
| 22.00 | 1.7812E+05 | -6.6396E+04 | -5.4704E+05 | 7.5968E+03 | -2.0125E+00 | 1.1799E-01 | 4.2381E+00 | 2.5022E+00 |
| 21.50 | 1.5097E+05 | -6.0458E+04 | -4.8099E+05 | 1.5603E+04 | -1.7383E+00 | 3.0394E-01 | 2.8560E+00 | 2.9779E+00 |
| 21.00 | 1.6367E+05 | -6.2344E+04 | -5.9533E+05 | 1.6192E+04 | -1.1282E+00 | 2.1937E-01 | 6.2070E-01 | 1.8563E+00 |

| | | | | | | | | |
|---|---|---|---|---|---|---|---|---|
| 20.50 | 1.2495E+05 | -6.7392E+04 | -4.8755E+05 | 2.7115E+04 | -8.7437E-01 | 3.8297E-01 | -2.7690E-03 | 1.5246E+00 |
| 20.00 | 3.4870E+04 | -2.6981E+04 | -2.2637E+05 | 2.6174E+04 | -2.5088E-01 | 2.5942E-01 | -9.6050E-01 | 4.1185E-01 |
| 19.50 | -3.9356E+04 | 2.7878E+03 | 2.0880E+04 | 1.2684E+04 | 2.3349E-02 | 1.1194E-01 | -8.8203E-01 | 1.7675E-01 |
| 19.00 | -7.3300E+04 | 8.3215E+03 | 1.6108E+05 | 2.0135E+04 | 2.1919E-01 | 1.6990E-01 | -7.8683E-01 | -1.9345E-01 |
| 18.50 | -8.1488E+04 | 1.9015E+04 | 1.8971E+05 | 1.0973E+04 | 3.1335E-01 | 1.0073E-01 | -5.2962E-01 | -6.8673E-02 |
| 18.00 | -9.5609E+04 | 3.7144E+04 | 2.2273E+05 | -7.2389E+03 | 4.1993E-01 | -6.5785E-02 | -2.7256E-01 | 1.2985E-01 |
| 17.50 | -1.0222E+05 | 4.1870E+04 | 2.1894E+05 | -1.4725E+04 | 5.0598E-01 | -1.6314E-01 | -1.0208E-01 | 9.4443E-02 |
| 17.00 | -8.5101E+04 | 4.1269E+04 | 1.9546E+05 | -1.5034E+04 | 4.8740E-01 | -1.7604E-01 | -9.4057E-02 | -2.3280E-02 |
| 16.75 | -9.2866E+04 | 5.1063E+04 | 1.9740E+05 | -2.3349E+04 | 5.5306E-01 | -2.8321E-01 | 1.8546E-01 | 5.7218E-01 |
| 16.50 | -7.1653E+04 | 4.3243E+04 | 1.6464E+05 | -2.0968E+04 | 5.1464E-01 | -2.9289E-01 | 5.6312E-02 | 4.7952E-01 |
| 16.25 | -6.4395E+04 | 4.0316E+04 | 1.5437E+05 | -1.8122E+04 | 4.9967E-01 | -2.8224E-01 | 1.1689E-01 | 5.5596E-01 |
| 16.00 | -6.7313E+04 | 4.5256E+04 | 1.5913E+05 | -1.9708E+04 | 5.0082E-01 | -3.1958E-01 | 7.7204E-02 | 9.0249E-01 |

**********

Ref.: 3-6
Author: Kussoy and Horstman
Geometry: 3-D Fin
Mach number: 8.2
Data: $p_{wall}$ ,$q_{wall}$ ,$c_f$ , flowfield pitot surveys

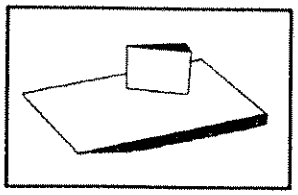

A detailed investigation of hypersonic sharp-fin interactions on a flat plate was carried out by M. I. Kussoy, K. C. Horstman, and C. C. Horstman of NASA-Ames Research Center (Refs. 3-6). Since a detailed data report (Ref. 3) has already been prepared on this experiment, the present treatment will be brief. The data included in the file KUSSOY3.DAT are exactly those given in Ref. 3 for sharp-fin interactions, plus some additional data (notably skin friction) supplied by the experimenters after Ref. 3 was published.

The data were obtained in the NASA-Ames 3.5-foot hypersonic wind tunnel, using a flat-plate model with a length of 220 cm. Natural transition occurred on this plate for all test conditions. While no turbulence data are available to establish the condition of the incoming boundary layer ahead of the interaction, a mean profile included in this dataset shows typical law-of-the-wall behavior, albeit with a lower wake-strength parameter than usual.

Fins of 5, 7.5, 10, 12.5, and 15 degree angle-of-attack were mounted on the flat plate. The fin leading-edge position was 176 cm aft of the plate leading-edge. The x,y,z coordinate frame used to describe the measurements is indicated in the sketch below. Given this information and the table of freestream properties in the data file, most of the measured distributions are self-explanatory.

One feature of this experiment is redundant data, considered a desirable aspect of benchmark experiments in Ref. 1. Similar heat transfer data are obtained by two different techniques. Redundant pressure and heat transfer data are included in the data file to establish the repeatability of the experiment.

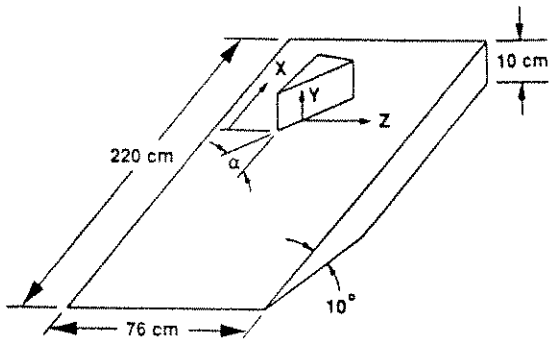


Users of these data should note that this fin interaction involves a relatively-thicker incoming boundary layer than the supersonic fin interactions included elsewhere in this database. The reason for this is the long flat-plate run required to naturally establish a turbulent boundary-layer at Mach 8. Thus the present fin is only 8 incoming-boundary-layer-thicknesses long, compared to relative fin lengths 5 times larger in the Penn State experiments at Mach 3 and 4. The net effect is that the present interaction lies entirely within its turbulent boundary-layer, while the supersonic interactions just referred to extend far outside their respective boundary-layers. The supersonic and Mach 8 cases are thus not directly comparable.

KUSSOY3.DAT

DATA FILES FROM NASA TM 103838 AND SUPPLEMENTARY DATA SUPPLIED BY THE EXPERIMENTERS ON A SINGLE-FIN, SWEPT SHOCK WAVE/ TURBULENT BOUNDARY-LAYER INTERACTION AT MACH 8.2

FREESTREAM CONDITIONS

| | |
|---|---|
| M INF | = 8.18 |
| T INF | = 81 K |
| P INF | = 430 N/M^2 |
| TW | = 300 K |
| U INF | = 1446 M/S |
| DELTA 0 | = 3.7 CM |
| DELTA* 0 | = 1.59 CM |
| THETA 0 | = 0.094 CM |
| TAUW INF | = 19.6 N/M^2 |
| Q INF | = 9900 W/M^2 |
| RE/M | = 4.9EE+06 |
| CF INF | = 0.98EE-03 |
| CH INF | = 0.53EE-03 |

S = DISTANCE ALONG FIN SURFACE MEASURED FROM LEADING EDGE

UPSTREAM BOUNDARY LAYER

| Y(cm) | M | P / P INF | RHO / RHO INF | T / T INF | U / U INF | RHOU / RHOU INF | TT / TT INF |
|---|---|---|---|---|---|---|---|
| 0.000 | 0.000 | 1.000 | 0.270 | 3.699 | 0.000 | 0.000 | 0.270 |
| 0.070 | 1.777 | 1.000 | 0.213 | 4.705 | 0.481 | 0.102 | 0.555 |
| 0.140 | 2.069 | 1.000 | 0.195 | 5.138 | 0.584 | 0.114 | 0.682 |
| 0.200 | 2.647 | 1.000 | 0.237 | 4.217 | 0.678 | 0.161 | 0.721 |
| 0.280 | 3.083 | 1.000 | 0.266 | 3.756 | 0.746 | 0.199 | 0.773 |
| 0.360 | 3.409 | 1.000 | 0.295 | 3.390 | 0.784 | 0.231 | 0.798 |
| 0.430 | 3.558 | 1.000 | 0.301 | 3.323 | 0.810 | 0.244 | 0.828 |
| 0.500 | 3.747 | 1.000 | 0.333 | 3.002 | 0.811 | 0.270 | 0.808 |
| 0.710 | 4.068 | 1.000 | 0.345 | 2.897 | 0.864 | 0.298 | 0.877 |
| 0.920 | 4.422 | 1.000 | 0.386 | 2.593 | 0.889 | 0.343 | 0.894 |
| 1.120 | 4.750 | 1.000 | 0.419 | 2.388 | 0.916 | 0.384 | 0.922 |
| 1.320 | 5.106 | 1.000 | 0.453 | 2.205 | 0.947 | 0.429 | 0.956 |
| 1.520 | 5.461 | 1.000 | 0.504 | 1.982 | 0.960 | 0.484 | 0.963 |
| 1.720 | 5.774 | 1.000 | 0.560 | 1.785 | 0.963 | 0.539 | 0.956 |
| 1.920 | 6.101 | 1.000 | 0.600 | 1.668 | 0.984 | 0.590 | 0.981 |
| 2.130 | 6.411 | 1.000 | 0.671 | 1.490 | 0.977 | 0.656 | 0.959 |
| 2.320 | 6.689 | 1.000 | 0.705 | 1.419 | 0.995 | 0.701 | 0.983 |
| 2.510 | 7.009 | 1.000 | 0.768 | 1.302 | 0.998 | 0.767 | 0.981 |
| 2.710 | 7.246 | 1.000 | 0.820 | 1.220 | 0.999 | 0.819 | 0.977 |
| 3.040 | 7.617 | 1.000 | 0.865 | 1.156 | 1.023 | 0.884 | 1.012 |
| 3.380 | 7.978 | 1.000 | 0.944 | 1.060 | 1.025 | 0.968 | 1.011 |
| 3.730 | 8.180 | 1.000 | 1.000 | 1.000 | 1.021 | 1.021 | 1.000 |
| 4.070 | 8.180 | 1.000 | 0.995 | 1.005 | 1.024 | 1.019 | 1.004 |

SURFACE STREAMLINE ANGLES ON FLAT PLATE WITH FIN

| 10 DEGREE FIN ANGLE | | 15 DEGREE FIN ANGLE | |
|---|---|---|---|
| Z(cm) | (deg) | Z(cm) | (deg) |
| 0.20 | 10.0 | 0.22 | 15.0 |
| 0.40 | 15.5 | 0.68 | 35.7 |
| 0.84 | 21.3 | 1.20 | 44.7 |
| 1.28 | 29.4 | 1.75 | 47.2 |
| 1.83 | 34.3 | 2.12 | 50.3 |
| 2.22 | 34.8 | 2.44 | 50.5 |
| 2.63 | 35.2 | 2.85 | 45.2 |
| 2.96 | 30.0 | 3.30 | 39.0 |
| 3.28 | 25.0 | 3.90 | 27.2 |
| 4.30 | 24.0 | 4.70 | 32.8 |
| 5.50 | 23.8 | 5.40 | 33.0 |
| 6.78 | 23.2 | 6.34 | 32.0 |
| 7.59 | 17.2 | 7.10 | 34.2 |
| 8.30 | 10.8 | 8.75 | 32.2 |
| 8.91 | 0.0 | 9.42 | 27.5 |
| | | 10.15 | 7.5 |
| | | 10.55 | 0.0 |

SURFACE PRESSURES ON FIN (P/P INF)

S = 18.34 cm

| Y(cm) | Fin Angle = 5 deg | 7.5 deg | 10 deg | 12.5 deg | 15 deg |
|---|---|---|---|---|---|
| 0.45 | 1.855 | 2.565 | 3.532 | 4.516 | 5.871 |
| 0.95 | 1.823 | 2.484 | 3.323 | 4.210 | 5.274 |
| 1.45 | 1.790 | 2.452 | 3.242 | 4.065 | 5.000 |
| 2.45 | 1.984 | 2.839 | 3.887 | 5.016 | 6.484 |
| 3.43 | 2.145 | 3.290 | 4.823 | 6.242 | 8.306 |
| 4.43 | 2.355 | 3.613 | 5.371 | 7.000 | 9.355 |
| 5.42 | 2.419 | 3.774 | 5.565 | 7.274 | 9.677 |
| 6.42 | 2.435 | 3.855 | 5.677 | 7.435 | 9.839 |
| 7.42 | 2.516 | 3.903 | 5.742 | 7.532 | 9.968 |
| 8.41 | 2.597 | 4.032 | 5.839 | 7.694 | 10.161 |
| 9.40 | 2.565 | 4.016 | 5.935 | 7.774 | 10.306 |
| 10.40 | 2.613 | 4.145 | 6.065 | 7.887 | 10.468 |

SURFACE PRESSURES ON FLAT PLATE WITH FIN

X = 18.19 cm

| Fin Angle = | 5 deg | | 7.5 deg | | 10 deg | |
|---|---|---|---|---|---|---|
| | Z(cm) | P/P INF | Z(cm) | P/P INF | Z(cm) | P/P INF |
| | 15.82 | 1.000 | 15.29 | 1.089 | 14.78 | 1.127 |
| | 14.82 | 0.979 | 14.29 | 1.050 | 13.78 | 1.102 |
| | 13.82 | 0.968 | 13.29 | 1.061 | 12.78 | 1.113 |
| | 12.83 | 0.990 | 12.30 | 1.050 | 11.79 | 1.098 |
| | 11.83 | 0.940 | 11.30 | 1.044 | 10.79 | 1.121 |
| | 10.80 | 1.027 | 10.27 | 1.103 | 9.76 | 1.113 |
| | 9.82 | 0.994 | 9.29 | 1.065 | 8.78 | 1.195 |
| | 8.82 | 0.990 | 8.29 | 1.123 | 7.78 | 1.363 |
| | 7.82 | 1.008 | 7.29 | 1.197 | 6.78 | 1.561 |
| | 6.82 | 1.115 | 6.29 | 1.358 | 5.78 | 1.758 |
| | 5.82 | 1.169 | 5.29 | 1.506 | 4.78 | 1.968 |
| | 4.82 | 1.324 | 4.29 | 1.661 | 3.78 | 2.065 |
| | 3.83 | 1.410 | 3.30 | 1.774 | 2.79 | 2.161 |
| | 2.83 | 1.497 | 2.30 | 1.935 | 1.79 | 2.742 |
| | 1.83 | 1.608 | 1.30 | 2.371 | 0.79 | 3.742 |
| | 0.83 | 2.000 | 0.30 | 2.887 | | |

| Fin Angle = | 12.5 deg | | 15 deg | |
|---|---|---|---|---|
| | Z(cm) | P/P INF | Z(cm) | P/P INF |
| | 14.27 | 1.229 | 13.72 | 1.021 |
| | 13.27 | 1.213 | 12.72 | 1.016 |
| | 12.27 | 1.226 | 11.72 | 1.037 |
| | 11.28 | 1.223 | 10.73 | 1.094 |
| | 10.28 | 1.252 | 9.73 | 1.292 |
| | 9.25 | 1.327 | 8.70 | 1.529 |
| | 8.27 | 1.500 | 7.72 | 1.839 |
| | 7.27 | 1.726 | 6.72 | 2.145 |
| | 6.27 | 1.968 | 5.72 | 2.339 |

| | | | |
|---|---|---|---|
| 5.27 | 2.194 | 4.72 | 2.452 |
| 4.27 | 2.371 | 3.72 | 2.452 |
| 3.27 | 2.387 | 2.72 | 2.613 |
| 2.28 | 2.758 | 1.73 | 4.113 |
| 1.28 | 3.984 | 0.73 | 6.387 |
| 0.28 | 5.065 | | |

Additional Surface Pressures on Flat Plate with Fin
x = 18.19cm

| 10 deg fin angle | | | | 15 deg fin angle | | | |
|---|---|---|---|---|---|---|---|
| z(cm) | P/PINF | z(cm) | P/PINF | z(cm) | P/PINF | z(cm) | P/PINF |
| 11.50 | 0.95 | 5.49 | 1.78 | 13.49 | 0.96 | 6.49 | 2.34 |
| 11.02 | 0.99 | 5.04 | 1.84 | 12.99 | 0.96 | 5.99 | 2.37 |
| 10.47 | 0.96 | 4.49 | 1.97 | 12.50 | 0.96 | 5.49 | 2.54 |
| 10.04 | 1.00 | 4.05 | 1.99 | 12.00 | 0.96 | 4.99 | 2.52 |
| 9.49 | 1.00 | 3.50 | 2.05 | 11.50 | 1.01 | 4.49 | 2.57 |
| 9.04 | 1.07 | 3.05 | 1.98 | 11.00 | 1.04 | 3.99 | 2.49 |
| 8.49 | 1.13 | 2.50 | 2.21 | 10.47 | 1.20 | 3.50 | 2.47 |
| 8.04 | 1.21 | 2.05 | 2.48 | 9.97 | 1.26 | 3.00 | 2.50 |
| 7.49 | 1.32 | 1.50 | 3.00 | 9.49 | 1.46 | 2.50 | 3.12 |
| 7.04 | 1.41 | 1.05 | 3.42 | 8.99 | 1.54 | 2.00 | 3.87 |
| 6.49 | 1.55 | 0.50 | 4.02 | 8.49 | 1.80 | 1.50 | 5.33 |
| 6.04 | 1.63 | 0.05 | 3.81 | 7.99 | 1.87 | 1.00 | 6.41 |
| | | | | 7.49 | 2.12 | 0.50 | 7.65 |
| | | | | 6.99 | 2.18 | 0.00 | 7.20 |

**********

HEAT TRANSFER ON FIN (Q/Q INF)

Thermocouples, S = 16.70 cm

| Y(cm) | Fin Angle = 5 deg | 7.5 deg | 10 deg | 12.5 deg | 15 deg |
|---|---|---|---|---|---|
| 0.47 | 1.28 | 2.06 | 3.04 | 3.82 | 5.01 |
| 0.95 | 1.17 | 1.80 | 2.86 | 3.47 | 4.24 |
| 1.45 | 1.30 | 2.11 | 2.99 | 3.69 | 4.55 |
| 2.45 | 1.40 | 2.37 | 3.27 | 4.20 | 5.50 |
| 3.45 | 1.44 | 2.32 | 3.02 | 3.83 | 5.30 |
| 4.45 | 1.43 | 1.98 | 2.54 | 2.90 | 4.02 |
| 5.45 | 1.30 | 1.85 | 2.31 | 2.60 | 3.35 |
| 6.43 | 1.25 | 1.68 | 2.07 | 2.35 | 3.05 |
| 7.43 | 1.19 | 1.65 | 2.03 | 2.41 | 3.09 |
| 8.43 | 1.20 | 1.69 | 2.06 | 2.38 | 3.08 |
| 9.40 | 1.21 | 1.67 | 2.04 | 2.39 | 2.93 |
| 10.38 | 1.16 | 1.67 | 2.02 | 2.42 | 2.94 |

Schmidt-Boelter Gauges, S = 19.62 cm

| Y(cm) | Fin Angle = 5 deg | 7.5 deg | 10 deg | 12.5 deg | 15 deg |
|---|---|---|---|---|---|
| 2.45 | 1.34 | 1.65 | 2.61 | 3.43 | 4.28 |
| 3.45 | 1.39 | 1.66 | 2.61 | 3.54 | 4.74 |
| 4.43 | 1.43 | 1.64 | 2.40 | 3.12 | 4.26 |
| 5.42 | 1.30 | 1.51 | 2.18 | 2.77 | 3.69 |
| 7.15 | 1.06 | 1.23 | 1.74 | 2.31 | 3.01 |
| 9.15 | 1.17 | 1.38 | 1.91 | 2.57 | 3.26 |

HEAT TRANSFER ON FLAT PLATE WITH FIN
X = 16.45 cm

| Fin Angle = | 5 deg | | 7.5 deg | | 10 deg | |
|---|---|---|---|---|---|---|
| | Z(cm) | Q/Q INF | Z(cm) | Q/Q INF | Z(cm) | Q/Q INF |
| | 15.75 | 0.86 | 15.27 | 0.95 | 14.76 | 0.99 |
| | 14.77 | 0.96 | 14.29 | 0.99 | 13.78 | 1.02 |
| | 13.76 | 0.94 | 13.28 | 1.06 | 12.77 | 1.05 |
| | 12.78 | 0.95 | 12.30 | 1.03 | 11.79 | 1.05 |
| | 11.82 | 0.92 | 11.34 | 1.01 | 10.83 | 1.07 |
| | 10.83 | 0.96 | 10.35 | 1.06 | 9.84 | 1.08 |
| | 9.82 | 0.98 | 9.34 | 1.10 | 8.83 | 1.07 |
| | 8.82 | 0.98 | 8.34 | 1.03 | 7.83 | 1.04 |
| | 6.80 | 0.96 | 6.32 | 1.03 | 5.81 | 1.20 |
| | 5.80 | 1.05 | 5.32 | 1.18 | 4.81 | 1.58 |
| | 4.80 | 1.11 | 4.32 | 1.30 | 3.81 | 1.58 |
| | 2.54 | 1.29 | 2.06 | 1.87 | 1.55 | 2.61 |
| | 1.79 | 1.47 | 1.31 | 2.31 | 0.80 | 3.23 |

| Fin Angle = | 12.5 deg | | 15 deg | |
|---|---|---|---|---|
| | Z(cm) | Q/Q INF | Z(cm) | Q/Q INF |
| | 14.35 | 0.99 | 13.89 | 0.98 |
| | 13.37 | 1.01 | 12.91 | 1.00 |
| | 12.36 | 1.02 | 11.90 | 1.03 |
| | 11.38 | 1.01 | 10.92 | 1.00 |
| | 10.42 | 1.02 | 9.96 | 0.94 |
| | 9.43 | 1.06 | 8.97 | 0.95 |
| | 8.42 | 1.00 | 7.96 | 0.95 |
| | 7.42 | 0.95 | 6.96 | 1.46 |
| | 5.40 | 1.58 | 4.94 | 2.01 |
| | 4.40 | 1.85 | 3.94 | 1.80 |
| | 3.40 | 1.56 | 2.94 | 1.75 |
| | 1.14 | 3.54 | 0.68 | 4.96 |
| | 0.39 | 4.07 | | |

Additional Heat Transfer on Flat Plate with Fin
x = 16.45cm

| 10 deg fin angle | | | | 15 deg fin angle | | | |
|---|---|---|---|---|---|---|---|
| z(cm) | Q/QINF | z(cm) | Q/QINF | z(cm) | Q/QINF | z(cm) | Q/QINF |
| 11.87 | 1.02 | 5.85 | 1.33 | 13.47 | 1.05 | 6.51 | 1.90 |
| 11.43 | 1.08 | 5.40 | 1.46 | 12.99 | 0.89 | 6.01 | 1.90 |
| 10.88 | 1.04 | 4.85 | 1.54 | 12.49 | 1.03 | 5.51 | 2.09 |
| 10.43 | 1.06 | 3.14 | 1.68 | 12.03 | 0.90 | 5.01 | 1.92 |
| 9.88 | 1.02 | 2.59 | 1.95 | 11.53 | 1.03 | 4.51 | 1.82 |
| 9.42 | 1.08 | 2.39 | 2.10 | 11.04 | 0.89 | 2.75 | 2.42 |
| 8.87 | 1.01 | 1.84 | 2.51 | 10.54 | 1.01 | 2.25 | 3.12 |
| 7.40 | 1.02 | 1.39 | 2.98 | 10.04 | 0.83 | 2.00 | 3.41 |
| 6.85 | 1.08 | 0.84 | 3.18 | 9.54 | 0.96 | 1.50 | 4.28 |
| 6.40 | 1.17 | 0.35 | 3.11 | 9.03 | 0.84 | 1.00 | 5.03 |
| | | | | 8.53 | 1.10 | 0.50 | 4.77 |
| | | | | 7.01 | 1.64 | | |

**********

Skin-friction on Flat Plate with Fin, X = 15.5cm
(replaces data in AIAA paper 91-1761 which was in error)

| Fin angle = 10 deg | | | 15 deg | | |
|---|---|---|---|---|---|
| z(cm) | Cf x 10 | uncertainty | z(cm) | Cf x 10 | uncertainty |
| 9.00 | 1.00 | +/- 0.18 | 9.00 | 1.00 | +/- 0.18 |
| 7.12 | 0.84 | +/- 0.10 | 2.73 | 2.40 | +/- 0.53 |
| 6.52 | 0.87 | +/- 0.21 | 1.35 | 4.59 | +/- 0.88 |
| 4.22 | 1.56 | +/- 0.33 | 1.05 | 4.50 | +/- 0.81 |
| 3.21 | 1.08 | +/- 0.20 | 0.60 | 5.86 | +/- 1.33 |
| 2.16 | 1.87 | +/- 0.48 | | | |
| 1.24 | 2.92 | +/- 0.54 | | | |
| 0.83 | 2.49 | +/- 0.56 | | | |

**********

FLOW FIELD YAW ANGLES (DEGREES)
10 DEGREE FIN ANGLE
X = 17.23 cm

| Y(cm) | Z(cm) = 0.64 | 1.27 | 1.91 | 2.54 | 3.81 | 5.08 |
|---|---|---|---|---|---|---|
| 0.00 | 16 | 25 | 35 | 35 | 25 | 24 |
| 0.25 | 14 | 17 | 20 | 22 | 21 | 15 |
| 0.50 | 14 | 15 | 18 | 19 | 15 | 9 |
| 0.75 | 13 | 14 | 16 | 15 | 10 | 4 |
| 1.00 | 13 | 13 | 14 | 11 | 5 | 2 |
| 1.25 | 13 | 12 | 12 | 7 | 2 | 1 |
| 1.50 | 12 | 11 | 10 | 5 | 1 | 1 |
| 1.75 | 12 | 11 | 9 | 3 | 0 | 0 |
| 2.00 | 12 | 10 | 9 | 2 | 0 | 0 |
| 2.25 | 11 | 10 | 9 | 2 | 0 | 0 |
| 2.50 | 11 | 10 | 9 | 2 | 0 | 0 |
| 2.75 | 11 | 10 | 9 | 2 | 0 | 0 |
| 3.00 | 11 | 10 | 10 | 2 | 0 | 0 |
| 3.25 | 11 | 10 | 11 | 2 | 0 | 0 |

FLOW FIELD PITOT PRESSURES (PT2/PT2 INF)
10 DEGREE FIN ANGLE
X = 17.23 cm

| Y(cm) | Z(cm) = 0.64 | 1.27 | 1.91 | 2.54 | 3.81 | 5.08 |
|---|---|---|---|---|---|---|
| 0.25 | 0.51 | 0.51 | 0.40 | 0.33 | 0.16 | 0.15 |
| 0.50 | 0.70 | 0.60 | 0.39 | 0.31 | 0.20 | 0.20 |
| 0.75 | 0.85 | 0.63 | 0.38 | 0.30 | 0.24 | 0.28 |
| 1.00 | 0.95 | 0.69 | 0.42 | 0.33 | 0.32 | 0.35 |
| 1.25 | 1.04 | 0.75 | 0.48 | 0.39 | 0.41 | 0.44 |
| 1.50 | 4.16 | 0.84 | 0.57 | 0.49 | 0.51 | 0.55 |
| 1.75 | 1.26 | 0.96 | 0.70 | 0.61 | 0.64 | 0.62 |
| 2.00 | 1.44 | 1.11 | 0.86 | 0.76 | 0.78 | 0.71 |
| 2.25 | 1.61 | 1.27 | 1.07 | 0.95 | 0.88 | 0.75 |
| 2.50 | 1.79 | 1.48 | 1.31 | 1.15 | 0.89 | 0.80 |
| 2.75 | 1.97 | 1.71 | 1.67 | 1.33 | 0.91 | 0.85 |
| 3.00 | 2.15 | 1.96 | 1.97 | 1.40 | 0.93 | 0.89 |
| 3.25 | 2.47 | 2.21 | 2.32 | 1.32 | 0.94 | 0.95 |

FLOW FIELD YAW ANGLES (DEGREES)
15 DEGREE FIN ANGLE
X = 17.44 cm

| Y(cm) | Z(cm) = 1.27 | 1.91 | 2.54 | 3.81 | 5.08 | 6.35 | 7.62 |
|---|---|---|---|---|---|---|---|
| 0.00 | 44 | 46 | 50 | 37 | 33 | 32 | 34 |
| 0.25 | 25 | 23 | 32 | 33 | 32 | 25 | 14 |
| 0.50 | 22 | 21 | 30 | 29 | 27 | 17 | 7 |
| 0.75 | 21 | 20 | 26 | 23 | 19 | 9 | 3 |
| 1.00 | 19 | 18 | 20 | 17 | 11 | 5 | 2 |
| 1.25 | 18 | 16 | 12 | 10 | 5 | 2 | 1 |
| 1.50 | 17 | 13 | 7 | 4 | 2 | 1 | 1 |
| 1.75 | 16 | 10 | 2 | 1 | 1 | 0 | 0 |
| 2.00 | 15 | 8 | 1 | 0 | 0 | 0 | 0 |
| 2.25 | 14 | 3 | 1 | 0 | 0 | 0 | 0 |
| 2.50 | 14 | 1 | 0 | 0 | 0 | 0 | 0 |
| 2.75 | 14 | | 1 | 0 | 0 | 0 | 0 |
| 3.00 | 14 | | 1 | 0 | 0 | 0 | 0 |
| 3.25 | 15 | | 1 | 0 | 0 | 0 | 0 |

FLOW FIELD PITOT PRESSURES (PT2/PT2 INF)
15 DEGREE FIN ANGLE
X = 17.44 cm

| Y(cm) | Z(cm) = 1.27 | 1.91 | 2.54 | 3.81 | 5.08 | 6.35 | 7.62 |
|---|---|---|---|---|---|---|---|
| 0.25 | 0.88 | 0.62 | 0.44 | 0.36 | 0.20 | 0.17 | 0.13 |
| 0.50 | 0.93 | 0.59 | 0.41 | 0.34 | 0.24 | 0.20 | 0.21 |
| 0.75 | 0.90 | 0.52 | 0.33 | 0.31 | 0.27 | 0.27 | 0.29 |
| 1.00 | 0.88 | 0.47 | 0.30 | 0.29 | 0.33 | 0.36 | 0.37 |
| 1.25 | 0.91 | 0.47 | 0.33 | 0.33 | 0.41 | 0.47 | 0.44 |
| 1.50 | 0.99 | 0.53 | 0.40 | 0.42 | 0.54 | 0.59 | 0.50 |
| 1.75 | 1.15 | 0.63 | 0.54 | 0.58 | 0.70 | 0.70 | 0.56 |
| 2.00 | 1.31 | 0.97 | 0.70 | 0.74 | 0.86 | 0.74 | 0.61 |
| 2.25 | 1.58 | 0.96 | 0.89 | 0.96 | 0.97 | 0.75 | 0.68 |
| 2.50 | 1.86 | 1.17 | 1.12 | 1.14 | 0.95 | 0.79 | 0.75 |
| 2.75 | 2.23 | | 1.35 | 1.15 | 0.89 | 0.86 | 0.83 |
| 3.00 | 2.49 | | 1.38 | 1.06 | 0.93 | 0.90 | 0.87 |
| 3.25 | 2.79 | | 1.22 | 0.98 | 0.98 | 0.95 | 0.93 |

**********END OF FILE**********

Ref.: 14
Author: Kussoy and Horstman
Geometry: Crossing Oblique Shock Waves
Mach number: 8.3
Data: $p_{wall}$, $q_{wall}$, flowfield pitot surveys

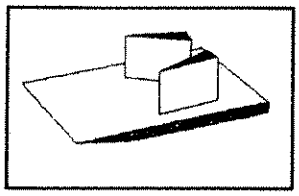

A detailed investigation of hypersonic crossing-shock interactions on a flat plate was carried out by M. I. Kussoy, K. C. Horstman, and C. C. Horstman of NASA-Ames Research Center (Refs. 14). Since a detailed data report (Ref. 14) has already been prepared on this experiment, the present treatment will be brief.

The data included in the file KUSSOY4.DAT are exactly those given in Ref. 14. These data were obtained in the NASA-Ames 3.5-foot hypersonic wind tunnel, using a flat-plate model with a length of 220 cm. Natural transition occurred on this plate for all test conditions. While no turbulence data are available to establish the condition of the incoming boundary layer ahead of the interaction, a mean profile included in this dataset shows typical law-of-the-wall behavior, albeit with a lower wake-strength parameter than usual.

Opposing pairs of fins, each having either 10 or 15 degree angles-of-attack were mounted on the flat plate as shown in the sketch below. The x,y,z coordinate frame used to describe the measurements is also indicated in the sketch. Given this information and the table of freestream properties in the data file, most of the measured distributions are self-explanatory.

As in the case of the Mach 8 single-fin interaction, Refs. 3-6, users of these data should note that this crossing-shock interaction involves a relatively-thicker incoming boundary layer than the supersonic crossing-shock interactions included elsewhere in this database. The supersonic and Mach 8 cases are thus not directly comparable.

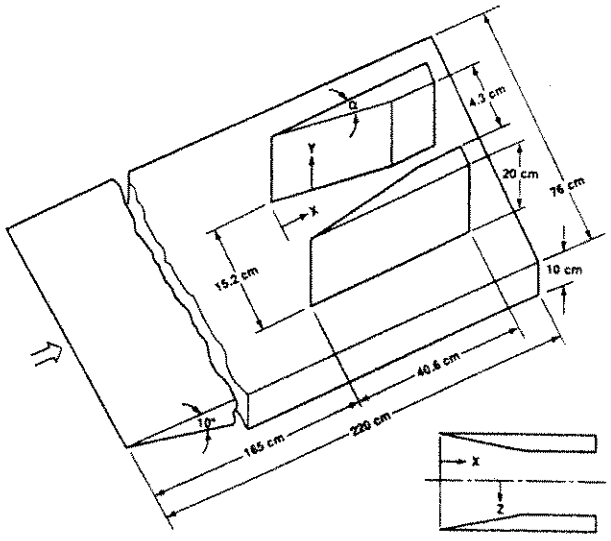

**********

KUSSOY4.DAT

DATA FILES FROM NASA TM 103909
ON A CROSSING-SHOCK-WAVE/
TURBULENT BOUNDARY-LAYER INTERACTION AT MACH 8.3

**********

FREESTREAM CONDITIONS

| | |
|---|---|
| M INF | = 8.28 |
| T INF | = 80 K |
| P INF | = 430 N/M^2 |
| RHO INF | =0.0186 KG/M^3 |
| TW | = 300 K |
| U INF | = 1483 M/S |
| DELTA 0 | = 3.25 CM |
| DELTA* 0 | = 1.26 CM |
| THETA 0 | = 0.083 CM |
| TAUW INF | = 21.6 N/M^2 |
| Q INF | = 10400 W/M^2 |
| RE/M | = 5.3EE+06 |
| CF INF | = 0.99EE-03 |
| CH INF | = 0.56EE-03 |

**********

UPSTREAM BOUNDARY LAYER

| Y (cm) | M | P / P INF | RHO / RHO INF | T / T INF | U / U INF | RHOU / RHOU INF | TT / TT INF |
|---|---|---|---|---|---|---|---|
| 0.000 | 0.000 | 1.000 | 0.267 | 3.744 | 0.000 | 0.000 | 0.270 |
| 0.110 | 2.330 | 1.000 | 0.243 | 4.109 | 0.571 | 0.139 | 0.609 |
| 0.210 | 3.252 | 1.000 | 0.290 | 3.445 | 0.730 | 0.212 | 0.753 |
| 0.320 | 3.530 | 1.000 | 0.318 | 3.148 | 0.758 | 0.241 | 0.770 |
| 0.420 | 3.772 | 1.000 | 0.338 | 2.957 | 0.785 | 0.265 | 0.795 |
| 0.520 | 4.058 | 1.000 | 0.356 | 2.811 | 0.823 | 0.293 | 0.840 |
| 0.620 | 4.297 | 1.000 | 0.380 | 2.631 | 0.843 | 0.320 | 0.859 |
| 0.720 | 4.550 | 1.000 | 0.406 | 2.464 | 0.864 | 0.351 | 0.879 |
| 0.820 | 4.703 | 1.000 | 0.423 | 2.362 | 0.874 | 0.370 | 0.889 |
| 0.930 | 5.076 | 1.000 | 0.490 | 2.043 | 0.877 | 0.430 | 0.873 |
| 1.030 | 5.247 | 1.000 | 0.499 | 2.002 | 0.898 | 0.448 | 0.902 |
| 1.130 | 5.477 | 1.000 | 0.526 | 1.903 | 0.914 | 0.480 | 0.921 |
| 1.240 | 5.678 | 1.000 | 0.559 | 1.789 | 0.919 | 0.514 | 0.921 |
| 1.340 | 5.891 | 1.000 | 0.582 | 1.718 | 0.934 | 0.544 | 0.942 |
| 1.440 | 6.039 | 1.000 | 0.600 | 1.666 | 0.943 | 0.566 | 0.953 |
| 1.540 | 6.259 | 1.000 | 0.628 | 1.591 | 0.955 | 0.600 | 0.968 |
| 1.640 | 6.371 | 1.000 | 0.636 | 1.572 | 0.966 | 0.614 | 0.986 |
| 1.750 | 6.571 | 1.000 | 0.670 | 1.492 | 0.971 | 0.651 | 0.989 |
| 1.850 | 6.765 | 1.000 | 0.700 | 1.429 | 0.978 | 0.685 | 0.997 |
| 1.950 | 7.005 | 1.000 | 0.746 | 1.341 | 0.981 | 0.732 | 0.996 |
| 2.050 | 7.171 | 1.000 | 0.783 | 1.278 | 0.980 | 0.767 | 0.991 |
| 2.150 | 7.373 | 1.000 | 0.817 | 1.224 | 0.987 | 0.806 | 0.998 |
| 2.250 | 7.492 | 1.000 | 0.843 | 1.186 | 0.987 | 0.832 | 0.996 |
| 2.350 | 7.647 | 1.000 | 0.869 | 1.150 | 0.992 | 0.862 | 1.003 |
| 2.450 | 7.800 | 1.000 | 0.901 | 1.110 | 0.994 | 0.896 | 1.004 |
| 2.550 | 7.875 | 1.000 | 0.918 | 1.090 | 0.994 | 0.912 | 1.003 |
| 2.650 | 7.949 | 1.000 | 0.936 | 1.068 | 0.994 | 0.930 | 1.001 |
| 2.750 | 8.023 | 1.000 | 0.944 | 1.059 | 0.999 | 0.943 | 1.009 |
| 2.850 | 8.074 | 1.000 | 0.941 | 1.063 | 1.007 | 0.948 | 1.023 |
| 2.940 | 8.132 | 1.000 | 0.960 | 1.042 | 1.004 | 0.964 | 1.017 |
| 3.030 | 8.189 | 1.000 | 0.962 | 1.039 | 1.010 | 0.972 | 1.027 |
| 3.120 | 8.233 | 1.000 | 0.988 | 1.012 | 1.002 | 0.990 | 1.011 |
| 3.220 | 8.275 | 1.000 | 0.999 | 1.001 | 1.001 | 1.000 | 1.009 |
| 3.310 | 8.275 | 1.000 | 1.009 | 0.991 | 0.996 | 1.005 | 1.000 |

**********



STREAMWISE CENTERLINE SURFACE PRESSURE AND HEAT TRANSFER DISTRIBUTION

10 x 10 DEGREE SHOCK GENERATOR
STREAMWISE CENTERLINE SURFACE PRESSURES ON FLAT PLATE

| X (cm) | P/P INF |
|---|---|
| 0.20 | 0.85 |
| 1.20 | 0.84 |
| 2.20 | 0.82 |
| 3.19 | 0.85 |
| 4.19 | 0.82 |
| 5.22 | 0.90 |
| 6.20 | 0.86 |
| 7.20 | 0.88 |
| 8.20 | 0.89 |
| 9.20 | 1.01 |
| 10.20 | 1.16 |
| 11.20 | 1.43 |
| 12.19 | 1.69 |
| 13.19 | 2.05 |
| 14.19 | 2.42 |
| 15.19 | 2.92 |
| 16.19 | 3.23 |
| 22.35 | 5.24 |
| 23.35 | 5.73 |
| 24.35 | 6.19 |
| 25.34 | 6.87 |
| 26.34 | 7.52 |
| 27.37 | 8.27 |
| 28.35 | 8.85 |
| 29.35 | 9.55 |
| 30.35 | 10.31 |
| 31.35 | 11.48 |
| 32.35 | 13.23 |
| 33.35 | 14.97 |
| 34.34 | 14.92 |
| 35.34 | 13.48 |
| 36.34 | 11.92 |
| 37.34 | 10.66 |
| 38.34 | 9.52 |

10 x 10 DEGREE SHOCK GENERATOR
STREAMWISE CENTERLINE SURFACE HEAT TRANSFER ON FLAT PLATE
FROM THERMOCOUPLES

| X (cm) | Q/Q INF |
|---|---|
| 4.03 | 1.02 |
| 5.01 | 1.00 |
| 6.02 | 1.02 |
| 7.00 | 0.99 |
| 7.96 | 1.01 |
| 8.95 | 1.01 |
| 9.95 | 0.98 |
| 10.96 | 0.91 |
| 12.98 | 1.09 |
| 13.98 | 1.39 |
| 14.98 | 1.73 |
| 17.24 | 2.34 |
| 17.99 | 2.37 |
| 18.99 | 2.61 |
| 20.03 | 2.74 |
| 22.50 | 3.21 |
| 23.48 | 3.48 |
| 24.49 | 3.79 |
| 25.47 | 4.04 |
| 26.43 | 4.47 |

| | |
|---|---|
| 27.42 | 4.94 |
| 28.42 | 5.21 |
| 29.43 | 5.59 |
| 31.45 | 6.38 |
| 32.45 | 7.21 |
| 33.45 | 8.02 |
| 35.71 | 7.33 |
| 36.46 | 6.48 |
| 37.46 | 5.84 |
| 38.50 | 5.28 |

15 x 15 DEGREE SHOCK GENERATOR
STREAMWISE CENTERLINE SURFACE PRESSURES ON FLAT PLATE

| X (cm) | P/P INF |
|---|---|
| 0.25 | 1.09 |
| 1.25 | 1.07 |
| 2.25 | 1.05 |
| 3.24 | 1.09 |
| 4.24 | 1.03 |
| 5.27 | 1.15 |
| 6.25 | 1.19 |
| 7.25 | 1.45 |
| 8.25 | 1.81 |
| 9.25 | 2.29 |
| 11.25 | 3.81 |
| 12.24 | 4.69 |
| 13.24 | 5.50 |
| 14.24 | 6.08 |
| 15.24 | 6.85 |
| 15.50 | 6.90 |
| 16.24 | 7.74 |
| 16.50 | 7.85 |
| 17.50 | 9.27 |
| 18.49 | 11.40 |
| 19.49 | 13.66 |
| 20.52 | 16.11 |
| 21.50 | 18.71 |
| 22.50 | 21.13 |
| 23.50 | 20.32 |
| 23.58 | 20.16 |
| 24.50 | 17.90 |
| 24.58 | 17.74 |
| 25.50 | 15.45 |
| 25.58 | 14.63 |
| 26.50 | 13.44 |
| 26.57 | 12.40 |
| 27.49 | 11.87 |
| 27.57 | 10.69 |
| 28.49 | 10.92 |
| 28.60 | 9.89 |
| 29.49 | 11.45 |
| 29.58 | 11.10 |
| 30.49 | 13.73 |
| 30.58 | 14.13 |
| 31.49 | 16.29 |
| 31.58 | 16.61 |
| 32.58 | 17.26 |
| 33.58 | 16.61 |
| 34.58 | 15.65 |
| 35.57 | 14.79 |
| 36.57 | 14.19 |
| 37.57 | 14.03 |
| 38.57 | 14.39 |
| 39.57 | 15.42 |

15 x 15 DEGREE SHOCK GENERATOR
STREAMWISE CENTERLINE SURFACE HEAT TRANSFER ON FLAT PLATE
FROM THERMOCOUPLES

| X (cm) | Q/Q INF |
|---|---|
| 2.00 | 0.74 |
| 2.98 | 0.87 |
| 3.99 | 0.78 |
| 4.97 | 0.75 |
| 5.93 | 0.78 |
| 6.92 | 0.74 |
| 7.92 | 0.58 |
| 8.93 | 0.59 |
| 10.95 | 1.76 |
| 11.95 | 2.60 |
| 12.95 | 3.42 |
| 14.00 | 4.02 |
| 14.98 | 4.38 |
| 15.21 | 4.60 |
| 15.96 | 4.68 |
| 15.99 | 4.72 |
| 16.96 | 5.20 |
| 16.97 | 5.16 |
| 17.93 | 6.22 |
| 18.00 | 6.36 |
| 18.92 | 7.63 |
| 19.92 | 8.90 |
| 20.93 | 10.28 |
| 22.95 | 12.09 |
| 23.95 | 11.69 |
| 24.95 | 10.28 |
| 27.21 | 7.14 |
| 27.96 | 6.31 |
| 28.96 | 6.14 |
| 30.00 | 6.88 |

**********

TRANSVERSE SURFACE PRESSURE, YAW ANGLE, AND HEAT TRANSFER DISTRIBUTION

10 x 10 DEGREE SHOCK GENERATOR
TRANSVERSE SURFACE QUANTITIES, STATION 1

Pressures (X = 18.2 cm)

| Z (cm) | P/P INF |
|---|---|
| 0.32 | 3.56 |
| 0.41 | 3.76 |
| 0.62 | 3.40 |
| 0.71 | 3.68 |
| 1.30 | 3.05 |
| 1.41 | 3.31 |
| 1.60 | 2.87 |
| 1.71 | 3.18 |
| 2.30 | 2.65 |
| 2.40 | 2.74 |
| 2.60 | 2.85 |
| 2.70 | 2.69 |
| 3.30 | 3.58 |
| 3.40 | 3.37 |

EXCERPT ONLY
SEE DATA FILE
KUSSOY4.DAT

Ref.: 10-11
Author: Lee and Settles
Geometry: 3-D Fin
Mach number: 3, 4
Data: $c_h$

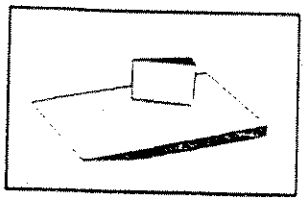

The Ph.D. research of Yeol Lee in the Penn State Gas Dynamics Laboratory involved measuring the heat transfer distributions beneath several sharp-fin interactions. The test conditions at Mach 3 and 4 and the fin angle-of-attack range were the same as those already documented here and in Ref. 1 for the Penn State series of sharp-fin experiments, which also includes surface pressures, surface flow directions, skin friction distributions, and flowfield density profiles. The present heat transfer data, listed in the file LEE.DAT, are thus supplementary data.

These heat transfer measurements required the development of a special heated-model technique for steady-state heat transfer in an otherwise near-adiabatic wind tunnel. The technique is discussed at length in Refs. 10 and 11. It was assumed, for simplicity of the instrumentation layout, that the quasiconical-flow approximation is valid for sharp-fin interactions (see, eg, Alvi and Settles, *AIAA Journal*, Vol. 30, Sept. 1992, pp. 2252-2258). 37 RTD heat transfer gages were thus arrayed in two adjacent circular arcs, centered at the fin leading edge location, with radii of 86.4 and 91.4 mm. The fin leading edge was 22.16 cm aft of the flat plate leading edge. The lateral spacing of the gages was such that their resolution was 2 degrees of the azimuthal interaction angle $\beta$ over a $\beta$ range of 6 to 78 degrees. the radii of the two gage rows was chosen to place them well outside the inception zones of all interaction cases studied.

A special feature of this dataset is the fact that adiabatic wall temperatures were actually measured rather than inferred, so the data are presented in terms of true heat transfer coefficients rather than dimensional heating rates. For more detail on this issue, please see Refs. 10 and 11.

```
**********************************************************************
LEE.DAT
     HEAT TRANSFER-
     SHARP FIN SHOCK/BL INTERACTION DATA - PENN STATE GAS DYNAMICS LAB
**********************************************************************

FREESTREAM CONDITIONS:

  Mach number 3.03 (Mach 3)
    stagnation pressure 120 psia (827 kPa)
    stagnation temperature 294 K
    Reynolds number 6.19E+07/m
    Tw/Taw = 1.06 (roughly adiabatic)

  Mach number 3.98 (Mach 4)
    stagnation pressure 221 psia (1524 kPa)
    stagnation temperature 293 K
    Reynolds number 6.79E+07/m
    Tw/Taw = 1.06 (roughly adiabatic)

INCOMING BOUNDARY LAYER PARAMETERS AT X=178 mm FROM FLAT-PLATE
LEADING EDGE

 Mach 3   (actual freestream Mach number was 2.91 for this survey)
  Delta = 3.02 mm
  Delta* = 0.895 mm
  Theta = 0.184 mm
  Cf = 0.001520
  Re(theta) = 9751

 Mach 4   (actual freestream Mach number was 3.88 for this survey)
  Delta = 2.87 mm
  Delta* = 0.950 mm
  Theta = 0.128 mm
  Cf = 0.001325
  Re(theta) = 9082
**********************************************************************
                        REFERENCE NORMALIZERS

MACH 3     CH INF =  0.86E-03
MACH 4     CH INF =  0.70E-03

**********************************************************************
                          TABULATED DATA
NOTE: Beta values are measured from fin leading edge, not VCO
**********************************************************************

MACH 3, 10DEG FIN INTERACTION
(max total uncertainty ± 10.9%)

BETA      CH/
(DEG)     CH INF
---------------
57.8      1.000
55.9      0.930
53.7      0.974
51.8      0.983
47.7      0.990
41.4      -----
39.5      0.922
33.2      0.940
31.2      0.970
29.0      0.998
27.0      1.172
24.9      1.361
22.9      1.508
20.7      1.727
18.7      1.911
16.6      2.065
12.5      1.963

MACH 3, 16DEG FIN INTERACTION
(max total uncertainty ± 8.8%)

BETA      CH/
(DEG)     CH INF
---------------
57.8      1.000
55.9      0.933
53.7      0.978
51.8      1.029
47.7      1.024
41.4      1.073
39.5      1.052
33.2      1.506
31.2      1.764
29.0      2.033
27.0      2.456
24.9      2.944
22.9      3.237
20.7      3.183
18.7      2.864

MACH 3, 20DEG FIN INTERACTION
(max total uncertainty ± 12.8%)

BETA      CH/
(DEG)     CH INF
---------------
57.8      1.000
55.9      0.940
53.7      0.965
51.8      1.032
47.7      1.270
41.4      1.686
39.5      1.400
33.2      2.438
31.2      2.693
29.0      3.939
27.0      4.110
24.9      3.455
22.9      3.074

MACH 4, 16DEG FIN INTERACTION
(max total uncertainty ± 9.5%)

BETA      CH/
(DEG)     CH INF
---------------
57.8      1.000
55.9      0.921
53.7      0.955
51.8      0.976
47.7      0.962
41.4      1.081
39.5      0.921
33.2      1.325
31.2      1.618
29.0      1.795
27.0      2.167
24.9      2.643
22.9      3.136
20.7      4.081
18.7      3.652

MACH 4, 20DEG FIN INTERACTION
(max total uncertainty ± 9.0%)

BETA      CH/
(DEG)     CH INF
---------------
57.8      1.000
55.9      0.948
53.7      0.976
51.8      1.034
47.7      1.177
41.4      1.616
39.5      1.455
33.2      2.082
31.2      2.492
29.0      2.992
27.0      4.227
24.9      5.120
22.9      4.452

**********************************END OF FILE****
```

Ref.: 7-9
Author: Rodi and Dolling
Geometry: 3-D Fin
Mach number: 4.9
Data: $p_{wall}$, $q_{wall}$, surface-flow traces

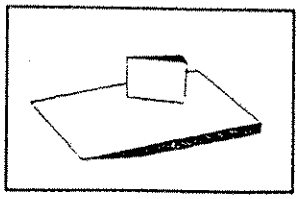

In this experiment, a single sharp fin was used to generate an attached oblique shock wave which interacted with an incoming turbulent boundary layer formed along a flat plate test surface. The freestream Mach number was 4.90, the nominal total pressure was 315 psia (2.7 MPa) and the nominal total temperature was 760 degrees R (422 K). The freestream Reynolds number was 11.7 x $10^6$/ft. (38.4 x $10^6$/m). The model was at ambient temperature before each run. This combination of tunnel total temperature and model temperature resulted in a cool wall condition with a wall temperature/recovery temperature ratio of 0.8. Pitot pressure surveys were made of the incoming boundary layer just ahead of the fin and are included in this dataset.

Mean surface heat transfer (using Schmidt-Boelter gages) and surface pressure data (using pressure taps and a scani-valve) were measured on the test surface along spanwise rows for a range of fin angle of attack. The kerosene-lampblack surface tracer technique was used to visualize the distribution of the local shear stress direction. Data were collected at six different fin angles of attack (6-, 8-, 10-, 12-, 14- and 16-degrees). Additional heat transfer data were taken along conical rays from the virtual conical origin (VCO) for fin angles of attack of 8- and 15-degrees. The investigator reported an error band of +/-8% for the heat transfer data and +/-3% for the pressure data.

The X-dimension is the downstream direction measured from the fin leading edge. The Y-dimension is the cross-stream direction measured from the fin leading edge, in the spanwise direction towards the compression side of the fin. The Z-direction is the vertical direction above the flat plate test surface.

Three different rotatable instrumentation "plugs" were used to make the present measurements. The "plug" used for wall pressure measurements had four rows of taps which were initially oriented in the spanwise (Y) direction (see diagram 1). The spanwise pressure data for 6, 8, 10, 12, and 14 degree fin angles were taken on the two downstream tap rows (rows 3 and 4 in diagram 1). Then, by rotating the instrumentation plug clockwise, the pressure-tap rows were reoriented to better approximate conical cross-planes (see diagram 2). For 8 and 16-degree fin angles, the plug was rotated 15 and 30 degrees clockwise, respectively, from its initial position. For these two fin angles, three rows of pressure data (rows 2, 3, and 4) are tabulated for both spanwise and rotated orientations of the instrumentation plug.

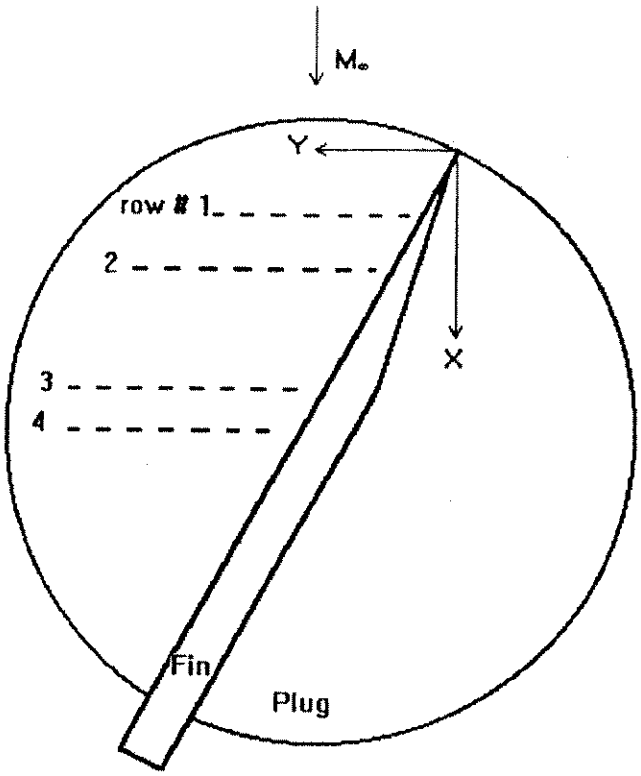


Diagram 1

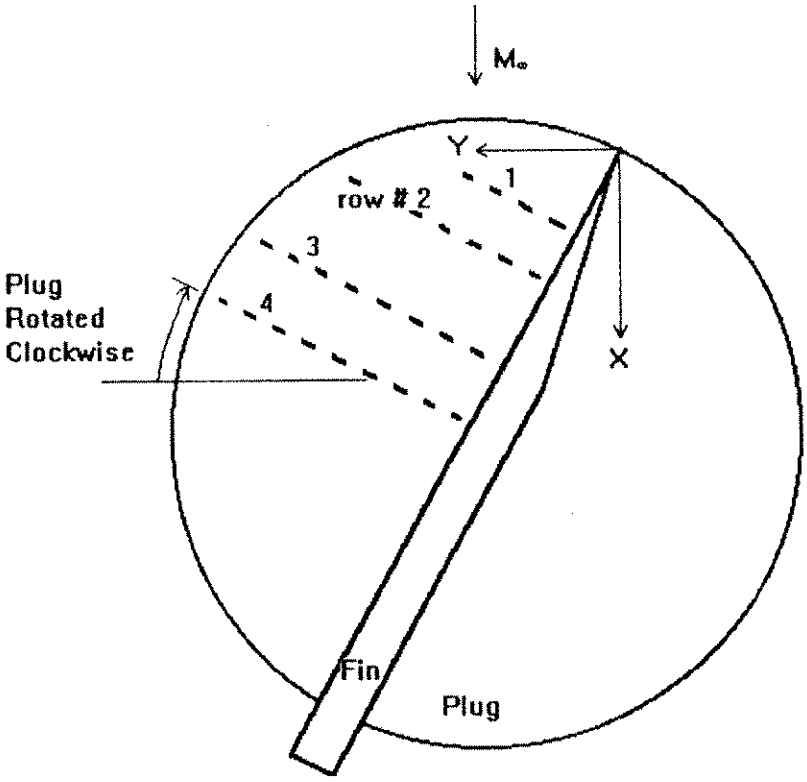


Diagram 2

**********

ROD1.DAT

SHARP-FIN-GENERATED SHOCK WAVE/TURBULENT BOUNDARY
LAYER INTERACTION DATA AT MACH 4.9, INCLUDING
HEAT TRANSFER MEASUREMENTS

**********

NOMENCLATURE

ALPHA = fin angle of attack, degrees
BETA = conical angle in plane of test surface, degrees
BETAO = angle of inviscid shock trace, degrees
BETAU = upstream influence angle, degrees
BETAS1 = primary separation angle, degrees
BEVCO = beta angle from VCO, degrees
BFLE = beta angle from fin leading edge, degrees
BLM = calculated local Mach number within boundary layer
BLP = assumed static pressure within boundary layer, psia
BLPO = measured total pressure within boundary layer, psia
BLTO = assumed total temperature within boundary layer, F
CH = Stanton number
CHE = Stanton number at interaction edge
DELTA = incoming boundary layer thickness, 0.25 in.
DELY = local spanwise distance from fin to tap/transducer, inches
L1 = length of leading edge inception region, inches
P = static wall pressure, psia
PE = pressure at interaction edge, psia
PO = tunnel total pressure, psia
QDOT = wall heat transfer, BTU/ft^2/sec
R = radial distance from VCO, inches
THETA = plug rotation angle, degree
TO = tunnel total temperature, degrees F
TW = wall temperature, degrees F
VCO= virtual conical origin
VCOp= VCO based upon the wall pressure distribution
VCOv= VCO based upon the surface tracer patterns
X = streamwise distance, inches
XLE = streamwise distance from fin leading edge, inches
Y = spanwise distance, inches
YS = local spanwise distance from fin to inviscid shock, inches
YYS = spanwise distance from fin normalized by the YS
YLE = spanwise distance from fin leading edge, inches
Z = vertical distance above plate, inches

**********

INCOMING BOUNDARY LAYER DOCUMENTATION

**********

The incoming turbulent boundary layer Pitot profile was measured 19.3 in. (49.0 cm.) downstream of the flat plate leading edge and approximately 0.5 in. (1.27 cm.) upstream of the fin leading edge. Height above the wall (Z) and Pitot pressure (BLPO) were measured directly, the local static pressure distribution (BLP) was assumed to be linear as was the local total temperature distribution (BLTO). Local Mach number (BLM) was calculated.

| INDEX | Z (in) | BLP (psia) | BLPO (psia) | BLM | BLTO (F) |
|---|---|---|---|---|---|
| 1 | 0.57008E-01 | 0.752 | 7.300 | 2.68 | 260.15 |
| 2 | 0.59449E-01 | 0.751 | 7.340 | 2.69 | 260.51 |
| 3 | 0.63031E-01 | 0.750 | 7.816 | 2.78 | 261.05 |
| 4 | 0.66614E-01 | 0.748 | 8.160 | 2.84 | 261.77 |
| 5 | 0.69449E-01 | 0.748 | 8.507 | 2.91 | 262.31 |
| 6 | 0.72008E-01 | 0.747 | 8.689 | 2.94 | 262.67 |
| 7 | 0.75866E-01 | 0.745 | 8.959 | 2.99 | 263.39 |
| 8 | 0.82834E-01 | 0.743 | 9.082 | 3.02 | 264.65 |
| 9 | 0.86260E-01 | 0.742 | 9.452 | 3.08 | 265.37 |
| 10 | 0.89291E-01 | 0.741 | 9.873 | 3.16 | 265.91 |
| 11 | 0.96575E-01 | 0.739 | 10.556 | 3.27 | 267.17 |
| 12 | 0.10024E+00 | 0.738 | 10.920 | 3.33 | 267.71 |
| 13 | 0.10571E+00 | 0.736 | 10.990 | 3.35 | 268.79 |
| 14 | 0.10866E+00 | 0.735 | 11.413 | 3.42 | 269.33 |
| 15 | 0.11327E+00 | 0.733 | 11.853 | 3.49 | 270.05 |
| 16 | 0.11949E+00 | 0.731 | 12.788 | 3.63 | 271.13 |
| 17 | 0.12524E+00 | 0.729 | 13.017 | 3.67 | 272.21 |
| 18 | 0.13209E+00 | 0.727 | 13.538 | 3.75 | 273.47 |
| 19 | 0.13776E+00 | 0.725 | 13.819 | 3.80 | 274.55 |
| 20 | 0.14559E+00 | 0.723 | 15.084 | 3.98 | 275.81 |
| 21 | 0.15303E+00 | 0.721 | 15.722 | 4.07 | 277.25 |
| 22 | 0.15929E+00 | 0.718 | 15.911 | 4.10 | 278.33 |
| 23 | 0.16587E+00 | 0.716 | 16.796 | 4.22 | 279.41 |
| 24 | 0.17480E+00 | 0.713 | 17.622 | 4.34 | 281.03 |
| 25 | 0.18327E+00 | 0.711 | 18.086 | 4.40 | 282.65 |
| 26 | 0.19091E+00 | 0.708 | 18.507 | 4.46 | 283.91 |
| 27 | 0.19795E+00 | 0.706 | 18.986 | 4.53 | 285.17 |
| 28 | 0.20594E+00 | 0.703 | 19.479 | 4.60 | 286.61 |
| 29 | 0.21563E+00 | 0.700 | 19.537 | 4.61 | 288.41 |
| 30 | 0.22791E+00 | 0.696 | 20.320 | 4.72 | 290.57 |
| 31 | 0.23752E+00 | 0.693 | 20.407 | 4.74 | 292.19 |
| 32 | 0.24787E+00 | 0.690 | 20.581 | 4.77 | 294.17 |
| 33 | 0.25882E+00 | 0.686 | 20.610 | 4.79 | 296.15 |
| 34 | 0.26827E+00 | 0.683 | 20.668 | 4.81 | 297.77 |
| 35 | 0.28004E+00 | 0.679 | 20.712 | 4.83 | 299.93 |
| 36 | 0.30000E+00 | 0.673 | 20.726 | 4.85 | 303.35 |
| 37 | 0.31067E+00 | 0.670 | 20.755 | 4.87 | 305.33 |

**********

SURFACE PRESSURE DATA

**********

Below are the spanwise pressure measurements for fin angles of attack = 6-, 10-, 12- and 14-degrees. The 8- and 16-degree spanwise data are plotted in conical coordinates along with the conical cross-plane data later. PE is defined as the edge pressure value along each spanwise row.

ALPHA= 6.0 BETAO= 16.1

| X (in.) | Y (in.) | DELY (in.) | YS (in.) | DELY/YS | P (psia) | P/PE |
|---|---|---|---|---|---|---|
| 2.009 | 1.852 | 1.640 | 0.369 | 4.450 | 0.777 | 1.000 |
| 2.009 | 1.712 | 1.500 | 0.369 | 4.070 | 0.770 | 0.991 |
| 2.009 | 1.572 | 1.360 | 0.369 | 3.690 | 0.761 | 0.979 |
| 2.009 | 1.432 | 1.220 | 0.369 | 3.311 | 0.766 | 0.986 |
| 2.009 | 1.292 | 1.080 | 0.369 | 2.931 | 0.765 | 0.985 |
| 2.009 | 1.152 | 0.940 | 0.369 | 2.551 | 0.822 | 1.058 |
| 2.009 | 1.012 | 0.800 | 0.369 | 2.171 | 0.907 | 1.167 |
| 2.009 | 0.872 | 0.660 | 0.369 | 1.792 | 1.001 | 1.288 |
| 2.009 | 0.732 | 0.520 | 0.369 | 1.412 | 1.032 | 1.328 |
| 2.009 | 0.592 | 0.380 | 0.369 | 1.032 | 1.066 | 1.372 |
| 2.009 | 0.452 | 0.240 | 0.369 | 0.652 | 1.142 | 1.470 |
| 2.009 | 0.312 | 0.100 | 0.369 | 0.273 | 1.244 | 1.601 |
| 2.378 | 1.852 | 1.602 | 0.436 | 3.670 | 0.755 | 1.000 |
| 2.378 | 1.712 | 1.462 | 0.436 | 3.350 | 0.759 | 1.005 |
| 2.378 | 1.572 | 1.322 | 0.436 | 3.029 | 0.761 | 1.008 |
| 2.378 | 1.432 | 1.182 | 0.436 | 2.708 | 0.768 | 1.017 |
| 2.378 | 1.292 | 1.042 | 0.436 | 2.387 | 0.827 | 1.095 |
| 2.378 | 1.152 | 0.902 | 0.436 | 2.066 | 0.911 | 1.207 |
| 2.378 | 1.012 | 0.762 | 0.436 | 1.745 | 0.976 | 1.293 |
| 2.378 | 0.872 | 0.622 | 0.436 | 1.425 | 1.019 | 1.350 |
| 2.378 | 0.732 | 0.482 | 0.436 | 1.104 | 1.051 | 1.392 |
| 2.378 | 0.592 | 0.342 | 0.436 | 0.783 | 1.070 | 1.417 |
| 2.378 | 0.452 | 0.202 | 0.436 | 0.462 | 1.178 | 1.560 |
| 2.009 | 1.642 | 1.430 | 0.369 | 3.880 | 0.770 | 1.000 |
| 2.009 | 1.502 | 1.290 | 0.369 | 3.501 | 0.764 | 0.992 |
| 2.009 | 1.362 | 1.150 | 0.369 | 3.121 | 0.792 | 1.029 |
| 2.009 | 1.222 | 1.010 | 0.369 | 2.741 | 0.792 | 1.029 |
| 2.009 | 1.082 | 0.870 | 0.369 | 2.361 | 0.867 | 1.126 |
| 2.009 | 0.802 | 0.590 | 0.369 | 1.602 | 1.034 | 1.343 |
| 2.009 | 0.662 | 0.450 | 0.369 | 1.222 | 1.057 | 1.373 |
| 2.009 | 0.522 | 0.310 | 0.369 | 0.842 | 1.110 | 1.442 |

| | | | | | | |
|---|---|---|---|---|---|---|
| 2.009 | 0.382 | 0.170 | 0.369 | 0.462 | 1.224 | 1.590 |
| 2.009 | 0.242 | 0.030 | 0.369 | 0.083 | 1.298 | 1.686 |
| 2.378 | 1.642 | 1.392 | 0.436 | 3.189 | 0.770 | 1.000 |
| 2.378 | 1.502 | 1.252 | 0.436 | 2.868 | 0.764 | 0.992 |
| 2.378 | 1.362 | 1.112 | 0.436 | 2.548 | 0.809 | 1.051 |
| 2.378 | 1.222 | 0.972 | 0.436 | 2.227 | 0.881 | 1.144 |
| 2.378 | 1.082 | 0.832 | 0.436 | 1.906 | 0.961 | 1.248 |
| 2.378 | 0.942 | 0.692 | 0.436 | 1.585 | 1.011 | 1.313 |
| 2.378 | 0.802 | 0.552 | 0.436 | 1.264 | 1.048 | 1.361 |
| 2.378 | 0.662 | 0.412 | 0.436 | 0.943 | 1.056 | 1.371 |
| 2.378 | 0.522 | 0.272 | 0.436 | 0.623 | 1.140 | 1.481 |
| 2.378 | 0.382 | 0.132 | 0.436 | 0.302 | 1.274 | 1.655 |

ALPHA= 10.0 BETAO= 19.6

| X (in.) | Y (in.) | DELY (in.) | YS (in.) | DELY/YS | P (psia) | P/PE |
|---|---|---|---|---|---|---|
| 2.002 | 1.992 | 1.639 | 0.360 | 4.553 | 0.779 | 1.000 |
| 2.002 | 1.852 | 1.499 | 0.360 | 4.164 | 0.758 | 0.973 |
| 2.002 | 1.712 | 1.359 | 0.360 | 3.775 | 0.753 | 0.967 |
| 2.002 | 1.992 | 1.639 | 0.360 | 4.553 | 0.779 | 1.000 |
| 2.002 | 1.852 | 1.499 | 0.360 | 4.164 | 0.758 | 0.973 |
| 2.002 | 1.712 | 1.359 | 0.360 | 3.775 | 0.753 | 0.967 |
| 2.002 | 1.572 | 1.219 | 0.360 | 3.386 | 0.765 | 0.982 |
| 2.002 | 1.432 | 1.079 | 0.360 | 2.997 | 0.844 | 1.083 |
| 2.002 | 1.292 | 0.939 | 0.360 | 2.608 | 0.992 | 1.273 |
| 2.002 | 1.152 | 0.799 | 0.360 | 2.219 | 1.104 | 1.417 |
| 2.002 | 1.012 | 0.659 | 0.360 | 1.830 | 1.186 | 1.522 |
| 2.002 | 0.872 | 0.519 | 0.360 | 1.441 | 1.184 | 1.520 |
| 2.002 | 0.732 | 0.379 | 0.360 | 1.052 | 1.194 | 1.533 |
| 2.002 | 0.592 | 0.239 | 0.360 | 0.663 | 1.409 | 1.809 |
| 2.002 | 0.452 | 0.099 | 0.360 | 0.274 | 1.762 | 2.262 |
| 2.371 | 1.992 | 1.574 | 0.426 | 3.692 | 0.757 | 1.000 |
| 2.371 | 1.852 | 1.434 | 0.426 | 3.363 | 0.763 | 1.008 |
| 2.371 | 1.712 | 1.294 | 0.426 | 3.035 | 0.757 | 1.000 |
| 2.371 | 1.572 | 1.154 | 0.426 | 2.706 | 0.905 | 1.196 |
| 2.371 | 1.432 | 1.014 | 0.426 | 2.378 | 1.037 | 1.370 |
| 2.371 | 1.292 | 0.874 | 0.426 | 2.049 | 1.119 | 1.478 |
| 2.371 | 1.152 | 0.734 | 0.426 | 1.721 | 1.177 | 1.555 |
| 2.371 | 1.012 | 0.594 | 0.426 | 1.393 | 1.190 | 1.572 |
| 2.371 | 0.872 | 0.454 | 0.426 | 1.064 | 1.182 | 1.561 |
| 2.371 | 0.732 | 0.314 | 0.426 | 0.736 | 1.355 | 1.790 |
| 2.371 | 0.592 | 0.174 | 0.426 | 0.407 | 1.683 | 2.223 |
| 2.002 | 1.782 | 1.429 | 0.360 | 3.969 | 0.757 | 1.000 |
| 2.002 | 1.642 | 1.289 | 0.360 | 3.580 | 0.755 | 0.997 |
| 2.002 | 1.502 | 1.149 | 0.360 | 3.191 | 0.784 | 1.036 |
| 2.002 | 1.362 | 1.009 | 0.360 | 2.802 | 0.900 | 1.189 |
| 2.002 | 1.222 | 0.869 | 0.360 | 2.413 | 1.057 | 1.396 |
| 2.002 | 0.942 | 0.589 | 0.360 | 1.635 | 1.200 | 1.585 |
| 2.002 | 0.802 | 0.449 | 0.360 | 1.246 | 1.196 | 1.580 |
| 2.002 | 0.662 | 0.309 | 0.360 | 0.857 | 1.284 | 1.696 |
| 2.002 | 0.522 | 0.169 | 0.360 | 0.468 | 1.648 | 2.177 |
| 2.002 | 0.382 | 0.029 | 0.360 | 0.079 | 1.899 | 2.509 |
| 2.371 | 1.782 | 1.364 | 0.426 | 3.199 | 0.770 | 1.000 |
| 2.371 | 1.642 | 1.224 | 0.426 | 2.871 | 0.831 | 1.079 |
| 2.371 | 1.502 | 1.084 | 0.426 | 2.542 | 0.993 | 1.290 |
| 2.371 | 1.362 | 0.944 | 0.426 | 2.214 | 1.096 | 1.423 |
| 2.371 | 1.222 | 0.804 | 0.426 | 1.885 | 1.159 | 1.505 |
| 2.371 | 1.082 | 0.664 | 0.426 | 1.557 | 1.197 | 1.555 |
| 2.371 | 0.942 | 0.524 | 0.426 | 1.228 | 1.175 | 1.526 |
| 2.371 | 0.802 | 0.384 | 0.426 | 0.900 | 1.222 | 1.587 |
| 2.371 | 0.662 | 0.244 | 0.426 | 0.571 | 1.509 | 1.960 |
| 2.371 | 0.522 | 0.104 | 0.426 | 0.243 | 1.948 | 2.530 |

ALPHA= 12.0 BETAO= 21.5

| X (in.) | Y (in.) | DELY (in.) | YS (in.) | DELY/YS | P (psia) | P/PE |
|---|---|---|---|---|---|---|
| 1.995 | 2.061 | 1.637 | 0.362 | 4.525 | 0.758 | 1.000 |
| 1.995 | 1.921 | 1.497 | 0.362 | 4.138 | 0.747 | 0.985 |
| 1.995 | 1.781 | 1.357 | 0.362 | 3.751 | 0.745 | 0.983 |
| 1.995 | 1.641 | 1.217 | 0.362 | 3.364 | 0.768 | 1.013 |
| 1.995 | 1.501 | 1.077 | 0.362 | 2.977 | 0.921 | 1.215 |
| 1.995 | 1.361 | 0.937 | 0.362 | 2.590 | 1.095 | 1.445 |
| 1.995 | 1.221 | 0.797 | 0.362 | 2.203 | 1.203 | 1.587 |
| 1.995 | 1.081 | 0.657 | 0.362 | 1.817 | 1.220 | 1.609 |
| 1.995 | 0.941 | 0.517 | 0.362 | 1.430 | 1.217 | 1.606 |
| 1.995 | 0.801 | 0.377 | 0.362 | 1.043 | 1.243 | 1.640 |
| 1.995 | 0.661 | 0.237 | 0.362 | 0.656 | 1.559 | 2.057 |
| 1.995 | 0.521 | 0.097 | 0.362 | 0.269 | 2.114 | 2.789 |
| 2.364 | 2.061 | 1.559 | 0.429 | 3.636 | 0.736 | 1.000 |
| 2.364 | 1.921 | 1.419 | 0.429 | 3.309 | 0.755 | 1.026 |
| 2.364 | 1.781 | 1.279 | 0.429 | 2.983 | 0.863 | 1.173 |
| 2.364 | 1.641 | 1.139 | 0.429 | 2.656 | 1.040 | 1.413 |
| 2.364 | 1.501 | 0.999 | 0.429 | 2.330 | 1.134 | 1.541 |
| 2.364 | 1.361 | 0.859 | 0.429 | 2.003 | 1.211 | 1.645 |
| 2.364 | 1.221 | 0.719 | 0.429 | 1.677 | 1.248 | 1.696 |
| 2.364 | 1.081 | 0.579 | 0.429 | 1.350 | 1.202 | 1.633 |
| 2.364 | 0.941 | 0.439 | 0.429 | 1.024 | 1.220 | 1.658 |
| 2.364 | 0.801 | 0.299 | 0.429 | 0.697 | 1.503 | 2.042 |
| 2.364 | 0.661 | 0.159 | 0.429 | 0.371 | 2.045 | 2.779 |
| 1.995 | 1.851 | 1.427 | 0.362 | 3.944 | 0.764 | 1.000 |
| 1.995 | 1.711 | 1.287 | 0.362 | 3.558 | 0.773 | 1.012 |
| 1.995 | 1.571 | 1.147 | 0.362 | 3.171 | 0.842 | 1.102 |
| 1.995 | 1.431 | 1.007 | 0.362 | 2.784 | 1.042 | 1.364 |
| 1.995 | 1.291 | 0.867 | 0.362 | 2.397 | 1.172 | 1.534 |
| 1.995 | 1.011 | 0.587 | 0.362 | 1.623 | 1.265 | 1.656 |
| 1.995 | 0.871 | 0.447 | 0.362 | 1.236 | 1.218 | 1.594 |
| 1.995 | 0.731 | 0.307 | 0.362 | 0.849 | 1.393 | 1.823 |
| 1.995 | 0.591 | 0.167 | 0.362 | 0.462 | 1.923 | 2.517 |
| 1.995 | 0.451 | 0.027 | 0.362 | 0.075 | 2.295 | 3.004 |
| 2.364 | 1.851 | 1.349 | 0.429 | 3.146 | 0.823 | 1.000 |
| 2.364 | 1.711 | 1.209 | 0.429 | 2.819 | 0.982 | 1.193 |
| 2.364 | 1.571 | 1.069 | 0.429 | 2.493 | 1.130 | 1.373 |
| 2.364 | 1.431 | 0.929 | 0.429 | 2.166 | 1.208 | 1.468 |
| 2.364 | 1.291 | 0.789 | 0.429 | 1.840 | 1.254 | 1.524 |
| 2.364 | 1.151 | 0.649 | 0.429 | 1.513 | 1.261 | 1.532 |
| 2.364 | 1.011 | 0.509 | 0.429 | 1.187 | 1.234 | 1.499 |
| 2.364 | 0.871 | 0.369 | 0.429 | 0.860 | 1.383 | 1.680 |
| 2.364 | 0.731 | 0.229 | 0.429 | 0.534 | 1.793 | 2.179 |
| 2.364 | 0.591 | 0.089 | 0.429 | 0.207 | 2.424 | 2.945 |

ALPHA= 14.0 BETAO= 23.5

| X (in.) | Y (in.) | DELY (in.) | YS (in.) | DELY/YS | P (psia) | P/PE |
|---|---|---|---|---|---|---|
| 1.986 | 2.131 | 1.636 | 0.368 | 4.441 | 0.779 | 1.000 |
| 1.986 | 1.991 | 1.496 | 0.368 | 4.061 | 0.768 | 0.986 |
| 1.986 | 1.851 | 1.356 | 0.368 | 3.681 | 0.777 | 0.997 |
| 1.986 | 1.711 | 1.216 | 0.368 | 3.300 | 0.886 | 1.137 |
| 1.986 | 1.571 | 1.076 | 0.368 | 2.920 | 1.118 | 1.435 |
| 1.986 | 1.431 | 0.936 | 0.368 | 2.540 | 1.250 | 1.605 |
| 1.986 | 1.291 | 0.796 | 0.368 | 2.160 | 1.334 | 1.712 |
| 1.986 | 1.151 | 0.656 | 0.368 | 1.780 | 1.345 | 1.727 |
| 1.986 | 1.011 | 0.516 | 0.368 | 1.400 | 1.267 | 1.626 |
| 1.986 | 0.871 | 0.376 | 0.368 | 1.020 | 1.336 | 1.715 |
| 1.986 | 0.731 | 0.236 | 0.368 | 0.640 | 1.779 | 2.284 |
| 1.986 | 0.591 | 0.096 | 0.368 | 0.260 | 2.600 | 3.338 |
| 2.355 | 2.131 | 1.544 | 0.437 | 3.534 | 0.767 | 1.000 |
| 2.355 | 1.991 | 1.404 | 0.437 | 3.214 | 0.879 | 1.146 |
| 2.355 | 1.851 | 1.264 | 0.437 | 2.893 | 1.095 | 1.428 |
| 2.355 | 1.711 | 1.124 | 0.437 | 2.573 | 1.226 | 1.598 |
| 2.355 | 1.571 | 0.984 | 0.437 | 2.252 | 1.299 | 1.694 |
| 2.355 | 1.431 | 0.844 | 0.437 | 1.932 | 1.336 | 1.742 |
| 2.355 | 1.291 | 0.704 | 0.437 | 1.611 | 1.324 | 1.726 |
| 2.355 | 1.151 | 0.564 | 0.437 | 1.291 | 1.257 | 1.639 |
| 2.355 | 1.011 | 0.424 | 0.437 | 0.970 | 1.351 | 1.761 |
| 2.355 | 0.871 | 0.284 | 0.437 | 0.650 | 1.759 | 2.293 |
| 2.355 | 0.731 | 0.144 | 0.437 | 0.329 | 2.593 | 3.381 |
| 1.986 | 1.921 | 1.426 | 0.368 | 3.871 | 0.769 | 1.000 |
| 1.986 | 1.781 | 1.286 | 0.368 | 3.490 | 0.825 | 1.073 |

EXCERPT
SEE DATA
FILE:
ROD1.DAT

********** Surface Flow Visualization Results **********

The following table lists the results from the SFVP study. The inception length (LI), and angles of upstream influence (BETAU) and primary separation line (BETAS1) are presented below (DELTA=0.25 in.).

| ALPHA (deg) | LI/DELTA | BETAU (deg) | BETAS1 (deg) |
|---|---|---|---|
| 6.0 | 4.44 | 22. | 20. |
| 8.0 | 4.28 | 26. | 23. |
| 10.0 | 3.76 | 29. | 27. |
| 12.0 | 3.16 | 34. | 31. |
| 14.0 | 2.72 | 36. | 34. |
| 15.0 (Gibson) | N/A | 36. | 34. |

Using the primary separation line (clearly seen on the SFVP) and the inviscid shock trace (calculated analytically) a VCO can be determined from the intersection of these two features.

Location of VCOv from Primary Separation Line and Inviscid Shock Wave

| ALPHA (deg) | X/DELTA | Y/DELTA |
|---|---|---|
| 6.0 | -6.64 | -2.04 |
| 8.0 | -5.48 | -1.76 |
| 10.0 | -4.52 | -1.60 |
| 12.0 | -3.48 | -1.36 |
| 14.0 | -3.24 | -1.40 |

The locations of the virtual conical origin of the pressure fields, obtained by matching features of the various cross plane distributions and extrapolating back to the VCOp, are list below.

Location of VCOp from Pressure Distributions

| ALPHA (deg) | X/DELTA | Y/DELTA |
|---|---|---|
| 8.0 | -3.55 | -1.44 |
| 16.0 | -1.90 | -0.91 |

********** Spanwise Heat Transfer Data **********

Next are given the spanwise heat transfer measurements for fin angles of attack of 6-, 8-, 10-, 12- ,14- and 16-degrees. Data from four runs were combined to produce a distribution with increased spatial resolution.

ALPHA= 6.000 BETAO= 16.100

TO= 299.04(F) CHE= 0.00050

| X (in.) | Y (in.) | DELY (in.) | YS | DELY/YS | TW (F) | QDOT (BTU/FT^2sec) | CH | CH/CHE |
|---|---|---|---|---|---|---|---|---|
| 2.009 | 1.886 | 1.675 | 0.369 | 4.54 | 78.53 | 0.696 | 0.00050 | 1.000 |
| 2.009 | 1.324 | 1.113 | 0.369 | 3.02 | 82.59 | 0.705 | 0.00052 | 1.040 |
| 2.009 | 1.043 | 0.832 | 0.369 | 2.26 | 81.23 | 0.790 | 0.00058 | 1.160 |
| 2.009 | 0.762 | 0.551 | 0.369 | 1.49 | 92.07 | 0.841 | 0.00066 | 1.320 |
| 2.009 | 0.481 | 0.270 | 0.369 | 0.73 | 87.39 | 1.346 | 0.00103 | 2.060 |

TO= 301.52(F) CHE= 0.00050

| X (in.) | Y (in.) | DELY (in.) | YS | DELY/YS | TW (F) | QDOT (BTU/FT^2sec) | CH | CH/CHE |
|---|---|---|---|---|---|---|---|---|
| 2.009 | 1.685 | 1.474 | 0.369 | 4.00 | 95.15 | 0.691 | 0.00055 | 1.100 |
| 2.009 | 1.404 | 1.193 | 0.369 | 3.24 | 94.20 | 0.632 | 0.00050 | 1.000 |
| 2.009 | 1.123 | 0.912 | 0.369 | 2.47 | 105.65 | 0.749 | 0.00064 | 1.280 |
| 2.009 | 0.842 | 0.631 | 0.369 | 1.71 | 99.27 | 0.792 | 0.00065 | 1.300 |
| 2.009 | 0.561 | 0.350 | 0.369 | 0.95 | 101.08 | 1.036 | 0.00086 | 1.720 |

TO= 303.45(F) CHE= 0.00049

| X (in.) | Y (in.) | DELY (in.) | YS | DELY/YS | TW (F) | QDOT (BTU/FT^2sec) | CH | CH/CHE |
|---|---|---|---|---|---|---|---|---|
| 2.009 | 1.746 | 1.535 | 0.369 | 4.16 | 103.76 | 0.577 | 0.00048 | 0.980 |
| 2.009 | 1.465 | 1.254 | 0.369 | 3.40 | 103.72 | 0.599 | 0.00050 | 1.020 |
| 2.009 | 1.184 | 0.973 | 0.369 | 2.64 | 105.50 | 0.685 | 0.00058 | 1.184 |
| 2.009 | 0.903 | 0.692 | 0.369 | 1.88 | 105.37 | 0.756 | 0.00064 | 1.306 |
| 2.009 | 0.622 | 0.411 | 0.369 | 1.11 | 114.88 | 0.843 | 0.00077 | 1.571 |
| 2.009 | 0.341 | 0.130 | 0.369 | 0.35 | 98.14 | 1.281 | 0.00103 | 2.102 |

TO= 301.94(F) CHE= 0.00050

| X (in.) | Y (in.) | DELY (in.) | YS | DELY/YS | TW (F) | QDOT (BTU/FT^2sec) | CH | CH/CHE |
|---|---|---|---|---|---|---|---|---|
| 2.009 | 1.816 | 1.605 | 0.369 | 4.35 | 86.19 | 0.668 | 0.00050 | 1.000 |
| 2.009 | 1.535 | 1.324 | 0.369 | 3.59 | 86.80 | 0.679 | 0.00051 | 1.020 |
| 2.009 | 1.254 | 1.043 | 0.369 | 2.83 | 89.36 | 0.724 | 0.00055 | 1.100 |
| 2.009 | 0.973 | 0.762 | 0.369 | 2.07 | 88.76 | 0.767 | 0.00058 | 1.160 |
| 2.009 | 0.692 | 0.481 | 0.369 | 1.30 | 97.39 | 0.828 | 0.00067 | 1.340 |
| 2.009 | 0.411 | 0.200 | 0.369 | 0.54 | 86.88 | 1.411 | 0.00106 | 2.120 |

ALPHA= 8.000 BETAO= 17.800

TO= 301.60(F) CHE= 0.00050

| X (in.) | Y (in.) | DELY (in.) | YS | DELY/YS | TW (F) | QDOT (BTU/FT^2sec) | CH | CH/CHE |
|---|---|---|---|---|---|---|---|---|
| 2.007 | 1.967 | 1.685 | 0.362 | 4.65 | 95.60 | 0.624 | 0.00050 | 1.000 |
| 2.007 | 1.405 | 1.123 | 0.362 | 3.10 | 97.08 | 0.633 | 0.00051 | 1.020 |
| 2.007 | 1.124 | 0.842 | 0.362 | 2.32 | 95.74 | 0.766 | 0.00061 | 1.220 |
| 2.007 | 0.843 | 0.561 | 0.362 | 1.55 | 108.30 | 0.804 | 0.00071 | 1.420 |
| 2.007 | 0.562 | 0.280 | 0.362 | 0.77 | 101.39 | 1.413 | 0.00118 | 2.360 |

TO= 300.61(F) CHE= 0.00049

| X (in.) | Y (in.) | DELY (in.) | YS | DELY/YS | TW (F) | QDOT (BTU/FT^2sec) | CH | CH/CHE |
|---|---|---|---|---|---|---|---|---|
| 2.007 | 1.756 | 1.474 | 0.362 | 4.07 | 97.62 | 0.672 | 0.00055 | 1.122 |
| 2.007 | 1.475 | 1.193 | 0.362 | 3.29 | 96.08 | 0.613 | 0.00049 | 1.000 |
| 2.007 | 1.194 | 0.912 | 0.362 | 2.52 | 108.52 | 0.802 | 0.00071 | 1.449 |
| 2.007 | 0.913 | 0.631 | 0.362 | 1.74 | 101.06 | 0.765 | 0.00064 | 1.306 |
| 2.007 | 0.632 | 0.350 | 0.362 | 0.97 | 104.13 | 1.179 | 0.00101 | 2.061 |

TO= 303.74(F) CHE= 0.00048

| X (in.) | Y (in.) | DELY (in.) | YS | DELY/YS | TW (F) | QDOT (BTU/FT^2sec) | CH | CH/CHE |
|---|---|---|---|---|---|---|---|---|
| 2.007 | 1.817 | 1.535 | 0.362 | 4.24 | 92.20 | 0.629 | 0.00048 | 1.000 |
| 2.007 | 1.536 | 1.254 | 0.362 | 3.46 | 94.04 | 0.654 | 0.00051 | 1.062 |
| 2.007 | 1.255 | 0.973 | 0.362 | 2.69 | 95.94 | 0.788 | 0.00062 | 1.292 |
| 2.007 | 0.974 | 0.692 | 0.362 | 1.91 | 95.73 | 0.826 | 0.00065 | 1.354 |
| 2.007 | 0.693 | 0.411 | 0.362 | 1.13 | 106.70 | 1.096 | 0.00094 | 1.958 |
| 2.007 | 0.412 | 0.130 | 0.362 | 0.36 | 89.25 | 1.699 | 0.00128 | 2.667 |

TO= 303.88(F) CHE= 0.00048

| X (in.) | Y (in.) | DELY (in.) | YS | DELY/YS | TW (F) | QDOT (BTU/FT^2sec) | CH | CH/CHE |
|---|---|---|---|---|---|---|---|---|
| 2.007 | 1.897 | 1.615 | 0.362 | 4.46 | 98.64 | 0.603 | 0.00048 | 1.000 |
| 2.007 | 1.616 | 1.334 | 0.362 | 3.68 | 97.71 | 0.613 | 0.00049 | 1.021 |
| 2.007 | 1.335 | 1.053 | 0.362 | 2.91 | 100.58 | 0.676 | 0.00055 | 1.146 |
| 2.007 | 1.054 | 0.772 | 0.362 | 2.13 | 100.04 | 0.727 | 0.00059 | 1.229 |
| 2.007 | 0.773 | 0.491 | 0.362 | 1.36 | 108.73 | 0.934 | 0.00081 | 1.688 |
| 2.007 | 0.492 | 0.210 | 0.362 | 0.58 | 99.36 | 1.565 | 0.00126 | 2.625 |

EXCERPT. SEE DATA FILE: RODI.DAT

Author: Settles, G. S., *et al*
Geometry: 2-D Compression Corner
Mach number: 3
Data: $p_{wall}$, $c_f$, mean flowfield pitot surveys

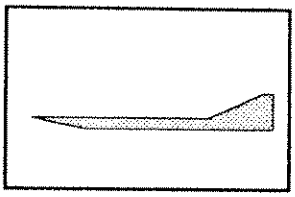

Settles, G. S., Fitzpatrick, T. J. and Bogdonoff, S. M., "Detailed Study of Attached and Separated Compression Corner Flowfields in High Reynolds Number Supersonic Flow," *AIAA Journal*, Vol. 17, No. 6, June 1979, pp. 579.

Settles, G.S., Gilbert, R.B. and Bogdonoff, S.M., "Data Compilation For Shock Wave/Turbulent Boundary Layer Interaction Experiments On Two-Dimensional Compression Corners," *Princeton University Report 1489-MAE*, Princeton Univ. 1980.

The data consist of both mean surveys of flow properties before and after two-dimensional compression corners at Mach numbers in the vicinity of 2.9. Compression corner angles of 8, 16, 20, and 24 degrees span the range from attached flow to large boundary-layer separation. Two-dimensionality of the experiments was demonstrated by studies of spanwise oil-flow patterns for all but the largest compression corner angle, where significant 3-D perturbations were observed.

The mean data include surface pressure and skin friction distributions, as well as pitot and static pressure distributions from which velocity and Mach number were deduced (the total temperature distribution through these interactions was nearly constant). *Note: the fluctuating data corresponding to this mean dataset were presented in the file SMITS.DAT in Ref. 1 and remain unchanged. The present correction and re-tabulation covers only the mean-flow data. It is given as file SETTLES2.DAT on the accompanying diskette.*

All units in the tables are SI. The x-coordinate is defined in the streamwise direction along the wind tunnel floor and compression corner surfaces. Thus locations upstream of the corner have negative x-values and those downstream have positive values. The compression corners were all located at 1.205 m downstream of the wind tunnel nozzle exit with the exception of the 24 degree corner for hot-wire measurements only, which was located 1.17 m downstream of the nozzle exit. The y-coordinate is measured upward from the test surface with its origin at that surface. The origin of the z-coordinate is on the wind tunnel centerline. It is taken positive to the left when looking downstream. See the diagram of the flow configuration reproduced below.

Users are encouraged to consult the cited references for detailed discussions of the data and their significance, which are beyond the present scope, as well as estimates of the various errors and discrepancies which serve to set confidence limits upon the data.

SCHEMATIC DIAGRAM OF FLOW CONFIGURATION

COMPRESSION CORNERS

PRINCETON HIGH REYNOLDS NUMBER SUPERSONIC WIND TUNNEL

TUNNEL WIDTH= 20.32 CM

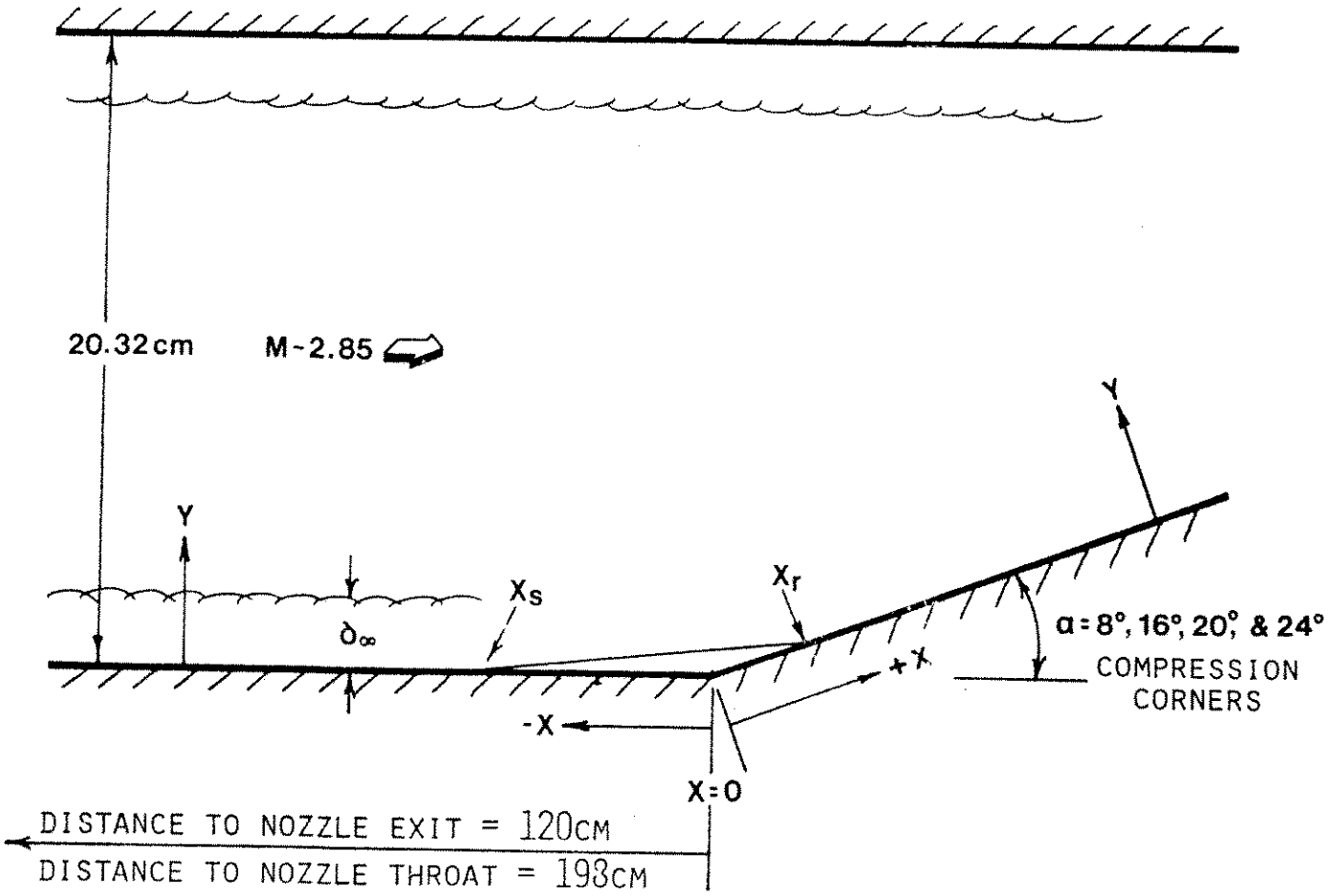

SETTLES2.DAT REVISED 7/18/93

**********MEAN-FLOW DATA**********

SETTLES et al 2-D COMPRESSION CORNER INTERACTIONS

**********

DEFINITIONS

alpha = compression corner angle, degrees
CF = TAUWAL/RHOINF*UREF**2
DELTA = boundary layer thickness, cm
DELTA* = boundary layer displacement thickness, cm
Mref = Nominal incoming freestream Mach number
PINF = Freestream static pressure, N/m**2
PT1 = Freestream total pressure, N/m**2
PW, Pwall = Wall pressure, N/m**2
RHOINF = Freestream density, kg/m**2
SECTION = Wind tunnel test section (1, 2, or 3; see source document)
TAUWAL = Wall shear stress, N/m**2
THETA = boundary layer momentum thickness, cm
TT1 = Freestream total temperature, K
TWINF = Flat-plate wall temperature ahead of interaction
UREF = Freestream velocity, m/s
X = Streamwise coordinate, zero at corner, measured along flat plate or ramp, m
Y = Vertical coordinate, zero at model, measured along direction of survey line, m
Z = Spanwise distance from model centerline, m

NOMINAL FREESTREAM AND INCOMING CONDITIONS

**********

All cases: freestream Re/m = 6.3E+07. Distance from nozzle to compression corner = 198 cm.

**********

| alpha | 8 | 16 | 20 | 24 |
|---|---|---|---|---|
| Mref | 2.87 | 2.85 | 2.85 | 2.84 |
| PINF | 2.30E+04 | 2.29E+04 | 2.32E+04 | 2.36E+04 N/m**2 |
| TT1 | 280 | 268 | 258 | 262 K |
| TWINF | 291 | 282 | 274 | 276 K |
| UREF | 592 | 576 | 562 | 569 m/s |
| DELTA | 2.6 | 2.6 | 2.5 | 2.3 cm |
| DELTA* | 0.67 | 0.63 | 0.66 | 0.61 cm |
| THETA | 0.13 | 0.13 | 0.13 | 0.12 cm |

**********UNCERTAINTIES**********

PWALL ± 2%
CFINF ± 15%
(PROFILE DATA)
U ± 5%
P ± 4%
M ± 3%

**********SURFACE-PRESSURE DISTRIBUTIONS**********

8 DEGREE RAMP

| X, cm | Pwall/PINF |
|---|---|
| -2.54 | 1.00 |
| -1.02 | 1.00 |
| -0.51 | 1.00 |
| -0.25 | 1.02 |
| -0.24 | 1.03 |
| -0.18 | 1.06 |
| -0.12 | 1.13 |
| -0.06 | 1.22 |
| 0.0 | 1.35 |
| 0.06 | 1.42 |
| 0.12 | 1.45 |
| 0.18 | 1.46 |
| 0.24 | 1.48 |
| 0.25 | 1.47 |
| 0.38 | 1.47 |
| 0.51 | 1.47 |
| 0.76 | 1.48 |
| 1.02 | 1.49 |
| 1.52 | 1.52 |
| 2.03 | 1.55 |
| 2.54 | 1.57 |
| 3.56 | 1.60 |
| 4.57 | 1.65 |
| 5.08 | 1.67 |
| 5.59 | 1.68 |
| 6.60 | 1.70 |
| 7.62 | 1.70 |
| 8.64 | 1.71 |
| 9.65 | 1.72 |
| 10.16 | 1.73 |
| 10.67 | 1.73 |
| 12.70 | 1.74 |
| 12.70 | 1.74 |
| 15.24 | 1.76 |

16 DEGREE RAMP

| X, cm | Pwall/PINF |
|---|---|
| -5.08 | 1.01 |
| -3.81 | 1.00 |
| -2.22 | 1.00 |
| -1.91 | 1.00 |
| -1.58 | 1.00 |
| -1.27 | 1.00 |
| -0.95 | 1.00 |
| -0.87 | 1.03 |
| -0.79 | 1.05 |
| -0.71 | 1.08 |
| -0.64 | 1.18 |
| -0.56 | 1.30 |
| -0.48 | 1.40 |
| -0.40 | 1.50 |
| -0.32 | 1.57 |
| -0.24 | 1.63 |
| -0.16 | 1.68 |
| -0.08 | 1.72 |
| 0.00 | 1.77 |
| 0.08 | 1.85 |
| 0.16 | 1.90 |
| 0.24 | 1.94 |
| 0.32 | 2.02 |
| 0.40 | 2.04 |
| 0.48 | 2.08 |
| 0.56 | 2.12 |
| 0.64 | 2.16 |
| 0.95 | 2.23 |
| 1.27 | 2.30 |
| 2.22 | 2.45 |
| 3.81 | 2.65 |
| 5.72 | 2.78 |
| 7.62 | 2.82 |
| 11.43 | 2.85 |

20 DEGREE RAMP

| X, cm | Pwall/PINF |
|---|---|
| -5.08 | 0.99 |
| -3.81 | 1.00 |
| -2.70 | 1.00 |
| -2.38 | 1.03 |
| -2.22 | 1.07 |
| -2.06 | 1.16 |
| -1.91 | 1.32 |
| -1.75 | 1.44 |
| -1.59 | 1.56 |
| -1.43 | 1.60 |
| -1.27 | 1.67 |
| -1.11 | 1.71 |
| -0.95 | 1.76 |
| -0.79 | 1.78 |
| -0.64 | 1.82 |
| -0.56 | 1.85 |
| -0.48 | 1.87 |
| -0.40 | 1.89 |
| -0.32 | 1.90 |
| -0.24 | 1.91 |
| -0.16 | 1.94 |
| -0.08 | 1.97 |
| 0.00 | 2.00 |
| 0.08 | 2.02 |
| 0.16 | 2.06 |
| 0.24 | 2.12 |
| 0.48 | 2.20 |
| 0.64 | 2.30 |
| 0.95 | 2.42 |
| 1.27 | 2.53 |
| 2.22 | 2.83 |
| 3.81 | 3.15 |
| 5.72 | 3.32 |
| 7.62 | 3.43 |
| 11.43 | 3.56 |

24 DEGREE RAMP

| X, cm | Pwall/PINF |
|---|---|
| -7.62 | 1.02 |
| -6.35 | 1.01 |
| -5.08 | 1.02 |
| -4.57 | 1.04 |
| -4.06 | 1.26 |
| -3.56 | 1.64 |
| -3.30 | 1.69 |
| -2.79 | 1.80 |
| -2.29 | 1.90 |
| -1.78 | 1.99 |
| -1.27 | 2.07 |
| -0.76 | 2.15 |
| -0.25 | 2.23 |
| 0.0 | 2.28 |
| 0.51 | 2.44 |
| 1.02 | 2.59 |
| 2.54 | 3.09 |
| 3.05 | 3.29 |
| 4.57 | 3.68 |
| 5.08 | 3.73 |
| 6.10 | 3.80 |
| 7.11 | 3.89 |
| 8.64 | 3.97 |
| 9.65 | 4.07 |
| 10.67 | 4.17 |
| 11.68 | 4.26 |
| 12.70 | 4.25 |

**********SKIN FRICTION DATA**********

ALL UNITS ARE SYSTEM INTERNATIONAL
FREESTREAM VALUES MAY NOT EXACTLY MATCH NOMINAL VALUES CITED

ALPHA=8 DEG RAMP, Z = -0.0127, PRESTON TUBE DIA. = 8.130E-04 m

| X | PT1 | TT1 | TAUWAL | CF |
|---|---|---|---|---|
| -2.540E-02 | 6.894E+05 | 2.780E+02 | 1.335E+02 | 1.003E-03 |

| | | | | |
|---|---|---|---|---|
| -1.520E-02 | 6.894E+05 | 2.780E+02 | 1.322E+02 | 9.925E-04 |
| -7.620E-03 | 6.894E+05 | 2.780E+02 | 1.315E+02 | 9.875E-04 |
| -5.080E-03 | 6.894E+05 | 2.780E+02 | 1.229E+02 | 9.225E-04 |
| -2.540E-03 | 6.894E+05 | 2.780E+02 | 1.237E+02 | 9.291E-04 |
| 0.000E+00 | 6.894E+05 | 2.780E+02 | 1.039E+02 | 7.800E-04 |
| 2.540E-03 | 6.894E+05 | 2.780E+02 | 1.021E+02 | 7.665E-04 |
| 5.080E-03 | 6.894E+05 | 2.780E+02 | 1.115E+02 | 8.369E-04 |
| 7.620E-03 | 6.894E+05 | 2.780E+02 | 1.199E+02 | 9.003E-04 |
| 1.020E-02 | 6.894E+05 | 2.780E+02 | 1.258E+02 | 9.447E-04 |
| 1.520E-02 | 6.894E+05 | 2.780E+02 | 1.360E+02 | 1.021E-03 |
| 2.030E-02 | 6.894E+05 | 2.780E+02 | 1.452E+02 | 1.091E-03 |
| 2.540E-02 | 6.894E+05 | 2.780E+02 | 1.543E+02 | 1.159E-03 |
| 3.050E-02 | 6.894E+05 | 2.780E+02 | 1.599E+02 | 1.201E-03 |
| 3.560E-02 | 6.894E+05 | 2.780E+02 | 1.638E+02 | 1.230E-03 |
| 4.060E-02 | 6.894E+05 | 2.780E+02 | 1.669E+02 | 1.253E-03 |
| 4.570E-02 | 6.894E+05 | 2.780E+02 | 1.726E+02 | 1.296E-03 |
| 5.080E-02 | 6.894E+05 | 2.780E+02 | 1.767E+02 | 1.327E-03 |
| 5.590E-02 | 6.894E+05 | 2.780E+02 | 1.796E+02 | 1.349E-03 |
| 6.600E-02 | 6.894E+05 | 2.780E+02 | 1.810E+02 | 1.359E-03 |
| 7.620E-02 | 6.894E+05 | 2.780E+02 | 1.890E+02 | 1.419E-03 |
| 8.640E-02 | 6.894E+05 | 2.780E+02 | 1.914E+02 | 1.437E-03 |
| 9.650E-02 | 6.894E+05 | 2.780E+02 | 1.996E+02 | 1.499E-03 |
| 1.070E-01 | 6.894E+05 | 2.780E+02 | 1.980E+02 | 1.487E-03 |
| 1.170E-01 | 6.894E+05 | 2.780E+02 | 2.022E+02 | 1.518E-03 |
| 1.270E-01 | 6.894E+05 | 2.780E+02 | 2.022E+02 | 1.518E-03 |
| 1.370E-01 | 6.894E+05 | 2.780E+02 | 2.075E+02 | 1.558E-03 |

ALPHA=16 DEG RAMP, Z = -0.0127, PRESTON TUBE DIA. = 8.38E-04 m

| X | PT1 | TT1 | TAUWAL | CF |
|---|---|---|---|---|
| -3.810E-02 | 6.894E+05 | 2.650E+02 | 1.338E+02 | 9.835E-04 |
| -2.540E-02 | 6.894E+05 | 2.650E+02 | 1.338E+02 | 9.835E-04 |
| -1.270E-02 | 6.894E+05 | 2.650E+02 | 1.385E+02 | 1.018E-03 |
| -9.530E-03 | 6.894E+05 | 2.650E+02 | 1.265E+02 | 9.299E-04 |
| -6.350E-03 | 6.894E+05 | 2.650E+02 | 8.351E+01 | 6.139E-04 |
| -3.180E-03 | 6.894E+05 | 2.650E+02 | 3.498E+00 | 2.572E-05 |
| 0.000E+00 | 6.894E+05 | 2.650E+02 | 3.270E+01 | 2.404E-04 |
| 3.180E-03 | 6.894E+05 | 2.650E+02 | 3.493E+01 | 2.568E-04 |
| 6.350E-03 | 6.894E+05 | 2.650E+02 | 7.186E+01 | 5.282E-04 |
| 9.530E-03 | 6.894E+05 | 2.650E+02 | 9.512E+01 | 6.993E-04 |
| 1.270E-02 | 6.894E+05 | 2.650E+02 | 1.069E+02 | 7.858E-04 |
| 1.910E-02 | 6.894E+05 | 2.650E+02 | 1.388E+02 | 1.021E-03 |
| 2.540E-02 | 6.894E+05 | 2.650E+02 | 1.473E+02 | 1.083E-03 |
| 3.810E-02 | 6.894E+05 | 2.650E+02 | 1.729E+02 | 1.271E-03 |
| 5.080E-02 | 6.894E+05 | 2.650E+02 | 1.973E+02 | 1.451E-03 |
| 7.620E-02 | 6.894E+05 | 2.650E+02 | 2.346E+02 | 1.725E-03 |
| 1.020E-01 | 6.894E+05 | 2.650E+02 | 2.574E+02 | 1.892E-03 |
| 1.270E-01 | 6.894E+05 | 2.650E+02 | 2.735E+02 | 2.011E-03 |
| 1.400E-01 | 6.894E+05 | 2.650E+02 | 2.825E+02 | 2.077E-03 |

ALPHA=20 DEG RAMP, Z = -0.0127, PRESTON TUBE DIA. = 8.13E-04 m

| X | PT1 | TT1 | TAUWAL | CF |
|---|---|---|---|---|
| -3.810E-02 | 6.894E+05 | 2.670E+02 | 1.417E+02 | 9.968E-04 |
| -2.220E-02 | 6.894E+05 | 2.670E+02 | 1.258E+02 | 8.854E-04 |
| -1.910E-02 | 6.894E+05 | 2.670E+02 | 8.131E+01 | 5.721E-04 |
| -1.590E-02 | 6.894E+05 | 2.670E+02 | 4.521E+01 | 3.181E-04 |
| -1.270E-02 | 6.894E+05 | 2.670E+02 | 2.056E+01 | 1.447E-04 |
| -1.110E-02 | 6.894E+05 | 2.670E+02 | 1.973E+01 | 1.388E-04 |
| -9.530E-03 | 6.894E+05 | 2.670E+02 | 1.124E+01 | 7.907E-05 |
| -6.350E-03 | 6.894E+05 | 2.670E+02 | 1.690E+01 | 1.189E-04 |
| -9.530E-03 | 6.894E+05 | 2.670E+02 | 3.883E+01 | 2.732E-04 |
| -1.270E-02 | 6.894E+05 | 2.670E+02 | 4.580E+01 | 3.222E-04 |
| -1.590E-02 | 6.894E+05 | 2.670E+02 | 7.370E+01 | 5.185E-04 |
| -1.910E-02 | 6.894E+05 | 2.670E+02 | 8.051E+01 | 5.665E-04 |
| -2.220E-02 | 6.894E+05 | 2.670E+02 | 8.936E+01 | 6.287E-04 |
| -2.540E-02 | 6.894E+05 | 2.670E+02 | 9.822E+01 | 6.911E-04 |
| -3.180E-02 | 6.894E+05 | 2.670E+02 | 1.181E+02 | 8.308E-04 |
| -4.130E-02 | 6.894E+05 | 2.670E+02 | 1.329E+02 | 9.351E-04 |

| | | | | |
|---|---|---|---|---|
| -5.720E-02 | 6.894E+05 | 2.670E+02 | 1.796E+02 | 1.263E-03 |
| -7.620E-02 | 6.894E+05 | 2.670E+02 | 2.243E+02 | 1.578E-03 |
| -9.530E-02 | 6.894E+05 | 2.670E+02 | 2.550E+02 | 1.794E-03 |
| -1.140E-01 | 6.894E+05 | 2.670E+02 | 2.726E+02 | 1.918E-03 |

ALPHA=24 DEG RAMP, Z = -0.0127, PRESTON TUBE DIA. = 1.57E-03 m

| X | PT1 | TT1 | TAUWAL | CF |
|---|---|---|---|---|
| -6.350E-02 | 6.894E+05 | 2.620E+02 | 1.406E+02 | 1.034E-03 |
| -5.080E-02 | 6.894E+05 | 2.620E+02 | 1.406E+02 | 1.034E-03 |
| -4.570E-02 | 6.894E+05 | 2.620E+02 | 1.180E+02 | 8.676E-04 |
| -4.320E-02 | 6.894E+05 | 2.620E+02 | 9.654E+01 | 7.100E-04 |
| -4.060E-02 | 6.894E+05 | 2.620E+02 | 9.174E+01 | 6.746E-04 |
| -3.810E-02 | 6.894E+05 | 2.620E+02 | 8.652E+01 | 6.363E-04 |
| -3.560E-02 | 6.894E+05 | 2.620E+02 | 8.549E+01 | 6.287E-04 |
| -3.300E-02 | 6.894E+05 | 2.620E+02 | 8.549E+01 | 6.287E-04 |
| -1.020E-02 | 6.894E+05 | 2.620E+02 | 1.244E+01 | 9.152E-05 |
| -1.520E-02 | 6.894E+05 | 2.620E+02 | 3.216E+01 | 2.365E-04 |
| -2.030E-02 | 6.894E+05 | 2.620E+02 | 4.197E+01 | 3.087E-04 |
| -3.050E-02 | 6.894E+05 | 2.620E+02 | 6.496E+01 | 4.777E-04 |
| -5.080E-02 | 6.894E+05 | 2.620E+02 | 1.180E+02 | 8.679E-04 |
| -6.100E-02 | 6.894E+05 | 2.620E+02 | 1.539E+02 | 1.132E-03 |
| -1.090E-01 | 6.894E+05 | 2.620E+02 | 2.133E+02 | 1.569E-03 |
| -1.020E-01 | 6.894E+05 | 2.620E+02 | 2.528E+02 | 1.859E-03 |
| -1.220E-01 | 6.894E+05 | 2.620E+02 | 2.910E+02 | 2.140E-03 |
| -1.420E-01 | 6.894E+05 | 2.620E+02 | 3.185E+02 | 2.342E-03 |

**********MEAN PROFILE DATA**********
FREESTREAM VALUES MAY NOT EXACTLY MATCH NOMINAL VALUES CITED EARLIER
**********

**********alpha = 8 degrees**********

MEAN PROFILE TABULATION
SURVEY NORMAL TO TUNNEL FLOOR-VERTICAL

| | |
|---|---|
| X | = -.2540E-01 |
| Z | = -.1270E-01 |
| Stagnation Pressure | = 0.6804E+06 |
| Stagnation Temperature | = 282.9 |
| M ref | = 2.870 |
| U ref | = 594.9 |
| P wall | = 0.2300E+05 |
| TAU wall | = 133.5 |

| Y, m | PT/PWALL | PS/PWALL | U/UREF | M |
|---|---|---|---|---|
| 0.7026E-03 | 2.060 | 0.9848 | 0.5630 | 1.083 |
| 0.8319E-03 | 2.519 | 0.9848 | 0.6292 | 1.250 |
| 0.9934E-03 | 2.780 | 0.9844 | 0.6607 | 1.335 |
| 0.1026E-02 | 3.010 | 0.9843 | 0.6847 | 1.402 |
| 0.1316E-02 | 3.204 | 0.9836 | 0.7037 | 1.458 |
| 0.1478E-02 | 3.313 | 0.9831 | 0.7130 | 1.487 |
| 0.1672E-02 | 3.487 | 0.9826 | 0.7289 | 1.536 |
| 0.1995E-02 | 3.639 | 0.9818 | 0.7413 | 1.575 |
| 0.2383E-02 | 3.834 | 0.9824 | 0.7565 | 1.625 |
| 0.2835E-02 | 3.996 | 0.9847 | 0.7665 | 1.660 |
| 0.3190E-02 | 4.176 | 0.9866 | 0.7784 | 1.703 |
| 0.3546E-02 | 4.387 | 0.9884 | 0.7909 | 1.749 |
| 0.3932E-02 | 4.552 | 0.9873 | 0.8016 | 1.789 |
| 0.4613E-02 | 4.713 | 0.9821 | 0.8110 | 1.825 |
| 0.5192E-02 | 4.909 | 0.9782 | 0.8250 | 1.874 |
| 0.5872E-02 | 5.096 | 0.9757 | 0.8353 | 1.917 |
| 0.6518E-02 | 5.348 | 0.9731 | 0.8483 | 1.974 |
| 0.7163E-02 | 5.470 | 0.9700 | 0.8545 | 2.002 |
| 0.7681E-02 | 5.709 | 0.9680 | 0.8651 | 2.051 |
| 0.8456E-02 | 5.883 | 0.9707 | 0.8698 | 2.080 |
| 0.9134E-02 | 6.057 | 0.9712 | 0.8782 | 2.115 |
| 0.9749E-02 | 6.243 | 0.9686 | 0.8863 | 2.151 |
| 0.1039E-01 | 6.400 | 0.9659 | 0.8940 | 2.186 |
| 0.1117E-01 | 6.578 | 0.9664 | 0.8997 | 2.214 |
| [illegible] | [illegible] | [illegible] | [illegible] | 2.257 |

NOTE: THE EXCERPT SHOWN HERE IS FOR SAMPLE PURPOSES ONLY. SPACE LIMITATIONS PRECLUDE A COMPLETE LISTING. SEE DISKETTE FILE SETTLES2.DAT

# REPORT DOCUMENTATION PAGE

*Form Approved*
*OMB No. 0704-0188*

Public reporting burden for this collection of information is estimated to average 1 hour per response, including the time for reviewing instructions, searching existing data sources, gathering and maintaining the data needed, and completing and reviewing the collection of information. Send comments regarding this burden estimate or any other aspect of this collection of information, including suggestions for reducing this burden, to Washington Headquarters Services, Directorate for information Operations and Reports, 1215 Jefferson Davis Highway, Suite 1204, Arlington, VA 22202-4302, and to the Office of Management and Budget, Paperwork Reduction Project (0704-0188), Washington, DC 20503.

| 1. AGENCY USE ONLY *(Leave blank)* | 2. REPORT DATE | 3. REPORT TYPE AND DATES COVERED |
|---|---|---|
| | April 1994 | Contractor Report |

**4. TITLE AND SUBTITLE**

Hypersonic Shock/Boundary-Layer Interaction Database: New and Corrected Data

**5. FUNDING NUMBERS**

NAG2-781

**6. AUTHOR(S)**

Gary S. Settles and Lori J. Dodson

**7. PERFORMING ORGANIZATION NAME(S) AND ADDRESS(ES)**

Department of Mechanical Engineering
Penn State University
University Park, PA 16802

**8. PERFORMING ORGANIZATION REPORT NUMBER**

A-94078

**9. SPONSORING/MONITORING AGENCY NAME(S) AND ADDRESS(ES)**

National Aeronautics and Space Administration
Washington, D.C. 20546-0001

**10. SPONSORING/MONITORING AGENCY REPORT NUMBER**

NASA CR-177638

**11. SUPPLEMENTARY NOTES**

Point of Contact: Joseph Marvin, Ames Research Center, MS 229-1, Moffett Field, CA 94035-1000
(415) 604-5390

**12a. DISTRIBUTION/AVAILABILITY STATEMENT**

Unclassified-Unlimited
Subject Category – 34

**12b. DISTRIBUTION CODE**

**13. ABSTRACT** *(Maximum 200 words)*

An effort was begun in 1989 at the Penn State University Gas Dynamics Laboratory to perform a critical review of the available hypersonic data and to assemble a selected database for purposes of computational fluid dynamics (CFD) code validation and turbulence modeling. The effort was sponsored by the National Aero-Space Plane (NASP) Program through NASA Ames Research Center, and was a part of an overall task to develop compressible turbulence models. NASA CR-177577, a database report on hypersonic shock wave/turbulent boundary-layer interactions, was the product of phase 1 of that effort. Phase 2 produced a similar database, NASA CR-177610, covering the topics of attached hypersonic boundary layers in pressure gradients and compressible turbulent mixing layers. The present report represents the result of the third and final phase: namely, recent additions and corrections to the hypersonic shock wave/turbulent boundary-layer interaction database originally given in NASA CR-177577. Seven new datasets are presented, consisting of supersonic and hypersonic experiments using single- and double-fin shock wave generators and a compression corner shock wave generator. Finally, typographical and other errors occurring in NASA CR-177577 have been corrected in a section of the present report, including clarification of some issues which were raised with regard to the original database by users in the interim.

**14. SUBJECT TERMS**

Hypersonic, Shock wave, Turbulent boundary layer, Shock wave/boundary-layer interaction

**15. NUMBER OF PAGES**

46

**16. PRICE CODE**

A03

| 17. SECURITY CLASSIFICATION OF REPORT | 18. SECURITY CLASSIFICATION OF THIS PAGE | 19. SECURITY CLASSIFICATION OF ABSTRACT | 20. LIMITATION OF ABSTRACT |
|---|---|---|---|
| Unclassified | Unclassified | | |

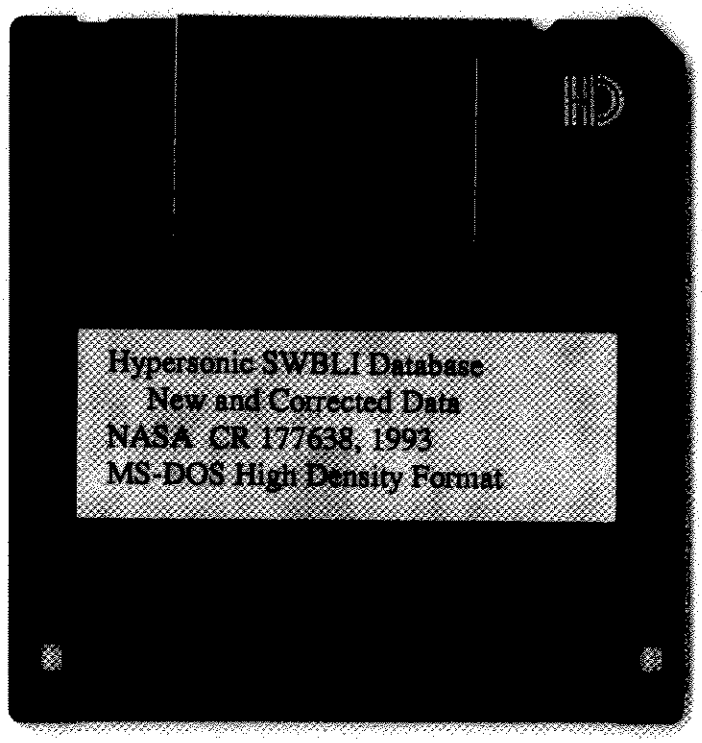


Also, NASA-CR177638Database.tgz